owtnm08.ewi.utwente.nl

OWTNM 2008 Eindhoven, The Netherlands Proceedings

OWTNM 2008

XVIIth International Workshop on Optical Waveguide Theory and Numerical Modelling

Eindhoven, The Netherlands
June 13 & 14, 2008

Proceedings

Contact information:

Dr. Hugo J.W.M. Hoekstra
University of Twente,
Faculty EEMCS,
P.O. Box 217,
7500 AE, Enschede,
The Netherlands;
Phone: +31 (0)53 489 2818
Fax: +31 (0)53 489 3343
E-mail: owtnm08@ewi.utwente.nl
Web: http://ioms.ewi.utwente.nl/

2008 University of Twente
Printed in Enschede, The Netherlands
ISBN: 978-90-365-2691-3

OWTNM 2008

XVII International Workshop on Optical Waveguide Theory and Numerical Modelling

13-14 June 2008, Eindhoven, The Netherlands

Proceedings

Acknowledgments

The organizers thank for shown interest and support:

MESA$^+$ Institute for Nanotechnology, University of Twente,
P.O. Box 217, 7500 AE Enschede, The Netherlands

PhoeniX Software, Software for micro- and nano technologies,
P.O. Box 545, 7500 AM Enschede, The Netherlands

NanoNed, Nanotechnology network in the Netherlands,
P.O. Box 3021, 3502 GA Utrecht, The Netherlands

Preface

This year the International Workshop on Optical Waveguide Theory and Numerical Modelling (OWTNM) will be held in Eindhoven on 13-14 June, in collocation with the ECIO (11-13 June, 2008; see also http://owtnm08.ewi.utwente.nl/). Since the beginning of the annually held OWTNM, in Teupitz, Germany, 1992, the workshop has been a forum for enthusiastic scientists in the field of integrated optics to exchange problems and new ideas related to optical theory and modelling and novel materials and devices in an open and relaxed atmosphere. The organizers hope and expect that the XVIIth OWTNM will be as successful as the previous meetings.
Topics of interest include but are not limited to: *theory and modelling* of passive, active and nonlinear waveguide devices, photonic integrated systems, grated waveguide structures, input/output waveguide coupling aspects, photonic bandgap structures and photonic crystals, photonic nanostructures, meta-materials and plasmonics, as well as *advances and new directions* in numerical methods, mode solvers and mathematical models.

The following remarks can be made on the traditional Special Issue of the Journal Optical Quantum Electronics:

1. Regarding the high level of all contributions, no distinction will be made between Oral and Poster presentations given at the workshop. Every participant is encouraged to write and submit a journal paper related to the OWTNM contribution
2. All papers should be submitted on-line via the Springer's Editorial Manager. Contributors shall personally submit their papers to Springer's electronic system, and choose the article type "Special Issue OWTNM 2008". Submission rules and guidance for authors can be found on the OQE official Web page http://www.editorialmanager.com/oqel/default.asp or http://owtnm08.ewi.utwente.nl/
3. All papers will be reviewed by referees appointed by the Guest Editors, being Bas de Hon, Manfred Hammer and Hugo J.W.M. Hoekstra.
4. The deadline for submission is strictly the 1st of September. The process of reviewing-revision-selection has to be completed by 30 November, 2008.

Enschede and Eindhoven, May 2008

The local organizing committee of OWTNM 2008

Organizers

Local Organizing Committee OWTNM 2008

- Hugo J.W.M. Hoekstra, University of Twente, Netherlands
- Manfred Hammer, University of Twente, Netherlands
- Bastiaan P. de Hon, Technical University of Eindhoven, Netherlands
- Alyona Ivanova, University of Twente, Netherlands
- So Van Pham, University of Twente, Netherlands
- Remco Stoffer, PhoeniX Software, Enschede, Netherlands

OWTNM Technical Committee

- Trevor Benson, University of Nottingham, UK
- Peter Bienstman, Ghent University, Belgium
- Jiří Čtyroký, Institute of Electronics and Photonics, Czech Republic
- Anand Gopinath, University of Minnesota, USA
- Hugo J.W.M. Hoekstra, University of Twente, Netherlands
- Andrei V. Lavrinenko, COM-DTU, Lyngby Kgs., Denmark
- Xavier Letartre, LEOM, Ecole Centrale de Lyon, France
- Andrea Melloni, DEI-Politecnico di Milano, Italy
- Olivier Parriaux, University of Saint Etienne, France
- Reinhold Pregla, FernUniversität Hagen, Germany
- Christoph Wächter, Fraunhofer IOF, Jena, Germany

Programme

Workshop schedule

Friday 13.06.2008

08:55	Welcome Address
09:00 - 10:15	Session OR-01: BPMs and Modal Methods: Waveguides and Fibres
10:15 - 10:45	*Coffee break*
10:45 - 12:00	Session OR-02: Optical Microcavities
12:00 - 13:00	*Lunch*
13:00 - 14:45	Session OR-03: (OWTNM-ECIO Joint Session) Dedicated Device Modelling
14:45 - 15:15	*Coffee break*
15:15 - 16:00	Session OR-04: Nano-Optical Components: Plasmonics
16:00 - 18:00	Poster Session
19:00 -	*Workshop Dinner*

Saturday 14.06.2008

09:00 - 10:15	Session OR-05: Active and Nonlinear Materials and Devices
10:15 - 10:45	*Coffee break*
10:45 - 12:00	Session OR-06: Nano-Optical Components: Photonic Crystals, and Meta-Materials
12:00 - 13:00	*Lunch*
13:00 - 14:45	Session OR-07: Advancements in Numerical Methods
14:45	Closing of the Workshop

Friday 13.06.2008

08:55		Welcome Address
09:00 - 10:15	**Session OR-01**	**BPMs and Modal Methods: Waveguides and Fibres**
09:00 - 09:15	OR-01.01	Rutger W. Smink, Bastiaan P. de Hon and Anton G. Tijhuis, *Refractive Index Profile Optimisation for the Design of Single-Mode Optical Fibres*
09:15 - 09:30	OR-01.02	Remco Stoffer and Jan Bos, *Fixed-Grid Finite Element Beam Propagation Method*
09:30 - 09:45	OR-01.03	S. S. A. Obayya, *Efficient Bidirectional Finite-Element Based Beam Propagation Method for Longitudinal Discontinuities*
09:45 - 10:00	OR-01.04	G. Renversez, F. Drouart, A. Nicolet and C. Geuzaine, *Spatial Kerr Solitons in Fibers of Finite Size Cross-Section: Beyond the Townes Soliton*
10:00 - 10:15	OR-01.05	O.V. (Alyona) Ivanova, Remco Stoffer, Manfred Hammer and E. (Brenny) van Groesen, *A Variational Vectorial Mode Solver*
10:15 – 10:45	***Coffee break***	
10:45 – 12:00	**Session OR-02**	**Optical Microcavities**
10:45 - 11:15	OR-02.01	T. M. Benson, P. Sewell, A. Vukovic and J. G.Wykes (invited), *3D Modelling of Resonant Cavities*
11:15 - 11:30	OR-02.02	C. Sauvan, S. Mazoyer, P. Lalanne and J.P. Hugonin, *Computational Concepts for Periodic Optical Waveguides: Application to Coupled Photonic Crystal Microcavities*
11:30 - 11:45	OR-02.03	T. Lauerman and J. Čtyroký, *Numerical Model of Nonlinear Pulse Propagation in a SOI Ring Microresonator*

11:45 - 12:00	OR-02.04	Elena I. Smotrova, Volodymyr O. Byelobrov, Trevor M. Benson, Phillip Sewell, Jiri Ctyroky and Alexander I. Nosich, *Understanding Thresholds of Microcavity Lasers Through Overlap Coefficients*
12:00 – 13:00	***Lunch***	
13:00 - 14:45	**Session OR-03**	**(ECIO-OWTNM Joint Session) Dedicated Device Modelling**
13:00 - 13:30	OR-03.01	A. Melloni, F. Morichetti, A. Canciamilla and C. Ferrari (invited), *Deeply Inside Tunable CROW Delay Lines*
13:30 - 14:00	OR-03.02	Wim Bogaerts, Lieven Vanholme, Paul Bradt and Peter Bienstman (invited), *Closed-Loop Modeling of Silicon Nanophotonics: From Design to Fabrication and Back Again*
14:00 - 14:15	OR-03.03	Jiro Ito, Kenji Iwamoto and Hiroyuki Tsuda, *Design of a Waveguide-Type Polarization Beam Splitter Incorporating Trenches Filled with Low-Refractive Index Material*
14:15 - 14:30	OR-03.04	Ken Kashiwagi, Shinji Yamashita, Katsunari Okamoto, and S. J. Ben Yoo, *Temperature Insensitive Silicon Slot Waveguides with Air Slot*
14:30 - 14:45	OR-03.05	A. Delâge, P.J. Bock, P Cheben, J.H. Schmid, D.-X. Xu, S. Janz and T.J. Hall, *A Demultiplexer with Blazed Waveguide Sidewall Grating*
14:45 – 15:15	***Coffee break***	
15:15 - 16:00	**Session OR-04**	**Nano-Optical Components: Plasmonics**
15:15 - 15:45	OR-04.01	J.M. Brok, O.T.A. Janssen and H.P. Urbach (invited), *Light Transmission Through Slits and Holes Using Waveguide Modes*

15:45 - 16:00 OR-04.02 Hung-Chun Chang, Chang-Chun Chung, Han-Chih Yeh, Chan-Huan Peng and Bang-Yan Lin,
Analysis of Triangular Metal Wedge Surface-Plasmon-Polariton Waveguides Using an Imaginary-Distance Finite-Element Beam Propagation Method

16:00 - 18:00 **Poster session**

PO-01 Samit Barai and Anurag Sharma,
Empirical Relations for the Propagation Characteristics of Integrated Optical Diffused Channel Waveguides

PO-02 Debjani Bhattacharya and Anurag Sharma,
A Semi-Vectorial Split-Step Non-Paraxial Method for Wave Propagation

PO-03 Debjani Bhattacharya and Anurag Sharma,
A New Scheme for Splitting of Operators in the 3D Finite Difference Split-Step Non-Paraxial Method

PO-04 S.S.A. Obayya, M.F.O.I. Hameed, P. Harrison, A.M. Nasr and M.I. Abou Elmaaty,
Artificial Neural Network Radial Basis Functions Approach for the Optimization of Photonic Crystal Fibres

PO-05 Alexander Nerukh, Helen Semenova and Nataliya Sakhnenko,
Alternative Calculations of Initial Value Problem for Electromagnetic Field in Dielectric Waveguide

PO-06 Vladimir A. Andreev, Anton V. Bourdine and Vladimir A. Burdin,
Some Samples of Perturbation Method Application for Improving FEM Algorithm of Singlemode Optical Fiber Dispersion Calculation

PO-07 Pavel Kwiecien, Ivan Richter and Jiří Čtyroký,
Aperiodic Rigorous Coupled Wave Analysis Applied to Photonic Nanostructure Modeling: a Critical Study

PO-08 Anna Vozianova, Alexander Nerukh and Nataliya Sakhnenko,
Surface Quasi-Plasmon-Polaritons at a Plane Boundary of Newly Created Plasma

PO-09 Indra Karnadi, Alexander A. Iskandar and May On Tjia,
Subwavelength Imaging with a Silver Lens

PO-21 Manfred Hammer,
Resonator Chains of 2-D Square Dielectric Optical Microcavities

PO-22 Nataliya Sakhnenko, Alexander Nerukh, Trevor Benson and Phillip Sewell,
Modeling of 2D Transient Responses in Stratified Cylindrical Structures

PO-23 Hovik V. Baghdasaryan, Tamara M. Knyazyan, Tigran H. Baghdasaryan and Grigori G. Eyramjyan,
Application of the Method of Single Expression for Analysis of Plane EM Wave Oblique Incidence on Multilayer Structures with Arbitrary Permittivity and Permeability

PO-24 Stefan F. Helfert and Reinhold Pregla,
Modeling of Waveguide Structures with Crossed Discretization Lines

PO-25 Nikolai Nikolaev,
Accurate Reconstruction of Gradient Index Profile of Planar Optical Waveguides by Two Sets of Measurements

19:00 - ***Dinner***

Saturday 14.06.2008

09:00 - 10:15	**Session OR-05**	**Active and Nonlinear Materials and Devices**
09:00 - 09:30	OR-05.01	John M. Arnold (invited), *Dynamical Systems in Nonlinear Optics: Maxwell-Bloch Models*
09:30 - 09:45	OR-05.02	R. Letizia and S. S. A. Obayya, *Efficient Multiresolution Time Domain Analysis for Second Harmonic Generation Integrated Devices*
09:45 - 10:00	OR-05.03	S. Schild, M. Ammann, N. Chavannes and N. Kuster, *A Novel Approach to Model Linear and Nonlinear Dispersion with ADE-FDTD*
10:00 - 10:15	OR-05.04	Holger Schmitz and Vladimir Mezentsev, *Full Vectorial Modelling of Femtosecond Bullets for Laser Inscription of Photonic Structures*
10:15 - 10:45	***Coffee break***	
10:45 - 12:00	**Session OR-06**	**Nano-Optical Components: Photonic Crystals, Gratings, and Meta Materials**
10:45 - 11:15	OR-06.01	S. Anantha Ramakrishna (invited), *Design and Control of Metamaterials with Negative Refractive Index*
11:15 - 11:30	OR-06.02	Hugo J.W.M. Hoekstra and Theo P. Valkering, *Transparent Expressions for Group Velocity and Sensitivity to Index Changes of Photonic Crystal Waveguide Modes*
11:30 - 11:45	OR-06.03	D. Pinto and S.S.A. Obayya, *Finite Volume Time Domain Analysis of Nonlinear Photonic Crystal Devices*
11:45 - 12:00	OR-06.04	Alexander A. Iskandar, Aimi Abass, Agoes Soehianie, Husin Alatas, May On Tjia and Hugo J.W.M. Hoekstra, *Effects of Lattice Variations on Confinement in Photonic Crystal Microcavity using Green Tensor Method*

12:00 – 13:00	***Lunch***	
13:00 – 14:45	**Session OR-07**	**Advancements in Numerical Methods**
13:00 - 13:30	OR-07.01	Ya Yan Lu (invited), *Application of Dirichlet-to-Neumann Maps in Numerical Modelling of Photonic Structures*
13:30 - 13:45	OR-07.02	Reinhold Pregla, *Analysis of Waveguides Bends and Junctions*
13:45 - 14:00	OR-07.03	E.A. Kolosovsky and A.V. Tsarev, *Use of the Coupled Modes Theory for Analysis of Light Scattering by the Inclined Reflector in Optical Waveguide*
14:00 - 14:15	OR-07.04	Niels Gregersen and Jesper Mørk, *An Improved Perfectly Matched Layer in the Eigenmode Expansion Technique*
14:15 - 14:30	OR-07.05	Jan Fiala, Ivan Richter and Milan Šiňor, *Interaction of Light with Subwavelength Apertures: a Comparison of Approximate and Rigorous Approaches*
14:30 - 14:45	OR-07.06	M. Maksimovic, M. Hammer and E. van Groesen, *Variational Coupled Mode Theory and Perturbation Analysis for 1D Photonic Crystal Structures using Quasi-Normal Modes*
14:45	Closing of the Workshop	

Abstracts

Refractive index profile optimisation for the design of single-mode optical fibres

Rutger W. Smink, Bastiaan P. de Hon, and Anton G. Tijhuis
Eindhoven University of Technology, P.O.Box 513, 5600 MB Eindhoven, The Netherlands
R.W.Smink@tue.nl, B.P.d.Hon@tue.nl, A.G.Tijhuis@tue.nl

With regard to several typical single-mode fibre properties, we have performed refractive index profile optimisation for the design of a single-mode fibre. Compared to a reference stochastic optimisation technique, algorithms based on exact gradient information win hands down in speed.

Introduction

Often, desired optical fibre properties are conflicting, e.g. minimum dispersion and dispersion slope are at odds with minimum bending losses. In addition, one would like to keep the mode-field diameter fixed. From a design point of view, it is a challenging task to adapt the refractive-index profile of an optical fibre to meet the specific demands. Fortunately, computer-based optimisation schemes can speed up this design step considerably. These schemes often lead to counterintuitive designs that could not have been contrived otherwise.

We have performed a refractive index profile optimisation with regard to the aforementioned fibre properties. Thus far, genuine optimisation methods have hardly ever been applied in the design of optical fibres. We have taken the work of Bingle et al. [1], as the point of departure for our gradient-based optimisation technique. As this is a local optimisation method, we have set our result against those obtained using a global stochastic optimisation technique.

Numerical approach

For the discretisation of the profile, we have chosen piecewise linear segments, with variable endpoints that serve as the free optimisation parameters. For the computation of the fibre quantities, we have implemented a full-wave (vectorial) modelling code for radially inhomogeneous optical fibres along the lines of early work by Dil and Blok [2].

Although many algorithms are available to perform the profile optimisation, we have chosen a modified-Newton (MN) algorithm and a simulated annealing (SA) scheme. The former is a gradient-based technique, whereas the latter is a global stochastic one. A cost function (CF) has been introduced that balances the fibre quantities. We have evaluated the gradients of the CF with respect to the optimisation parameters in terms of Fréchet derivatives.

Results and conclusions

We have performed optimisation runs consisting of five to thirteen optimisation parameters with both optimisation schemes. For a fair comparison, we have left the CF unchanged throughout. It has turned out that optimisation with the MN algorithm is at least two orders of magnitude faster than with an SA scheme, while the difference in the attained local minima are marginal. Moreover, for an increasing number of parameters, the MN algorithm tends to find better local minima than the "global" SA optimiser. A disadvantage of the MN algorithm is its dependence on the initial profile. However, by a systematic selection of several initial profiles, we have thus far always attained a minimum comparable or better than the one found with SA.

References

[1] M. Bingle, B.P. de Hon and M.J.N. van Stralen, *Proc. 2001 URSI Int. Symp. Electromagn. Theory, Victoria, Canada*, 515–517, (2001).

[2] J.G. Dil and H. Blok, *Opt. Quant. Electron.* **5**, 415–428 (1973)

Fixed-grid Finite Element Beam Propagation Method

Remco Stoffer and Jan Bos
PhoeniX BV, P.O. Box 545, 7500AM Enschede, The Netherlands
remco.stoffer@phoenixbv.com

A fixed-grid finite element BPM is proposed in which the location of interfaces between materials inside the elements is taken into account accurately.

Summary

Despite advances in more general, omnidirectional simulation methods, unidirectional Beam Propagation Methods (BPM) are still used extensively in the modeling of integrated optical components. The most prominent of these are finite difference (FD) and finite elements (FE). An advantage of FD is that the structure of the matrices in the equations is constant from one step to the next; in those parts of the window in which nothing changes the matrix elements do not need to be re-calculated. However, material interfaces between grid points are hard to take into account. The FE scheme, on the other hand, can deform its mesh to follow the material interfaces. The mesh thus needs to be recreated each step, implying a potentially expensive re-gridding step, a recalculation of all involved matrices, and interpolation to the new finite element nodes.

This paper proposes a new FE full-vectorial BPM. The FE grid is kept constant from one calculation step to the next, which helps in avoiding recalculations of matrices. Contrary to standard FE methods, inside each grid cell, the refractive index may be arbitrary, so it is not necessary to adjust the grid to the interfaces. All distinct material sections in a cell are taken into account in the calculation of the integrals that result from the weak formulation of Maxwell's equations. Slanted interfaces are treated accurately; even waveguides with very few or no points in the guide are simulated reasonably well.

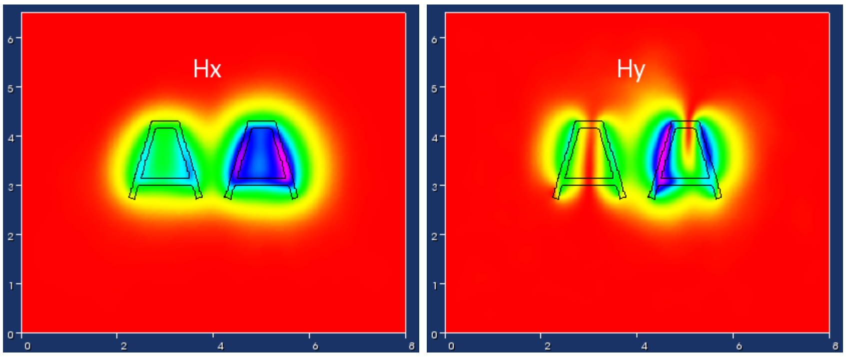

Absolute value of the field in a coupler of slanted box-shaped TriPleX waveguides [1] 75 μm after the mode of the left waveguide is launched.

References

[1] F. Morichetti et al, *IEEE Journal of Lightwave Technology* 25 (**36**), 2579–2589 (2007).

Efficient Bidirectional Finite-Element Based Beam Propagation Method for Longitudinal Discontinuities

S. S. A. Obayya[1]
[1] *University of Leeds, School of Electronics and Electrical Engineering, LS2 9JT Leeds, UK*
s.s.a.obayya@leeds.ac.uk

Summary

Many photonic devices involve longitudinal optical waveguide discontinuities which will certainly result in power reflectivities. The problem of the numerical modelling of power reflectivity caused by arbitrary longitudinal discontinuities, such as, e.g., optical fibres facets, can be approached using different numerical techniques such as the finite difference time domain (FDTD). However, it takes a very long time before obtaining stable results for the reflected waves. Alternatively, the analytical free space radiation method (FRSM) has been suggested in [1] as has been proven to give accurate modelling of the optical fibre facet problem. However, its applicability is only limited to the cases where the refractive index difference between the core and cladding is less than 10%. In this paper, an alternative numerical technique based on the versatile finite element method will be suggested for the problem of multiple and arbitrary longitudinal optical waveguide discontinuities. For each side of each discontinuity, and by "lumping" the mass matrix entries into the diagonal locations, this matrix renders itself to be diagonal, and hence its inversion and multiplication with the original characteristic matrix will result in a modified characteristic matrix as sparse as the original one. By applying Talyor's series expansion to represent the square root of the modified characteristic matrix and satisfying the interface boundary condition at the discontinuity plane, both the reflected and transmitted fields can be efficiently solved for. Therefore, the presented finite element method not only avoids the modal solution stage, but also, does not require any matrix inversion to approximate the square root operator of the characteristic matrix using higher order Talyor's series expansions. This approach has also been combined with an iterative "unidirectional" BPM scheme so as to build the basis of our bidirectional BPM method to account accurately for the reflected and transmitted waves. The excellent agreement of the results, shown in Fig. 2, for the waveguide terminating by double-layer antireflection (AR) coating of Fig. 1 obtained using the presented finite element approach and the FDTD [1], reveals its high numerical accuracy. In the presentation, more examples showing the versatility and efficiency of the presented finite element approach will be presented.

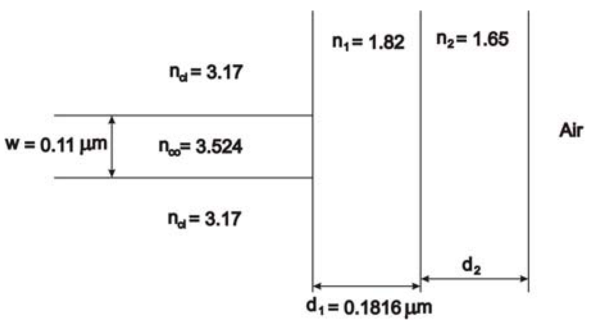

Fig. 1 Schematic diagram of waveguide terminating by double layer AR coating.

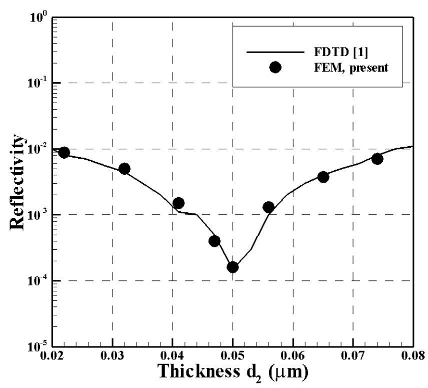

Fig.2 Power reflectivity spectrum.

[1] Feng et al., J. Lightwave Technol., vol. 21, pp. 281-285, Jan. 2003.

Spatial Kerr solitons in fibers of finite size cross-section: beyond the Townes soliton

G. Renversez[1], F. Drouart[1], A. Nicolet[1] and C. Geuzaine[2]
[1]*Institut Fresnel, Université Aix-Marseille, Marseille, France*
gilles.renversez@fresnel.fr

[2]*Institut Montefiore, Université de Liège, Liège, Belgique*

We propose a new numerical method to find spatial solitons in fibers with a nonlinear Kerr effect. Results for step-index and microstructured optical fibers with a finite cross-section are described. These solutions are different from the Townes soliton but converges toward it at small wavelengths.

Summary

Rigorous techniques for modeling the *linear* properties of microstructured optical fibers have been available for several years [1]. Modeling the *nonlinear* properties of fibers (and in particular the optical Kerr effect) is inherently more complex, and while several techniques have been proposed, none is completely satisfactory. On the one hand, there are numerous works based on the nonlinear Schrödinger equation, which do not deal with the finite size of the waveguide cross-section, but focus on the transient evolution of pulse propagation along the fiber axis. On the other hand, there are works based directly on Maxwell's equations or their scalar approximation, which take into account the optogeometric profile of the fiber. Our study belongs to the second group: it is based on the direct numerical solution of Maxwell's equations with nonsaturable Kerr-type nonlinearities, using the finite element method [1, 2].

We improve previous studies in several ways. First, while the numerical method we propose is closely related to the one proposed by Ferrando et al. [3] , we do not artificially periodize the cross-section of the fiber. Its symmetry properties are thus fulfilled more easily, since no unit cell must be defined to implement the periodic boundary conditions. Second, and more importantly, we do not use the "fixed-power" algorithm proposed in [3]. In this algorithm, at each step of the iterative process defined to obtain the nonlinear solution, the power of the intermediate solution is renormalized to the power arbitrarily fixed at the beginning of the algorithm. Our new algorithm determines the power of the solution by itself, relying only on residue minimization. Finally, in contrast to a related work by Snyder et al. [4], our algorithm can deal with inhomogeneous media and both the scalar case and the vector one.

We demonstrate that the nonlinear self-coherent solution, corresponding to the spatial soliton with the highest reachable energy avoiding the self-focusing instability in optical fibers, is different from the Townes soliton. We demonstrate that not only this solution is different from the one obtained in the homogeneous medium but also that it depends on the finite size of the structure. Indeed, the variation of the spatial soliton for various core sizes of the step-index fiber and for various air-hole sizes or various number of air-hole rings of the microstructured optical fiber is illustrated. Besides, we prove that this nonlinear solution of high energy converges toward the Twones soliton at small wavelengths. We also show that the amplitude of the nonlinear self-coherent solution, as taken into account by our algorithm, depends on the fiber geometry.

References

[1] F. Zolla, G. Renversez, *et al.*. *Foundations of Photonic Crystal Fibres.* ICP, London, 2005.
[2] A. Nicolet, F. Drouart, G .Renversez, and C. Geuzaine. *COMPEL*, 26(4):1105–1113, 2007.
[3] A. Ferrando, M. Zacarés, P. Fernandez de Cordoba, *et al.* . *Optics Express*, 11(5):452–459, 2003.
[4] A. W. Snyder, D. .J. Mitchell, and Y. Chen. *Optics Letters*, 19(8):524–526, 1994.

A Variational Vectorial Mode Solver

O.V. (Alyona) Ivanova, Remco Stoffer, Manfred Hammer and E. (Brenny) van Groesen
MESA+ Institute for Nanotechnology, AAMP group, University of Twente, The Netherlands
o.v.ivanova@math.utwente.nl

A variational method for the fully vectorial mode analysis of lossless dielectric waveguides with piecewise constant rectangular refractive index distributions is proposed.

Summary

An extension of the scalar Mode Expansion Mode Solver [1] to fully vectorial simulations is discussed. The method uses a six component variational formulation of the Maxwell equations [2] together with approximations of each component of the vector field by specific superpositions of some given basis functions, depending on one of the coordinates, times unknown coefficient functions that are defined on the entire second coordinate axis. In principle there is some freedom in choosing the basis functions; we use the vector field components of modes of the constituting vertical slices of the waveguide.

It turns out that with our field template the problem of finding the unknown lateral coefficient-functions reduces to finding those, which correspond to only two field components; the computational effort becomes comparable to the scalar case [1] or the Film Mode Matching method [3].

Just like the scalar approach this method can be used with only a few terms in the expansion for rough approximations; the technique can then be compared to a semi-vectorial Effective Index Method. With a suitable choice of basis fields a reasonable approximation can be achieved with a relatively low number of terms. On the other hand, higher order expansions lead to rigorous simulations. Both limits are discussed.

The present method can also be seen as a step towards solving the scattering problem in 3D using a similar approach.

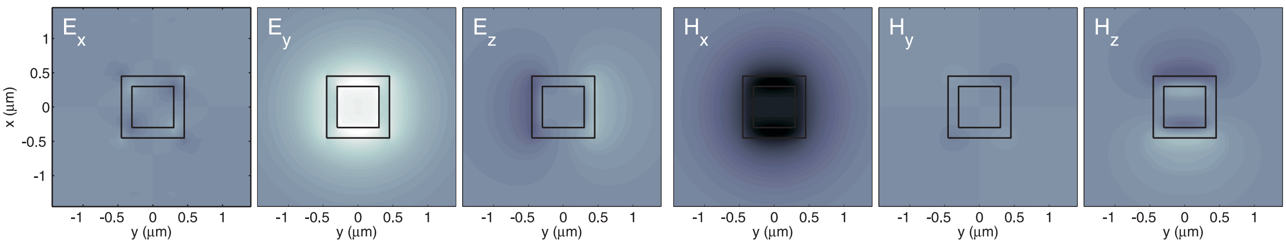

Vectorial field profile of the fundamental mode of the box-shaped waveguide from [4]. The Si_3N_4 (n=1.99) shell around the $0.6 \times 0.6\,\mu m^2$ SiO_2 (n=1.4456) core is 150 nm thick and surrounded by SiO_2; the wavelength is 1.55 μm. The effective index is 1.52436.

This research was supported by NanoNed, a national nanotechnology program coordinated by the Dutch Ministry of Economic Affairs.

References

[1] O.V. Ivanova, M. Hammer, R. Stoffer and E. van Groesen. A variational mode expansion mode solver. *Optical and Quantum Electronics*, **39**, 849–864 (2007).

[2] C. Vassallo. *Optical Waveguide Concepts*. Elsevier, Amsterdam, 1991.

[3] A.S. Sudbø. Film mode matching: a versatile numerical method for vector mode field calculation in dielectric waveguides. *Pure Appl. Opt.* **2**, 211-233 (1993).

[4] F. Morichetti, A. Melloni, M. Martinelli, R.G. Heideman, A. Leinse, D.H. Geuzebroek and A. Borreman. Box-shaped dielectric waveguides: a new concept in integrated optics? *Journal of Lightwave Technology*, **25** (9), 2579–2589 (2007).

3D Modelling of Resonant Cavities

T. M. Benson, P. Sewell, A. Vukovic, J. G.Wykes.
George Green Institute for Electromagnetics Research, University of Nottingham, University Park, Nottingham NG7 2RD, UK.
Trevor.benson@nottingham.ac.uk

The difficulties and challenges when modelling micro-resonators are discussed. Recent progress towards their 3D modelling using time-domain codes will be described.

Summary

Micro-resonators are critical optical components that have many exciting applications in fields such as telecommunications, novel laser sources, quantum cryptography and optical signal processing. A recent overview of the physics and applications of micro-resonators can be found in [1]. Fabrication techniques allow many different designs of micro-resonator to be realised, but at present their optimisation and simulation remain firmly entrenched in 2D. The geometrical complexity of many micro-resonators prevents detailed analytic study. Thus there is a strong demand for comprehensive 3D numerical simulations. In this paper we will discuss some of the difficulties and challenges that must be faced when modelling the electromagnetic properties of micro-resonators. Recent progress towards their 3D modelling using time-domain codes will then be described.

[1] Virtual Focus Issue, Physics and Applications of Microresonators (PAM), V. N. Astratov (Coordinating Associate Editor), Optics Express, Vol. 15, Issue 25, Dec 2007, http://www.opticsexpress.org/virtual_issue.cfm?vid=51

Computational Concepts for Periodic Optical Waveguides: Application to Coupled Photonic Crystal Microcavities

C. Sauvan, S. Mazoyer, P. Lalanne and J.P. Hugonin

Laboratoire Charles Fabry de l'Institut d'Optique, CNRS, Univ. Paris Sud
Campus Polytechnique, RD 128, F-91127 Palaiseau Cedex, France
christophe.sauvan@institutoptique.fr

We present a rigorous modal formalism for modelling light propagation in 3D periodic waveguides. By applying this formalism, we propose a semi-analytical model for Photonic Crystal coupled-resonator waveguides. This model provides simple analytical expressions for the delay and the losses and allows to compare various geometries.

Summary

A coupled-resonator optical waveguide (CROW) consists of a chain of resonators in which light propagates by virtue of the evanescent coupling between adjacent resonators [1]. By tailoring the coupling and the resonators, it is possible to control the group velocity of optical pulses. The physical origin of the coupling between the resonators can be either purely refractive, e.g. an air gap between two high refractive-index regions, or based on distributed Bragg reflection. The first strategy generates CROWs made of coupled ring resonators, for example, and the second strategy generates CROWs made of coupled Photonic Crystal (PC) microcavities. In the case of coupled ring resonators, the three formalisms most commonly used to model the structure are the tight-binding approximation, the transfer matrix method and the temporal coupled-mode theory [2]. These formalisms provide simple analytical expressions for the main CROW characteristics in the limit of weakly coupled resonators with negligible coupling losses. But in the case of coupled PC cavities, the coupling losses are predominant and can not be neglected compared to the propagation losses in the resonators. Therefore, a straightforward generalization of previous works to PC-based CROWs provides inaccurate results for the attenuation.

In order to correctly take into account the specificities of PC geometries (intrinsic radiation losses and large dispersion), we have developed a semi-analytical model based on an extension of the classical transfer matrix formalism to three-dimensional (3D) periodic structures with radiation losses. This generalization is based on a rigorous modal formalism that allows to model light propagation in 3D periodic waveguides [3]. We will first present this 3D modal formalism before applying it to the case of coupled PC resonators. We will show that our formalism allows us to propose a semi-analytical model for the light propagation in these structures. The model provides simple analytical expressions for the delay, bandwidth and attenuation of the CROW. These expressions evidence the important physical parameters, such as the coupling coefficient, the coupling losses, the group velocity inside each resonator and the penetration length in the distributed mirrors. They allow to easily discuss the trade-off between delay and losses.

References

[1] A. Yariv, Y. Xu, R.K. Lee and A. Scherer, Opt. Lett. **24**, 711 (1999).
[2] J.K.S. Poon *et al.*, J. Opt. Soc. Am. B **21**, 1665 (2004).
[3] G. Lecamp, J.P. Hugonin and P. Lalanne, Opt. Express **15**, 11042 (2007).

Numerical model of nonlinear pulse propagation in a SOI ring microresonator

T. Lauerman[1,2] and J. Čtyroký[1]
[1] *Institute of Photonics and Electronics ASCR, v.v.i, Chaberska 57, 18251 Praha 8, Czech Republic*
ctyroky@ufe.cz

[2] *Czech Technical University, Faculty of Nuclear Sciences and Physical Engineering, Brehova 7, 11519, Praha 1, Czech Republic*
lauerman@troja.fjfi.cvut.cz

A numerical algorithm for nonlinear pulse progation in ring microresonator based devices is presented. The resonant behaviour of the optical feedback is rigorously accounted for by an iterative procedure, whereas the pulse evolution is governed by the NLSE adapted to SOI waveguides.

Summary

We present a numerical model of a nonlinear propagation of optical pulses in a ring microresonator coupled to two straight bus waveguides. As known, microresonator devices has been studied with the aim at performing all-optical signal processing and switching, realizing that the main feature of microresonators arises from their capability to enhance the nonlinear behavior of the waveguide material by the resonant response of the structure itself.
In the view of this, we describe an efficient iterative method for modeling nonlinear properties of microresonator devices, which is "platform" independent and can be easily modified for other types of resonant waveguide cavities like FP resonators, too.
In the treatment adopted here, the distributed coupling between bus and ring guides is assumed to be linear, localized and nondispersive, which is justified in case of a ring resonator. The nonlinear propagation of the optical pulse out of the coupling points can be described in a formal way as an action of a nonlinear operator, e.g. represented by the nonlinear Schrodinger equation (NLSE). The resonant behavior of the optical feedback, the phase and group delays in the ring are then fully taken into account by the application of an iterative numerical procedure [1].
Even though the concept of our treatment has been designed to be general, to demonstrate its key features, it is applied to model the optical pulse propagation in a silicon-on-insulator ring microresonator. The nonlinear propagation in the bus waveguides and in the ring as well is governed by the NLSE introducing following effects optical pulses can exhibit in SOI waveguides: SPM, XPM, SRS, TPA, FCA and the plasma dispersion effect [2, 3, 4].

References

[1] J.Čtyroký and T.Lauerman, OSA Toppical Meeting IPNRA and SL 2007 Technical Digest, paper ITuF4.
[2] A.Liu, H.Rong, M.Paniccia, O.Cohen and D.Hak, *Optics Express* **12**, 4261–4268 (2004).
[3] V.M.N.Passaro and F.De Leonardis, *Journal of Lightwave Technology* **24**, 2920–2931 (2006).
[4] Q.Lin, O.J.Painter and G.P.Agrawal, *Optics Express* **15**, 16604–16644 (2007)

Understanding Thresholds of Microcavity Lasers through Overlap Coefficients

Elena I. Smotrova[1], Volodymyr O. Byelobrov[1], Trevor M. Benson[2], Phillip Sewell[2], Jiri Ctyroky[3], Alexander I. Nosich[1]

[1] *Institute of Radio-Physics and Electronics NASU, Kharkov 61085, Ukraine*
anosich@yahoo.com
[2] *G. Green Institute for Electromagnetics Research, University of Nottingham, NG7 2RD, Nottingham, UK*
[3] *Institute of Photonics and Electronics AS CR, v.v.i. 182 51 Prague 8, Czech Republic*

Summary

Although comprehensive microcavity laser models try to account for several physical mechanisms such as transport of carriers, heating, and optical confinement, a considerable amount of useful information can be obtained if all non-electromagnetic effects are neglected, and the optical modes are viewed as eigensolutions of linear Maxwell equations.

Until recently, linear modelling of microdisk and other microcavity lasers has implied exclusively the calculation of the natural modes of the *passive* open dielectric resonators. Mathematically this means solving the time-harmonic Maxwell eigenvalue problem with the outgoing-wave radiation condition at infinity for the complex-valued natural frequencies, *k*. These eigenvalues form a *discrete* set and can be numbered, say, by using the index *s*. Then the modes with the largest Q-factors, $Q_s = \mathrm{Re}\, k_s / 2|\mathrm{Im}\, k_s|$, are associated with the lasing.

However, the lasing phenomenon is not addressed directly through the Q-factor – neither the presence of active region, nor the specific value of material gain that is needed to force a mode to become lasing is included in the formulation. Therefore in [1] we have formulated the Lasing Eigenvalue Problem (LEP) in which we introduce macroscopic gain, γ, as the active imaginary part of the complex-valued refractive index, $\nu = \alpha - i\gamma$, $\alpha, \gamma > 0$ assigned to the active region and look for the real-valued pairs of (k_s, γ_s) as eigenvalues. We emphasize that the LEP and Q-factor problems cannot be reduced to each other by transformations and changes of variables.

Tailoring of the active region shape can be an efficient tool for the threshold control and manipulation, while keeping the emission frequency essentially untouched. The latter is true so far as the gain-induced contrast in the cavity is small, which is valid for the low-threshold modes such as whispering-gallery (WG) ones or those confined using distributed Bragg reflectors (DBRs) [1,2].

We present several numerical examples demonstrating the nontrivial interplay between passive and active parts of the laser cavities in their competition for the mode field, even in the simplest configurations such as 1-D DBR-equipped cavity with a quantum well and an active-disk microcavity inside an annular DBR. Applying the Optical Theorem to the lasing mode field, we derive expressions that provide a rigorous definition of the mode volume and the mode active-region overlap factor – this, in fact, bridges the gap between the Maxwell theory and the cavity quantum electrodynamics, where these two quantities are widely used. Our results indicate that, if the material mode threshold is small, say $\gamma_s < 10^{-2}$, then this quantity and the overlap factor behave as inverse values of each other while the mode volume and radiation loss are almost constant. In such a case, we have found that approximate identity holds true: $\gamma_s = (\Gamma_s^{(0)} Q_s^{(0)})^{-1} + O(\gamma_s^2, \mathrm{Im}^2\, k_s)$, where the mode overlap coefficient $\Gamma_s^{(0)}$ and the Q-factor $Q_s^{(0)}$ are the values calculated using the optical field expressions neglecting the presence of γ_s or $\mathrm{Im}\, k_s$, respectively.

References

[1] E.I. Smotrova, A.I. Nosich, *Optical and Quantum Electronics*, **36**, 213-221 (2004)
[2] V.O. Byelobrov, A.I. Nosich, *Optical and Quantum Electronics* **39**, 927-937 (2007)

Deeply inside tunable CROW delay lines

A. Melloni[1], F. Morichetti[1,2], A. Canciamilla[1], C. Ferrari[1]
[1] *Dipartimento di Elettronica e Informazione, Politecnico di Milano*
Via Ponzio 34/5, 20133 Milano, Italy
[2] *CORECOM, via G. Colombo 81, 20133 Milano, Italy*
E-Mail: melloni@elet.polimi.it

A chip-scale continuously tunable delay-line is presented and both experimental and numerical results are discussed. The focus of the work is mainly on the open issues, involving both theoretical and practical aspects to take care of or still to solve.

Summary

A slow-wave coupled-resonator optical waveguide (CROW) has been successfully employed to realize a tunable delay line able to introduce a continuously controllable delay of several bits on optical signals modulated at several Gbit/s [1]. Experimental results obtained with thermally activated rings fabricated in 4.5% index contrast silicon oxynitride (SiON) technology demonstrated a continuously tuneable fractional delay from 0 to 8 bits at 10 Gbit/s (overall delay 800 ps) and 25 Gbit/s (320 ps). Thanks to the high storage efficiency, exceeding 1 bit/RR, the device reconfiguration can be easily handled and the device footprint is below 7 mm^2. System performance and signal degradation were also investigated, showing a fractional loss below 1 dB/bit and error-free operation (BER < 10^{-9}) at 10 Gbit/s for fractional delays up to 3 bits.

This device is an excellent demonstration of the optimal trade-off achieved between all the variables and parameters of the structure and the synergy between the optical circuit, the technology constraint and the management of the reconfigurability. There are several critical points to tackle with and to optimize: the choice of the technology and the architecture, the impedance matching (or apodization) impacts on backreflections, the slow down factor should be high enough to increase the storage efficiency but not too high to reduce the technological sensitivity to tolerances, the limitations imposed by the index contrast, mainly the minimum bending radius, the effect of waveguide roughness, the impact of coupling coefficient disorder and phase disorder, the tuning mechanism and its management, thermal cross-talk and so on. Moreover, one has to face with waveguide losses, chromatic dispersion and impedance matching, the three main limiting factor of the ultimate performances of this architecture, and find the right trade-off to achieve acceptable system performance.

In the talk we will highlight the main features and limits, the open issues and the tricks for proper operation with a brief overview on the possible applications.

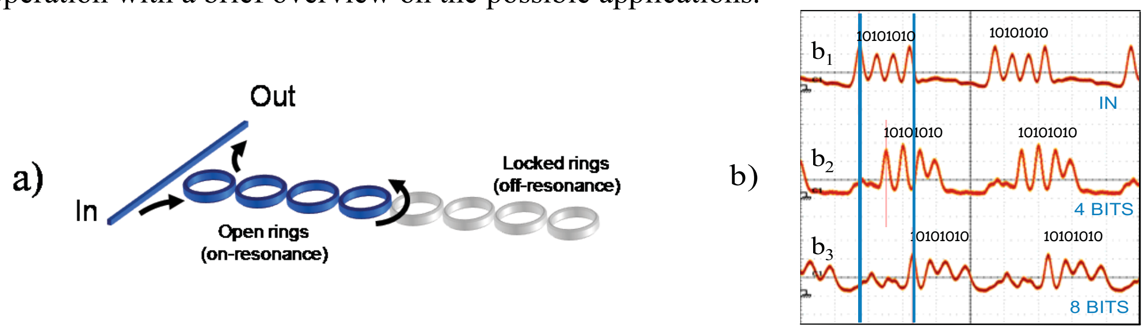

Fig. 1. a) Schematic of a tunable CROW delay line; b) Time traces of the delayed 25 Gbit/s sequence 10101010-00000000 at the output of the CROW delay line: (b_1) zero delay, (b_2) 4-bit 160 ps delay and (b_3) 8-bit 320 ps delay.

References

[1] F. Morichetti et al., "*A reconfigurable architecture for continuously variable optical slow-wave delay lines*," Opt. Express **15**, 17273, Dec. 2007.

Closed-loop Modeling of Silicon Nanophotonics: From Design to Fabrication and Back Again

(invited paper)

Wim Bogaerts, Lieven Vanholme, Paul Bradt and Peter Bienstman
Ghent University, Department of Information Technology, Sint-Pietersnieuwstraat 41, 9000 Gent, Belgium
Wim.Bogaerts@UGent.be

We present a system for closed-loop modeling of silicon nanophotonics, where the properties of the fabrication process are taken into account in the design and optimization of nanophotonic components.

Summary

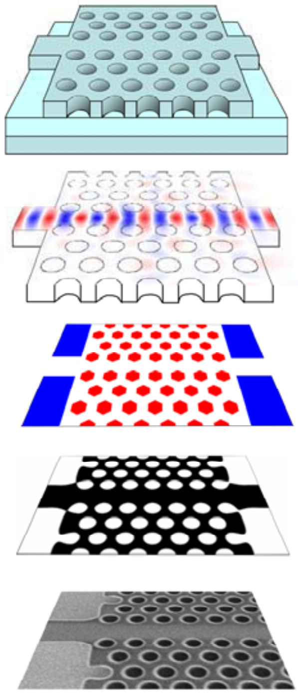

When fabricating nanophotonic components, several aspects come into play. There is the detailed electromagnetic simulation of the component, the generation of the mask layout, and the properties of the fabrication process which make that the fabricated structure is often not exactly identical to the one that was originally designed. We present a framework where all of these aspects are integrated in such a way that the properties of the fabrication can be taken into account during the design phase.
The framework is held together with Python, a flexible programming language especially suitable for scientific applications [1]. Currently, the framework has a python interface to an electromagnetic simulator based on eigenmode expansion [2], a library for mask layout design, and a simulator for optical projection lithography. This last library is calibrated against actual fabrication processes using the 248nm and 193nm steppers used by IMEC for the fabrication of nanophotonic waveguide circuits [3].
In addition, python makes it exceptionally easy to include new interfaces to existing software tools (commercial and free), including advanced optimization routines such as genetic algorithms.
To demonstrate this framework we optimize an in-line DBR reflector in a photonic wire. A design with rectangular grating teeth will be deformed by the optical lithography, because for submicron features the lithography acts as a spatial low-pass filter, rounding sharp corners. Therefore, while an optimization routine on the rectangular design might yield an efficient component, the actual fabricated structure would be very different. Thus, we included the lithography in the optimization loop. Starting from a mask design, we perform a virtual lithography, and the resulting pattern is fed to CAMFR. The result is used to modify the mask layout, taking into account design rules such as minimal spacing. This whole cycle is then managed by an optimization routine, in this case a relatively simple steepest descent method.

References

[1] Special issue on Python of *Computing in Science & Engineering*, vol. 9(3) (2007)
[2] P. Bienstman and R. Baets, *Opt. Quantum. Electron* 33(4/5), p.327 (2001)
[3] W. Bogaerts et al. *J. Lightwave Technol.* 23(1), p.401 (2005)

Design of a Waveguide-Type Polarization Beam Splitter Incorporating Trenches Filled with Low-Refractive Index Material

Jiro Ito[1], Kenji Iwamoto[1] and Hiroyuki Tsuda[1]

[1]Department of Electronics and Electrical Engineering, KEIO University
jiro-i.23@tsud.elec.keio.ac.jp

Abstract. *We propose a waveguide-type polarization beam splitter (PBS) incorporating trenches filled with low-refractive index material, which exhibits a low insertion loss of less than 2 dB and a high polarization extinction ratio of more than 20 dB over a wide wavelength range from 1525-1630 nm.*

Introduction

The concept of a waveguide-type polarization beam splitter (PBS) is very promising because such a device could be easily integrated with other circuits. A silica-based waveguide-type PBS which utilizes waveguide birefringence and which is dependent on the core-width has been reported [1]. This device exhibited low-insertion loss and a high polarization extinction ratio. Silica-based waveguides have been very popular in the field of passive optical components because they offer low fiber-to-chip coupling losses and low propagation losses. However, these devices require the use of long waveguide arms because the waveguide birefringence is low. PBS devices fabricated using silicon-on-insulator waveguides have also been studied [2]. Since they feature large waveguide birefringence which depends on the rib width, the size of these devices can be more compact than silica-based designs. However, it is difficult to achieve a high polarization extinction ratio and a low coupling loss between single mode fibers without mode-size conversion when using a silicon-based waveguide-type PBS.

We have proposed and fabricated a compact silica-based PBS [3] by including trenches filled with low-refractive index material with a refractive index of 1.3335. This device exhibited a high polarization extinction ratio around the center wavelength. In this paper, we have optimized such a PBS structure which incorporates trenches in order to obtain a high polarization extinction ratio over a wide wavelength range, and we have confirmed the transmission characteristics of the PBS that we designed by using simulations based on the beam propagation method (BPM).

Design of PBS

Our proposed PBS structure with trenches filled with low-refractive index material is shown in Fig. 1. It has a Mach-Zehnder interferometer (MZI) configuration, and consists of two 3-dB couplers and two waveguide arms with trenches of different lengths. We used multimode interference (MMI) devices as a 3-dB coupler, and the trenches were introduced along both sides of the core. Because of the local laterally-enhanced optical confinement, the propagation constants of the embedded waveguides containing low-refractive index material strongly depend on the polarization. Therefore, the size of such a PBS can be reduced. To balance the light intensities in both waveguide arms, we inserted trenches into both of them. The straight trenches were inserted gradually into the core to reduce the junction loss between the conventional waveguide and the low-refractive index material embedded waveguide.

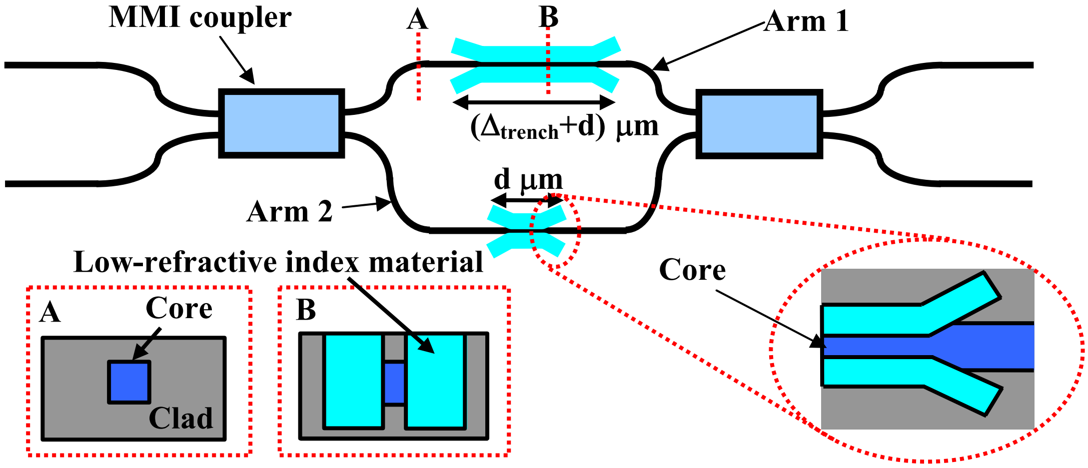

Fig. 1. Schematic configuration of our proposed PBS

The wavelength dependences of the effective refractive indices for both the conventional waveguides and the low-refractive index material embedded waveguides are shown in Fig. 2. The value of the difference in optical pass-length between the two waveguide arms *Δ(nL)* changes according to the wavelength because the effective refractive index of a low-refractive index material embedded waveguide depends on the wavelength. Therefore, we can't obtain a high polarization extinction ratio over a broad wavelength range with this configuration.

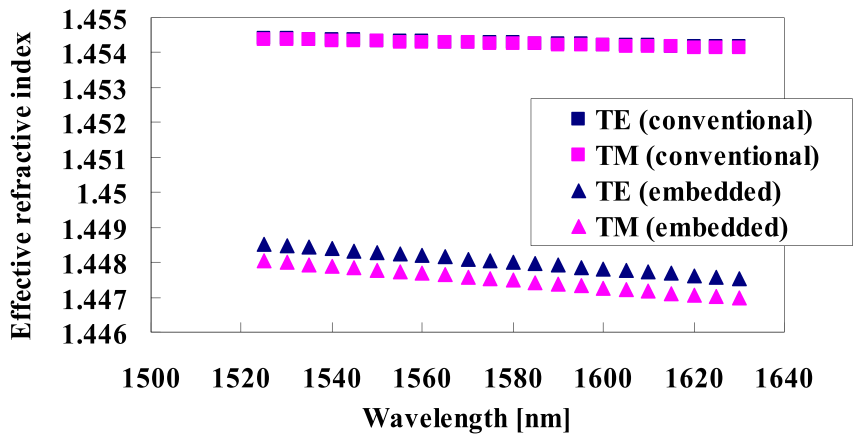

Fig. 2. Wavelength dependences of the effective refractive indices of both conventional waveguides and low-refractive index material embedded waveguides with mesa widths of 3.0 μm.

We solved this problem by taking the wavelength dependence of the effective refractive index into account. From Fig. 2, we can assume that the wavelength dependence of the effective refractive index decreases almost linearly as a function of wavelength. The conditions in which the PBS has a broad bandwidth are expressed by

$$n1_{TE}(\lambda)(\Delta_{trench}+\Delta L)-n2_{TE}(\lambda)\Delta_{trench}=m\lambda, \quad (1)$$

$$n1_{TM}(\lambda)(\Delta_{trench}+\Delta L)-n2_{TM}(\lambda)\Delta_{trench}=\left(n+\frac{1}{2}\right)\lambda, \quad (2)$$

where $n1_{TE(TM)}$ and $n2_{TE(TM)}$ respectively express the effective refractive indices of TE(TM) mode for a conventional waveguide and a low-refractive index material embedded waveguide (whose values depend on the wavelength), Δ_{trench} is the difference in length between the trenches in the two waveguide arms, ΔL is the difference in length between the two waveguide arms, λ is the wavelength of the incident light, and m and n are integers. From (1) and (2), the optimum values for Δ_{trench} and ΔL can be determined. However, it is difficult to set the parameters in order to completely satisfy (1) in relation to (2) because the slopes of the effective refractive indices of TE and TM mode as a function of wavelength for a low-refractive index material embedded waveguide do not share the same values. Although we can adjust these by changing the mesa width, they are not independently controllable. Therefore, we obtained a wide bandwidth by making a small sacrifice in terms of the extinction ratio by designing the parameters such that the values of m and n almost become integers.

Simulation results

We optimized the parameters and confirmed the characteristics of the wavelength dependence by using a two dimensional (2D) beam propagation method (BPM). ΔL was 3.59 µm. The mesa width was 3 µm. The birefringence of a waveguide fabricated using trenches filled with low-refractive index material is shown in Fig. 3, and it can be seen that it depends strongly on the mesa width. Smaller mesa widths exhibit larger birefringence; therefore, this enables the use of shorter waveguide arms. However, the difference between the slopes of the effective refractive indices between TE and TM modes as a function of wavelength for a low-refractive index embedded waveguide becomes larger and therefore narrows the working bandwidth. Moreover, narrow mesa widths are difficult to fabricate. Therefore, we determined that the mesa width should be 3 µm, Δ_{trench} was 764 µm, and the straight length of the shorter trench, d was 10 µm. The length of the longer trench, including the taper parts, was less than 1130 µm. The transmission characteristics are shown in Fig. 4.

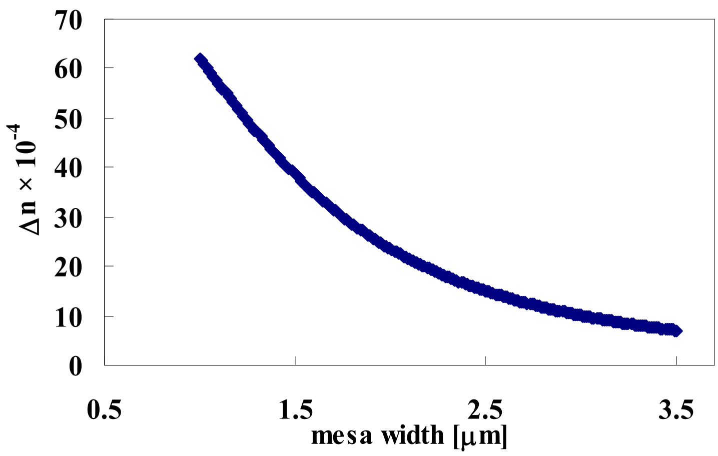

Fig. 3. Birefringence of a low-refractive index material embedded waveguide as a function of mesa width.

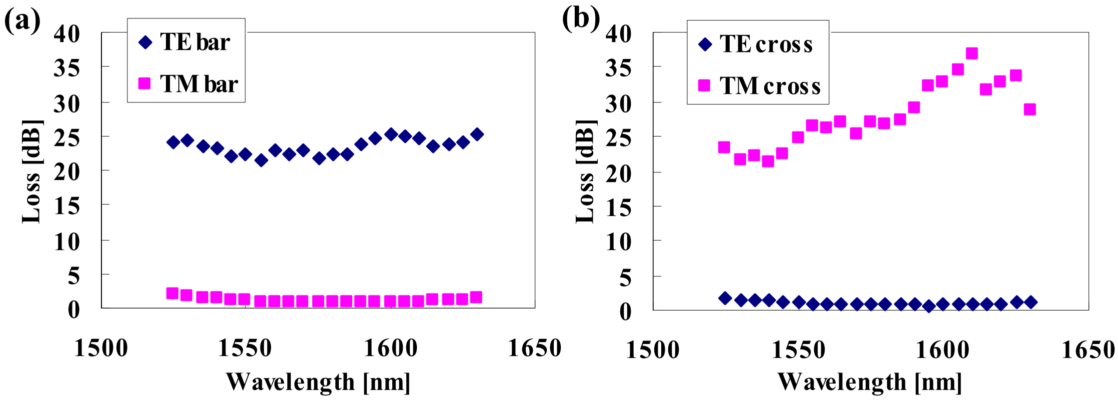

Fig. 4. Wavelength dependence of transmission characteristics.
(a) through-path. (b) cross-path.

The insertion loss was less than 2 dB. The polarization extinction ratio was greater than -20 dB over a wide wavelength range from 1525-1630 nm for both polarizations. Although the trench length becomes longer, higher polarization extinction ratios can be obtained by widening the mesa width.

Conclusion

We improved the wavelength-dependence of a PBS incorporating trenches filled with low-refractive index material by taking the wavelength-dependence of the effective refractive index into account. We confirmed that a PBS fabricated using our proposed design method exhibited a low insertion loss of less than 2 dB and a high polarization extinction ratio of more than 20 dB over a wide wavelength range from 1525 to 1630 nm by making 2D BPM simulations.

References

[1] Y. Hashizume, R. Kasahara, T. Saida, Y. Inoue and M. Okano, “Integrated polarization beam splitter using waveguide birefringence dependence on waveguide core width,” Electron. Lett., vol. 25, no. 25, pp. 1517-1518, 2001.

[2] T. K. Liang and H. K. Tsang, “Integrated polarization beam splitter in high index contrast silicon-on-insulator waveguides,” IEEE Photon. Technol. Lett., vol. 17, no. 2, pp. 393-395, 2005.

[3] J. Ito, Y. Ikuma, K. Iwamoto and H. Tsuda, “Compact polarization beam splitter using trenches filled with low-refractive index material,” in Proceedings of the APLS 2008, 2008, pp.181.

Temperature Insensitive Silicon Slot Waveguides with Air Slot

Ken Kashiwagi[1], Shinji Yamashita[1], Katsunari Okamoto[2], S. J. Ben Yoo[2]

[1]Department of Electronic Engineering, Graduate School of Engineering, The University of Tokyo
kasiwagi@sagnac.t.u-tokyo.ac.jp
[2]Department of Electrical and Computer Engineering, University of California, Davis

Abstract. *We report numerical simulation about thermal stabilities of silicon slot waveguide. A polymer cladding, which has negative thermo-optic(TO) coefficient, was used to compensate positive TO coefficient of silicon and silicon-dioxide(SiO_2). We found athermal waveguide can be realized with air slot, and even with SiO_2 slot.*

Introduction

High index contrast waveguides are very attractive, with the advantage of small footprint and large nonlinearity due to their high optical density because of their sub-micron sized dimensions. Novel nonlinear devices have been proposed and demonstarated by using sub-micron sized silicon (Si) waveguides. Si has, however, high thermo-optic (TO) coefficient which is one magnitude larger than that of silicon-dioxide (SiO_2) which is utilized for various photonic applications in industry. Very accurate and power consumable temperature controller should be used to stabilize the device performance, especially the devices which have wavelength dependent characteristics, such as arrayed waveguide gratings (AWGs), ring resonators, Bragg gratings, Mach-Zehnder interferometers.

Recently, a novel design of high index contrast waveguide, called slot waveguide, have been proposed[1],[2]. Since it can confine a light in low index region, we can employ various materials as optical nonlinear materials by filling the slots with them. High optical intensity in the slot enhances their optical nonlinearity. One of the advantages of the slot waveguides is the design flexibility. Slot width can be another design degree of freedom additional to the height and width of the waveguides. However, when we use Si as a host material of a waveguide, thermal stability should be suffered from the large TO coefficient of Si. A thermally stable ring resonator based on Si slot waveguide was proposed and experimentally demonstrated using a polymer as over cladding and slot region[3]. In this paper, we investigate on thermal stability of Si slot waveguides focusing on slot materials. We found that filling slot regions with polymer materials is not necessary to achieve temperature insensitive slot waveguides.

Athermal silicon slot waveguides with polymer slot

Fig. 1 shows a schematic cross-sectional structure of a slot waveguide. The slot waveguide has a slot region which is embedded with two high index regions, and the structure is surrounded by under cladding and over cladding which have lower refractive index comparing to that of high index region. A material of slot region can be the same with those of over cladding or under cladding as far as the material has lower refractive index comparing to that of high index regions. In this paper, we assume symmetric waveguides, or two high index regions have the same width.

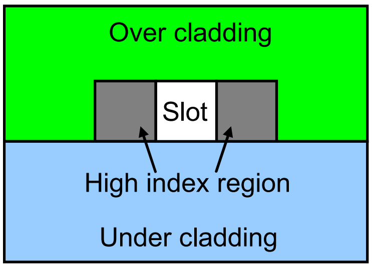

Fig. 1 Cross-sectional schematic structure of a slot waveguide

In this section, we assume slot waveguides which consist of SiO_2 under cladding, Si high index region, and slot region and over cladding polymethyl methacrylate (PMMA). In the simulation, the refractive indecies of Si, SiO_2 and PMMA were 3.48, 1.46 and 1.481[4], and their TO coefficients were 1.84×10^{-4}, 1.0×10^{-5} and -1.0×10^{-4}, respectively. We fixed the waveguide heights as 250 nm, and calculated effective refractive index (n_{eff}) with changing Si and slot width using finite different method based modesolver. Only TE mode was considered in this paper since light confinement in the slot region appears only in TE modes.

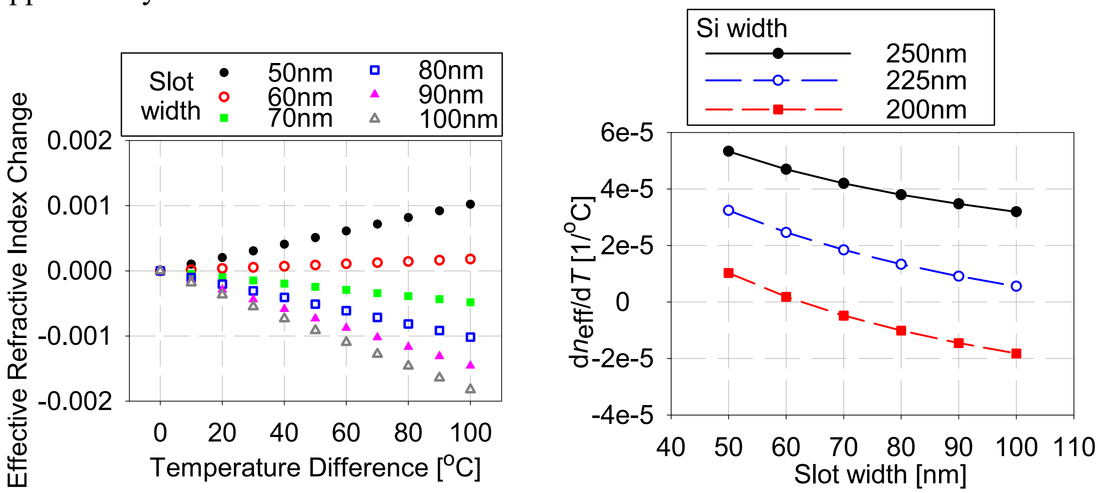

Fig. 2(a) Simulated temperature dependence of effective indecies with several slot width

(b) Simulated effective index change slope as a function of slot width, 250nm height

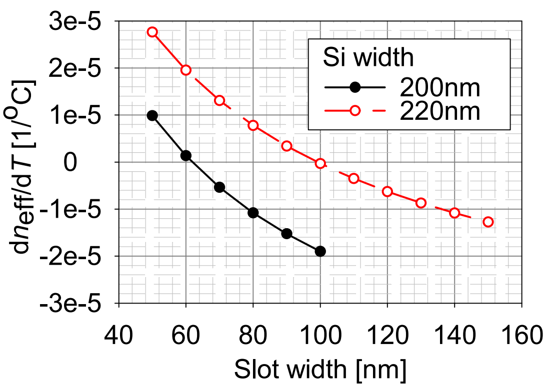

Fig. 3 Temperature insensitivity design with different Si width without changing waveguide heights (250nm)

Fig. 2(a) and (b) show the simulated temperature dependence of effective index of the waveguide with several slot widths and the slot width dependence of effective index slope (dn_{eff}/dT) with three different Si widths, respectively. In the case that a waveguide is temperature independent, effective refractive index change stay zero at any temperature. Widening slot width decreased dn_{eff}/dT from positive to negative slope shown in Fig. 2(a). A zero-crossing point in Fig. 2(b) are the temperature insensitive waveguide structure, and ~62 nm slot width was the optimum for Si width of 200 nm.
Temperature independence can be achieved in various waveguide designs without changing their heights. Fig. 3 shows temperature dependence of the Si slot waveguides with two different Si widths. Waveguide heights were 250 nm. 100 nm slot width was the optimum size for Si slot waveguides whose Si width is 220 nm.

Athermal silicon slot waveguides with air slot

In practical fabrication process, it is difficult to fill the slot region with a material, such as PMMA. However, temperature insensitive slot waveguides can be realized without filling any materials in the slots, or with air slots. Fig. 4 shows the effective index slope of slot waveguides as a function of slot width. The refractive index and TO coefficient of air were assumed as 1.0 and 0, respectively. The waveguide heights were fixed at 250nm. Under cladding were SiO_2. For the case of Si width of 200nm and 220nm, athermal Si slot waveguides could be achieved with the slot width of ~65nm and ~125nm, respectively.
The refractive index of air is much smaller than that of PMMA and the light is much highly confined inside the slot region. Since the TO coefficient of air is zero, temperature insensitivity could be realized with air slot, covering slot structures was sufficient to compensate the TO coefficient of Si and SiO_2.

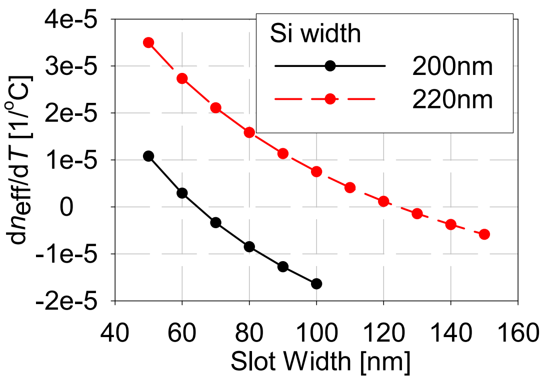

Fig. 4 Effective refractive index slopes of Si slot waveguides with air slots, 250nm heights, TE modes

Athermal silicon slot waveguides with SiO_2 slot

We reported the athermal Si slot waveguide filled with air in previous section. While the waveguides are easier to fabricate than the PMMA slot waveguides, we cannot utilize the advantage of slot waveguides, enhancement of optical nonlinearity due to the high optical concentration inside the slots. To use the advantage, the slots must be filled with a material. In this section, we report simulation results of athermal Si slot waveguides which had SiO_2 slot and PMMA over cladding.

The simulation results of Si slot waveguides with SiO_2 slots are shown in Fig. 5. Their heights were 250nm, same as the waveguides in the previous sections. Under cladding was SiO_2. For the case of Si width of 200nm and 210nm, athermal Si slot waveguides could be achieved with the slot width of ~103 nm and ~145 nm, respectively.

The SiO_2 slot itself cannot compensate the positive TO coefficients of Si and under cladding SiO_2. For this reason, the wider slot and narrower Si width were necessary than those of PMMA and air slot. Narrow Si width and wide slot width decrease the optical component inside the Si region. This permits the compensation of positive TO coefficient mainly comes form Si part, by PMMA over cladding. By using a polymer material which has larger negative TO coefficient than that of PMMA, athermal slot waveguides can be realized by narrower slot and wider Si width.

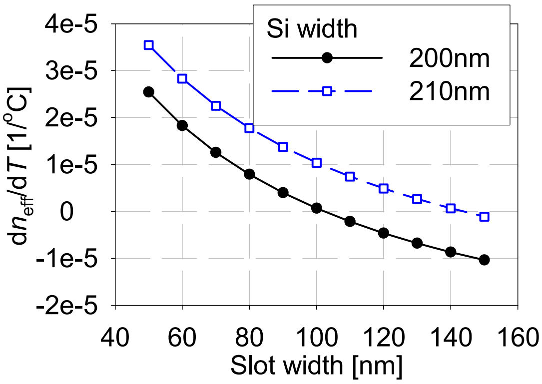

Fig. 5 Effective refractive index slopes of Si slot waveguides with SiO_2 slots, 250nm heights, TE modes

Summary

We reported the numerical simulation of temperature insensitive Si slot waveguide to achieve thermally stable optical devices. The positive TO coefficients of Si and SiO_2 can be compensated using PMMA, whose TO coefficient is negative, as an over cladding material of Si slot waveguides. We showed temperature insensitive design of Si slot waveguides whose slot regions were filled with PMMA. Temperature insensitive waveguides with air slots were proposed for easy fabrication. SiO_2 was employed as an example of slot material to use the advantage of slot waveguides, the enhancement of optical nonlinearity.

References

[1] Vilson R. Almeida, Qianfan Xu, Carlos A. Barrios, and Michal Lipson, “Guiding and confining light in void nanostructure, ” Optics Letters, vol. 29, pp.1209-1211, 2004.

[2] Qianfan Xu, Vilson R. Almeida, Roberto R. Panepucci, and Michal Lipson, “Experimental demonstration of guiding and confining light in nanometer-size low-refractive-index material, ” Optics Letters, vol. 29, pp.1626-1628, 2004.

[3] Jong-Moo Lee, Duk-Jun Kim, Gwan-Ha Kim, O-Kyun Kwon, Kap-Joong Kim, and Gyungock Kim, “Controlling temperature dependence of silicon waveguide using slot structure,” Optics Express, vol. 16, pp.1645-1652, 2008.

[4] Y. Kokubun, S. Yoneda and S. Matsuura, “Temperature-insensitive optical filter at 1.55μm wavelength using a silica-based athermal waveguide,” Electronics Letters, vol. 34, pp.367-369, 1998.

A Demultiplexer with Blazed Waveguide Sidewall Grating

A. Delâge[1], P.J. Bock[1,2], P Cheben[1], J.H. Schmid[1], D.-X. Xu[1], S. Janz[1], and T.J. Hall[2]

[1]*Institute for Microstructural Sciences, National Research Council Canada, Ottawa, K1A 0R6 Canada*
Andre.Delage@nrc-cnrc.gc.ca
[2]*University of Ottawa, Centre for Research in Photonics, Ottawa, Canada*

We propose a new type of waveguide diffraction grating demultiplexer with a very small footprint, designed for the silicon-on-insulator platform.

Summary

Integrated waveguide de-multiplexers as AWG's and etched echelle gratings (EEG) have been designed in the last decade to accommodate the specifications of telecommunication for narrow channel spacing. Now, with new applications with relaxed specifications (such as FTTH, optical sensing, etc.), new designs have emerged for compact coarse WDM devices. Among them we have been interested in the performance of the dispersive waveguide grating recently published by Hao et al [1], and we propose the use a sub-wavelength antireflection structure to improve its design.

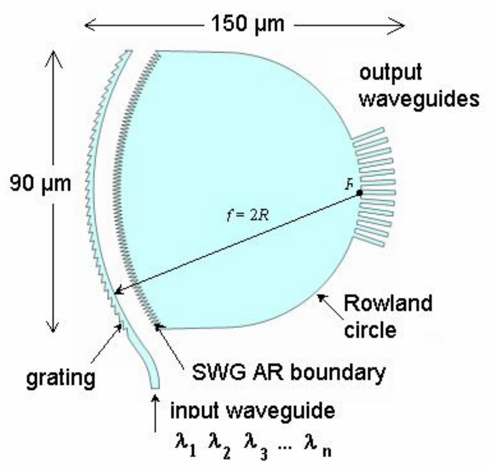

Fig 1: Waveguide grating demultiplexer

The device is presented in Fig. 1; it consists essentially of a curved waveguide on the left of the picture, in which the external wall is etched as a first order grating in order to diffract the light, originally in the waveguide, towards the output waveguides at the right. The arrangement is based on a Rowland circle (RC) configuration, with the radius of curvature of the waveguide equal to twice the Rowland radius. The focus point of the diffracted light is expected to lie on the RC in front of the output waveguides. The light is confined in the vertical direction, justifying the 2D simulations that are used to describe the device. To be efficient, this demultiplexer should also include an anti-reflection boundary that could be provided by a sub-wavelength grating as described in reference [2]. Contrary to AWG and EEG, the size of the focused spot in front of the output waveguides is not related to the input waveguide nor the grating waveguide width or mode profile; but rather to the total span of the grating and to the apodisation brought to the shape of the grating. This paper will present the properties of this device and its performance as a coarse wavelength de/multiplexer.

These properties have been studied by two different approaches: a two dimensional Kirchhoff-Huygens diffraction integral and by FDTD to account for more specific details. The first method is particularly adequate to establish the fundamental properties and limits of an ideal device. For R=70 um in silicon, it indicates the possibility of more than 10 channels separated by 25 nm with cross-talk of -40 dB. More realistic results have been then obtained with a 2D-FDTD technique that includes the grating shape and the AR-layer. This model uses a straight waveguide on a 100 μm × 3 μm calculation window from which the far-field is calculated using a standard Fourier transform. Our present design produces a 15 channel configuration with 25 nm spacing with only a supplementary penalty of –10 dB in cross-talk compared to the ideal case.

References

[1] Y. Hao, Y. Wu, J. Yang, X. Jiang and M. Wang, *Opt. Express* **14**, 8630-8637 (2006).
[2] J. H. Schmid, P. Cheben, S. Janz, J. Lapointe, E. Post and D.-X. Xu, *Opt. Lett*. **32**, 1794-1796 (2007).

Light Transmission Through Slits and Holes Using Waveguide Modes

J.M. Brok[1], O.T.A. Janssen[1] and H.P. Urbach[1]
[1]*Delft University of Technology, Optics Research Group, P.O. Box 5046, 2600 GA Delft, The Netherlands*
h.p.urbach@tudelft.nl

We study the transmission of light through slits and holes in a metal plate. Plasmon excitation and its influence on the transmission will be discussed and a waveguide model will be treated.

Summary

A plasmon wave is an electromagnetic surface wave which propagates parallel to the interface between a metal and a dielectric. The electric field of the plasmon is perpendicular to the surface while its magnetic field is perpendicular to the the plane through the normal on the surface and the real part of the wave number. When the plate is illuminated by a p-polarized plane wave at perpendicular incidence, the magnetic field of the plasmon scattered by the slit is parallel to the slit, i.e. parallel to the magnetic field of the incident field. It was found [1] that, provided the width of the slit is smaller than the wavelength, the phase difference between the magnetic fields of the plasmon wave and the incident field at the center of the slit is π. With this property one can explain for the case of two parallel slits the modulation of the transmission as function of the distance between the slits. Furthermore, by using the π phase difference, a grating structure consisting of grooves can be designed for which the transmission though the slit at the center of the grating is more than 90 times the energy that is incident on the slit [2].

We also consider the transmission through several rectangular holes using wave guide theory [3], [4]. The metal is considered perfectly conducting. In that case the plasmon surface wave becomes a plane wave which propagates parallel to the surface. The transmission of a Laguerre-Gaussian beam with phase singularity at the center through a rectangular hole will be explained.

References

[1] O.T.A. Janssen, H.P. Urbach and G. 't Hooft, *Optics Express*, **14**, 11823-11833 (2006).
[2] O.T.A. Janssen, H.P. Urbach and G. 't Hooft, *Physical Review Letters* **99**, 043902 (2007).
[3] J.M. Brok and H.P. Urbach *J. Mod. Optics*, **51**, 2059-2077 (2004).
[4] J.M. Brok and H.P. Urbach, *Optics Express*, **14**, 2552-2572 (2006).

Fig. 1. The amplitude of the **scattered** magnetic field when a metal plate with two parallel slits of widths equal to a quarter of the wavelength, is illuminated by a p-polarized plane wave from the top. At the left the distance between the slits is such that a minimum of transmission occurs, at the right the distance gives a maximum.

Analysis of Triangular Metal Wedge Surface-Plasmon-Polariton Waveguides Using an Imaginary-Distance Finite-Element Beam Propagation Method

Hung-chun Chang, Chang-Chun Chung, Han-Chih Yeh, Chan-Huan Peng, and Bang-Yan Lin
Department of Electrical Engineering, Graduate Institute of Photonics and Optoelectronics, and Graduate Institute of Communication Engineering, National Taiwan University, Taipei, Taiwan 106-17, R.O.C.
hcchang@cc.ee.ntu.edu.tw

Surface-plasmon-polariton modes on triangular metal wedge waveguides are investigated in detail using a finite element analysis with curvilinear hybrid edge/nodal elements by considering different wedge angles and wavelengths. Not only wedges rounded with an arc radius but also the ideal sharp wedges are analyzed.

Summary

Metal waveguides of different cross-sectional shapes for confining surface-plasmon-polariton (SPP) modes in the transverse plane have recently been investigated experimentally and theoretically. Due to their highly localized field distribution and vector-mode characteristics at the metal-dielectric interfaces, the SPP waveguides are more difficult to analyze compared to conventional optical waveguides for obtaining accurate complex propagation constants. In this paper we investigate modal characteristics of triangular metal wedge waveguides [1]. Such structures have been recently analyzed in detail based on the finite element method (FEM) [2]. The FEM has the advantages of better treating material interface boundary conditions through adaptive mesh distribution. Here we employ a full-vectorial imaginary-distance finite-element beam propagation method (ID-FE-BPM) based on curvilinear hybrid edge/nodal elements with triangular shape and incorporated with perfectly matched layer (PML) absorbing boundary conditions (ABCs) as the mode solver [3, 4] for calculating the real and imaginary parts of the modal propagation constants from which the effective index and the loss in dB/mm can be derived respectively. We consider both the sharp and rounded air/silver wedges, as depicted in Figs. 1(a) and 1(b), respectively, where $2r$ in Fig. 1(b) is the diameter of the tip arc. Due to the geometrical symmetry, we can consider only half of the cross-section with the symmetry plane replaced with a perfect magnetic conductor (PMC), as indicated in Fig. 1(c), where PML regions of thickness 1 μm are placed around the three sides. We examine the effect of different values of the tip arc radius, including the ideal sharp-wedge case (zero arc radius) not shown in [2], at 0.633-μm and 1.55-μm wavelengths. It is observed that the ideal sharp-wedge structures obviously possess better mode confinement near the tip and significantly larger losses.

References

[1] D. F. P. Pile, T. Ogawa, D. K. Gramotnev, T. Okamoto, M. Haraguchi, M. Fukui, and S. Matsuo, Appl. Phys. Lett. **87**, 061106 (2005).
[2] M. Yan and M. Qiu, J. Opt. Soc. Am. B **24**, 2333-2342 (2007).
[3] K. Saitoh and M. Koshiba, IEEE J. Quantum Electron. **38**, 927-933 (2002).
[4] S. M. Hsu, H. J. Chen, and H. C. Chang, Proc. SPIE **5623**, 316-324 (2005).

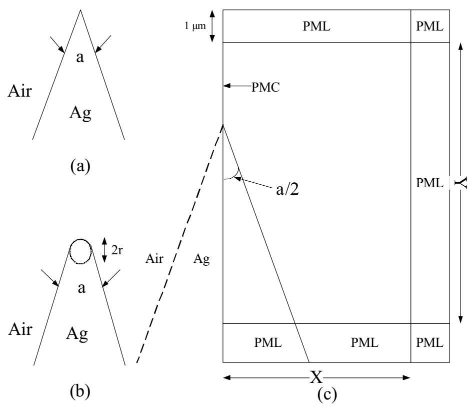

Fig. 1. (a) Sharp air/silver wedge. (b) Rounded air/silver wedge. (b) Schematic of the computational domain with PML regions.

Empirical Relations for the Propagation Characteristics of Integrated Optical Diffused Channel Waveguides

Samit Barai[1,2] and Anurag Sharma[1]

[1] *Physics Department, Indian Institute of Technology Delhi, New Delhi – 110016, India*

asharma@physics.iitd.ac.in

[2] *KLA Tencor Software India Pvt. Ltd., Kandanchavadi, Chennai – 600096, India*

Empirical relations for the propagation characteristics of the diffused channel waveguides have been developed. These are based on the evanescent secant-hyperbolic (ESH) field, which has earlier shown to have very good accuracy. As an application, the coupling length of a directional coupler has been obtained

Summary

We have shown earlier that the evanescent secant hyperbolic field profile, involving only two adjustable parameters, is a very good approximation for the mode of diffused channel waveguides [1,2]. We have developed empirical expressions for these field parameters in terms of the characteristics parameters of the waveguides with the commonly occurring refractive-index profiles, namely, Gaussian-Gaussian, Error function-Gaussian and Error function-exponential. The procedure adopted is that we first obtain the optimized values of the parameter using the variational method [1,2] and then use the least square-fitting procedure to obtain a judiciously chosen functional dependence of these parameters. As an example, we include here the empirical relation for the mode of waveguides with error function- Gaussian index profile:

$$\Psi(x,y)=\psi_x(x)\ \psi_y(y) \quad \text{with} \quad \psi_x(x)=\operatorname{sech}^{\delta}(x/a)\,;$$

$$\psi_y(y>0)=[1+W_c\sinh(y/D)\operatorname{sech}^{\tau}(y/D)] \quad \text{and}$$

$$\psi_y(y<0)=\exp(W_c y/D)$$

where, $b=\left(1.32514/\sqrt{r}\right)-1.57656+0.41271V-0.03803V^2$

$$\delta=-2.77890+1.45556r-0.37672r^2+1.26574V-0.09746V^2$$

$$\tau=3.12852-2.71429r+0.34709r^2+1.35839V-0.08386V^2$$

Here, $b=[(\beta/k_0)^2-n_s^2]/(2n_s\Delta n)$, r, diffusion width to depth ratio, $V=k_0D\sqrt{(2n_s\Delta n)}$, β is the propagation constant, $W_c=D(\beta^2-k_0^2n_c^2)^{1/2}$ n_s the substrate index, Δn is the peak index change and $k_0=2\pi/\lambda$; the cover is taken to be air ($n_c=1$). The obtained field profile for V = 3.0, n_s = 2.203, Δn = 0.03 and r = 1.5 is given in Fig. 1.

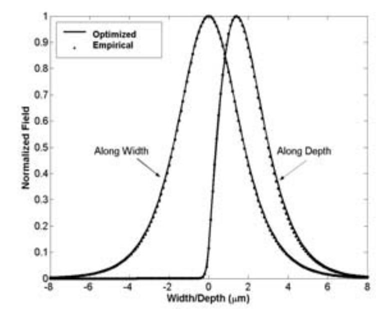

Fig. 1 Comparison of field profile obtained using empirical relation with the optimized field profile.

As an example of application, we have obtained the coupling length of a direction coupler made of two parallel waveguides with V = 2.0, n_s = 2.203, Δn = 0.03 and r = 1.875 using the empirical fields and the coupled mode theory. The variation of the coupling length with the separation distance (2*s*) is shown in Fig. 2, These results show that the empirical formulae can be used for estimating characteristics of directional couplers and similar devices. It is expected that these relations will help reduce device design cycle time.

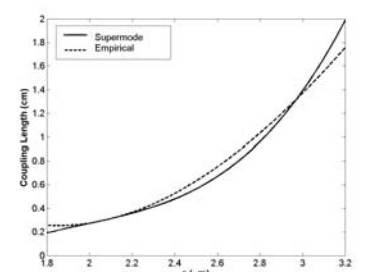

Fig. 2 Coupling length obtained using coupled-mode theory with field from empirical relations and that using super-mode theory with optimized ESH fields [2] as a function of *s*, half the waveguide separation

References:

[1] A. Sharma and P. Bindal, *IEEE J. Quantum Electron.* **29**, 150-153 (1993).

[2] A. Sharma and P. Bindal, *J. Opt. Soc. Am. A* **11**, 2244-2248 (1994).

A Semi-Vectorial Split-Step Non-Paraxial Method for Wave Propagation

Debjani Bhattacharya and Anurag Sharma
Physics Department, Indian Institute of Technology Delhi, New Delhi, India-110016
asharma@physics.iitd.ac.in

We present a semi-vectorial beam propagation method, which is based on the finite difference split step non-paraxial method. A new splitting procedure is used to take care of the continuity conditions at the interface.

Summary

In devices with high index contrast, the electric field becomes discontinuous and hence a semi-vectorial method is required. Earlier we had developed a 3D finite difference split-step non-paraxial (FDSSNP) method for scalar beam propagation [1]. Based on [1], a semi-vectorial method has now been developed. The semi-vectorial equation for the quasi-TE mode is

$$\frac{\partial^2 E_x}{\partial z^2}+\frac{\partial}{\partial x}\left[\frac{1}{n^2}\frac{\partial\left(n^2 E_x\right)}{\partial x}\right]+\frac{\partial^2 E_x}{\partial y^2}+k_0^2 n^2(x,y,z)E_x=0 \qquad (1)$$

where $n^2(x,y,z)$ is the refractive index variation of the guiding structure. The time dependence of the field is assumed to be $\exp(i\omega t)$ and $k_0=\omega/c$. In Eq.(1), n^2E_x and $(1/n^2)\partial(n^2E_x)/\partial x$ are continuous and thus the derivatives can be evaluated directly. A new method of splitting of operators is used to maintain the continuity conditions. A higher order series is used for the $\partial/\partial x$ operator and it is evaluated analytically. In other semi-vectorial methods [2, 3] the matrix elements for the second order derivative, at interfaces, are found analytically. But the continuity conditions are matched only till the third order derivative [2] or the fourth order derivative [3]. This gives very good accuracy for calculating modes, but for wide-angle propagation these may not be sufficient.

As an example we consider propagation of the fundamental mode through a square-core waveguide of core-width is $5\mu m$, n_{co}= 3.5 and n_{cl}=3.1693. We consider propagation in the *x-z* plane, at 30° with the *z*-axis. We use $\Delta x = 0.1443\mu m$ and $\Delta z = 0.0625\mu m$ at $\lambda = 1\mu m$. We compare three methods. First, the scalar 3D-FDSSNP is used for calculating the mode and for propagation. Second, the interface conditions [2,3] are used to evaluate the mode, while the propagation is scalar using 3D-FDSSNP. Finally we use our semi-vectorial method for propagation, while the mode is computed using the interface conditions [2,3]. The last method has very good accuracy (Fig. 1). It was seen with the FDSSNP method that higher order approximation for the derivatives required for the finite difference representation as the tilt angle increases; hence the three/five-point formula [2,3] is inadequate for wide-angle propagation. More examples will be presented at the workshop.

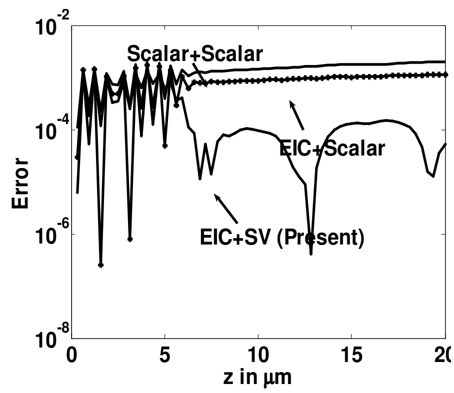

Fig.1: Error in propagation of the fundamental mode of a square core wave-guide, tilted at 30° to the z-axis.

References

[1] D. Bhattacharya and A. Sharma, *Opt. Quantum Electron*. **39**, 865-876 (2007). [also at OWTNM-2007].

[2] J. Yamauchi, *Propagating Beam Analysis of Optical Waveguides,* Research Studies Press, Baldock, Hertfordshire, England.(2003).

[3] R. Stoffer, H.J.W.M. Hoekstra, *Opt. and Quantum Electron*. **30,** 375-383 (1998).

A New Scheme for Splitting of Operators in the 3D Finite Difference Split-Step Non-Paraxial Method

Debjani Bhattacharya and Anurag Sharma
Physics Department, Indian Institute of Technology Delhi, New Delhi, India-110016
asharma@physics.iitd.ac.in

We present a new method for splitting of operators used in the 3D Finite Difference Split Step Non-paraxial (FDSSNP) method and discuss its advantages.

Summary

We have recently developed a finite difference split step non-paraxial method for 3D scalar wave propagation [1]. A single propagation step is split into three operators (Method-1, say):

$$\Phi(z+\Delta z) = \mathbf{PQP}\Phi(z) \tag{1}$$

where Φ is a column vector containing the field and its first order derivative with respect to z. The operator **P** represents propagation in a homogeneous medium of refractive index n_{ref} over a distance $\Delta z/2$, and involves the square root of $\partial^2/\partial x^2 + \partial^2/\partial y^2 + k_0^2 n_{ref}^2$. The operator **Q** represents the effect of the refractive index variation. In the new splitting method (Method-2), the $\partial^2/\partial x^2$ term or the $\partial^2/\partial y^2$ term or both (depending on the structure to be analyzed) are shifted to the matrix **Q** from matrix **P**. The evaluation of **P** and **Q** remains analytical as in [1]. This procedure has several advantages: **i)** In a semi-vectorial equation, Method-2 is necessary in order to keep the terms continuous; **ii)** Method-2 is more accurate even though $\partial^2/\partial x^2$ and $\partial^2/\partial y^2$ may not be operating simultaneously at the same x-y plane; **iii)** Method-2 is more efficient in terms of speed and memory requirement as it involves only sparse matrices; and **iv)** the PML boundary condition can be applied very easily to both the semi-vectorial and scalar methods, as now it requires only two extra diagonal matrix multiplications and the whole method is analytical.

As an example, we consider the scalar wave propagation of the fundamental mode of a square core waveguide tilted at 30° to the z-axis in the x-z plane [1]. We compare three cases: Method-1, Method-2 with $\partial^2/\partial x^2$ in **Q,** and Method-2 with both $\partial^2/\partial x^2$ and $\partial^2/\partial y^2$ in **Q**. Figure 1 shows that the second and the third cases have almost similar accuracy, which is much better than that in Method-1. As mentioned above, the new splitting procedure also reduces the propagation time significantly. For the example considered above, the typical computation times for single step propagation for the three cases, respectively, are 1.3009s, 0.2834s and 0.0451s. More examples further illustrating the advantages of the new splitting procedure will be presented at the Workshop.

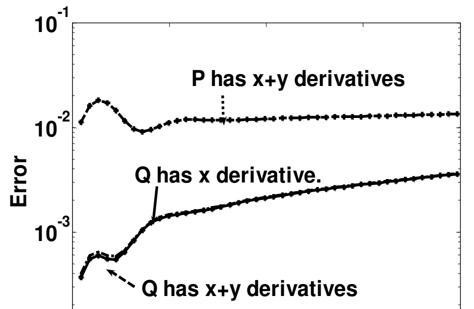

Fig. 1. Comparison of the various splitting methods.

Reference

[1] D. Bhattacharya and A. Sharma, *Opt. and Quantum Electron*. **39**, 865-876 (2007). [also at OWTNM 2007]

Artificial neural network radial basis functions approach for the optimization of photonic crystal fibres

S.S.A.Obayya , M.F.O.I. Hameed , P.Harrison, A.M.Nasr[1], M. I. Abou Elmaaty[1]
School of Electronic and Electrical Engineering , University of Leeds
TEL:. +44 113 343 2079, FAX.: +44 113 343 2032 email: S.S.A..OBAYYA@LEEDS.AC.UK
[1], Faculty of Engineering,University of Mansoura, Egypt.

Photonic crystal fibers (PCFs) [1] have been under intensive study as they offer design flexibility in controlling the modal properties. PCFs are usually formed by a central defect region surrounded by multiple air holes in a regular triangular lattice. These fibers have some extraordinary properties, such as wide single-mode wavelength range, unusual chromatic dispersion, and large effective mode area. With the growing interest in PCFs, accurate numerical modeling is mandatory to predict the light propagation properties in PCFs. Various methods have been developed for modal analysis of PCFs such as finite difference time domain, finite difference method (FDM) and finite element method (FEM). However, these numerical modal solution techniques are time consuming as they should rely on fine meshes for an acceptable accuracy. In this paper, an Artificial neural network approach based on radial basis function [2] is suggested as an alternate efficient and yet an accurate model for the prediction of various mode properties in PCF. Particularly, the use of radial basis function guarantees a very quick convergence and efficiency during ANN learning. Hence the computation efficiency has significantly improved. In addition, this approach enables us to calculate the propagation properties in PCFs for a small change in the structure of the PCFs which overcomes the meshing problems in some numerical modal solution techniques. Furthermore, this method takes a very little time compared to the other modal methods. Fig.1 shows an example of PCF structure. As shown in Fig.2, the results of this ANN approach agrees with those obtained using FVFDM. In the presentation, we will introduce more results to show the robustness and the accuracy of the ANN approach.

References

[1] J.Broeng, D.Mogilevstev, S.E.Barkou, and A.Bjarklev, *Opt. Fiber Technol*. **5**, 305-330. (1999)
[2] S. Haykin, *Neural Networks a Comprehensive Foundation* ,(1999)

Figures

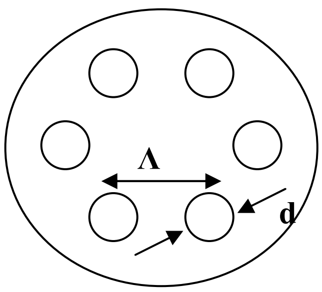

Fig.1.Cross section of PCF of one ring which contains 6 holes which are arranged in a silica background. Each hole has a diameter d and the distance between the holes is Λ

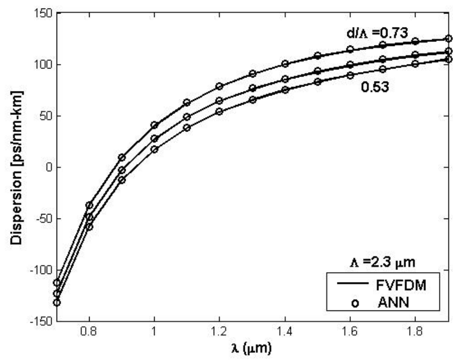

Fig.2.Variation of the dispersion of the fundamental mode H^x_{11} as a function of wavelength when Λ= 2.3 μm for different d/Λ ratios.

Alternative Calculations of Initial Value Problem for Electromagnetic Field in Dielectric Waveguide

Alexander Nerukh, Helen Semenova, Nataliya Sakhnenko
Kharkov National University of Radio Electronics, 14 Lenin Ave., Kharkov, 61166, Ukraine
e-mail: nerukh@ddan.kharkov.ua

Two ways for calculation of an initial value problem in a dielectric waveguide is presented. Each way describes one of two complementary approaches. Evolution of a transient electromagnetic field in the waveguide after instant change of its permittivity is considered and calculated.

Summary

Guided-wave dynamics can be organized around two complementary approaches – progressing and oscillatory – that are closely related to local versus global descriptions [1]. Progressing-way objects (wave-fronts) are responsible for point-to-point propagation, and sample the physical environment locally along their trajectory. Oscillatory-wave objects (modes or resonances) form standing waves over extended (global) portions of physical environment [2].

This paper presents calculation of an initial value problem for transformation of an electromagnetic wave in a dielectric waveguide after instant changing of its permittivity. The calculation is made (i) by tracing the Brillouin wave fronts and (ii) by summation of generated secondary modes. The evolution of the electromagnetic field and its spectrum is shown in Fig. 1.

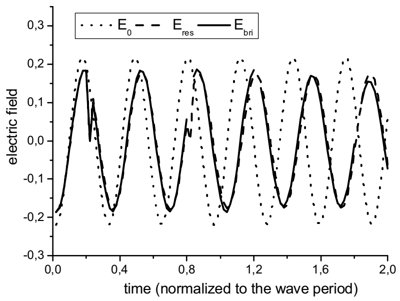

a)

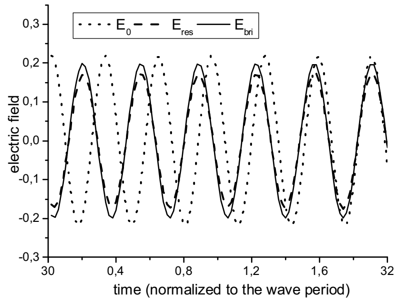

b)

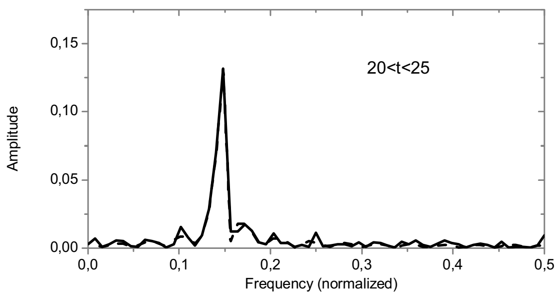

c)

Fig. 1. The evolution of the electromagnetic field (a, b) and its spectrum (c).

The field evolution immediately after the permittivity change is given in Fig. 1(a) and after 70 periods of the initial wave in Fig. 1(b). The initial wave is marked by the dotted line. The results obtained by virtue of two ways is coincide in the early stage of the process as well as after long period. The same is true for the field spectra, Fig. 1(c).

The progressing way turns out to be preferable because it does not need calculation of eigen-numbers for new modes that may be a rather difficult problem.

References

[1] L. B. Felsen and N. Marcuvitz, *Radiation and Scattering of Waves,* Englewood Cliffs, NJ, Prentice-Hall, (1973); reissue by Piscataway, NJ, IEEE Press, (1994).
[2] L. Sevgi, F. Akleman, L. B. Felsen, *IEEE Antannas and Propagation Magazine*, vol. 49, No 3, pp. 76-94, (2007).

Some Samples of Perturbation Method Application for Improving FEM Algorithm of Singlemode Optical Fiber Dispersion Calculation

Vladimir A. Andreev[1], Anton V. Bourdine[1] and Vladimir A. Burdin[1]
[1]*Department of Communication Lines, Povolzhskaya State Academy of Telecommunications and Informatics(PSATI), 67, Moscow Av., Samara, Russia;*
burdin@psati.ru

Perturbation method application for improving finite elements method (FEM) algorithm of single mode optical fiber dispersion calculation and some samples of it's using for optical fiber with various transverse structure are presented.

Summary

Perturbation theory formalism gives efficient way for the calculation of response of the device properties to small variation of different parameters of optical waveguides with various designing. It is well known application of perturbation method for derivation approximate analytical solution for non-uniform waveguides and analytical correction of numerical method for optical waveguides properties calculations [1, 2]. For example for determining eigenvalues of optical waveguides with two-dimensional transverse refractive index profile algorithm with analytical perturbation correction method combined with the finite difference approximation was developed [3]. By using common perturbation theory for linear operators [4] the fast and accuracy algorithm was achieved [5]. Another approach is based on the plane wave expansion method, where computation procedure requires one calculation of the frequency and the field distribution of the Bloch modes for the given Bloch vector and then determines the corrections as functions of the introduced perturbation parameters [6].

Introduced in this work algorithm correction calculating is based on widely used in perturbation method applications for optical waveguide propagation constant definition equation [1].

$$\beta=\bar{\beta}_C+k_0\frac{\int_A\left(\bar{n}_C-n\right)\bar{\Phi}_C\,ds}{\int_A\bar{\Phi}_C\,ds} \qquad (1)$$

The main idea of proposed algorithm is based on calculation on coarse and precise meshes. Eigenvalue problems of single mode fiber on 2D plane are solved by FEM algorithm on coarse mesh. Correction is calculated on more precise mesh after electromagnetic component and refractive index overdetermination by interpolation methods. It is possible to repeat correction procedure.

Application introduced method for some fiber optical structure, which included microstructural fiber, demonstrated sufficient high efficiency. For the same accuracy it works about 5-10 times faster then traditional FEM algorithm.

References

[1] A. W. Snyder and J. D. Love, *Optical Waveguide Theory,* London, Chapman and Hall (1983).
[2] A.K. Ghatak, I.C. Goyal, et al. *Can. J. Phys ./ Rev. can. phys.* **76**, 351-359 (1998).
[3] R.C. Partha, A.K. Ghatak, B.P. Pal and C. Lu, *Opt. laser technol.,* **37**, 61-67 (2005).
[4] T. Kato, *Perturbation theory for linear operators,* Berlin, Springer-Verlag (1966).
[5] J. Fini, *Optics Express*, **12**, 4535-4545 (2004).
[6] V. Zabelin, R. Houdre, *OWTNM 2007 Proceedings*, OR-01.05 (2007).

Aperiodic Rigorous Coupled Wave Analysis Applied to Photonic Nanostructure Modeling: a Critical Study

Pavel Kwiecien,[1] Ivan Richter[1], and Jiří Čtyroký[2]
[1] *Czech Technical University in Prague, Faculty of Nuclear Sciences and Physical Engineering, Department of Physical Electronics, Břehová 7, 11519 Prague 1, Czech Republic*
ivan.richter@fjfi.cvut.cz
[2] *Institute of Photonics and Electronics, Academy of Sciences of the Czech Republic, Chaberská 57, 18251 Prague 8, Czech Republic*

The aperiodic rigorous coupled wave analysis (ARCWA) method is analyzed, implemented and successfully applied to modeling various photonic nanostructures, including plasmonic and photonic wire, crystal and waveguide structures. The attention is given to numerical performance and its comparison to other approaches.

Summary

Today, photonic nanostructures represent a broad range of very perspective structures, often of artificial origin. They include various photonic crystals and wire based structures, plasmonic and subwavelength structures, as well as new classes of metamaterials. In order to fully explore the advantages and potential applications of such novel structures, the rigorous modelling and optimization process is always required. In this contribution, we have successfully modified the well known rigorous coupled-wave analysis algorithm (RCWA, also called the Fourier-modal method, FMM), applicable to periodic (grating) diffraction problems, following the original Lalanne's idea [1], to describe and model a broad range of general 2D aperiodic photonic nanostructures. First, our RCWA method implementation has included all modern techniques and approaches (as e.g. the application of proper Fourier factorization rules, scattering and enhanced transmittance matrix algorithms) as well a range of other important algorithm expansions, necessary for a proper accurate modelling (as e.g. the application of various schemes of dispersion relations, a possibility of near-field calculations, conical diffraction), to keep the numerical performance as high as possible. Based on this effective RCWA implementation, we have modified the approach to be used efficiently for the numerical analysis of 2D aperiodic finite photonic nanostructures, resulting in the Matlab-based effective numerical tool [2,3]. The modification has been achieved by introducing a virtual periodicity and incorporating artificial absorbers at the boundaries of the elementary cells of periodic structures. As artificial absorbers, we use complex nonlinear coordinate transformation combined with the perfectly-matched layer (PML) concept. According to a specific problem studied, these two approaches can be either switched on separately or combined together. A detailed critical study of the numerical performance of the method will be presented, together with a comparison with other available ARCWA implementations, as well as with some other methods (especially modal methods based on bidirectional expansion and propagation algorithm, and direct numerical techniques as the finite difference time domain method). The attention will be given to convergence study, the effect of boundary condition selection. Finally, several simulation and optimization examples of photonic nanostructures will be discussed.

References

[1] E. Silberstein et al., Use of grating theories in integrated optics, JOSA A **18**, 2865 (2001).
[2] I. Richter, P. Kwiecien, M. Šiňor, A. Haiduk, SPIE Proceedings **6581**, 2007.
[3] I. Richter, P. Kwiecien, M. Šiňor, J. Čtyroký, OSA Annual Meeting & Laser Science XXIII, Frontiers in Optics, San Jose, CA, USA, September 2007, paper JWC25.

Surface Quasi-Plasmon-Polaritons at a Plane Boundary of Newly Created Plasma

Anna Vozianova[1], Alexander Nerukh[1], Nataliya Sakhnenko[1]

Kharkov National University of Radio Electronics
Lenin Ave., 14, Kharkov, 61166, UKRAINE
[1]nerukh@ddan.kharkov.ua

***Abstract*— Creation of surface quasi-plasmon-polaritons at a plane boundary of newly created plasma is considered. The initial field is generating by a point source and the plasma density is above critical value with respect to the source frequency.**

Summary

Plasmon polaritons are attracting great attenuation now with their wide applications in nano-technology. The plasmon polaritons are created at an interface between a dielectric and a material with the negative permittivity. The latter can be a metal as well as plasma of great electron density. Plasma is a medium which can easily change its parameters, the electron density among them, and can be easily generated in originaly dielectric medium. If an electromagnetic field has existed in this medium the generation of plasma changes the field magnitude and frequency. If this initial field is radiation of the frequency ω then after the plasma generation the field consists of the ways of the frequencies ω and $\Omega = \sqrt{\omega_e^2 + c^2\kappa^2}$ where ω_e is a plasma frequency, $\kappa = \omega / v$ and v is the wave phase velocity in the dielectric [1, 2]. The structure of these waves inside different to outside of the spherical wave front. $\mathbf{E}_{11}^{\pm}$ are waves of the frequency Ω and $\mathbf{E}_{10}$ is the frequency ω wave. The wave of the frequency Ω converges to the source point, so this point is the singularity one for this wave.

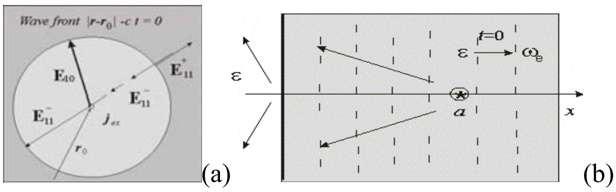

Fig. 1. The field structure after plasma creation in unbounded space (a); the wave output from bounded plasma (b).

This process alters profoundly if plasma is generated in a bounded medium. In this case the converged wave of the frequency Ω is limited at the point source and the condition for appearing of plasmon polaritons at the plasma boundary can occur. Such a case is investigated in the presented paper where electromagnetic field transformation caused by jump medium ionisation in the half-space $x \geq 0$ is considered. It is assumed that undisturbed electromagnetic field is radiation of a point harmonic source $\mathbf{E_0} = \mathbf{I}\exp(i\omega t - i\kappa|\mathbf{r} - \mathbf{r}_0|)/|\mathbf{r} - \mathbf{r}_0|$, $\kappa = \omega / v$, which is located in ionisable region at the point $\mathbf{r}_0 = (a, 0, 0)$, and newly created plasma is characterised by plasma frequency ω_e.

It is shown that appearing bounded plasma covering a radiation point source eliminates singularity of the secondary converging wave. The wave outgoing from plasma is like to a plasmon polariton at the frequency of the initial wave.

References

[1] F. R. Morgenthaler, Velocity modulation of electromagnetic waves, *IRE Trans. on Microwave Theory and Technique,* vol. 6, pp. 167-172, 1958).

[2] L. B. Felsen, G. M. Whitman, *IEEE Trans. on Antennas and Propag*., vol. AP-18, p.242, 1970.

Subwavelength Imaging with a Silver Lens

Indra Karnadi[1], Alexander A. Iskandar[2] and May On Tjia[2]
[1] *Pelita Harapan University, Department of Physics, Lippo Karawaci,Tangerang 15811, Indonesia*
ind_karnadi@yahoo.co.id
[2] *Institut Teknologi Bandung, Physics of Magnetism and Photonics Group, Jl. Ganesa 10, Bandung 40132, Indonesia*
iskandar@fi.itb.ac.id

We present a study of subwavelength image formation by a silver lens. It was found that an image with a good quality can be reproduced a certain distance from the lens. A relation between this distance and the absorption coefficient was derived.

Summary

Subwavelength imaging has been an active research topics as it overcomes the diffraction limit of a conventional optics which is only capable of transmitting the propagating components emanating from the source while the evanescent waves that carry subwavelength information about the object decay exponentially in a medium. To regain this subwavelength information, a superlens of the form of a thin slab of material with negative permittivity or permeability, or both, is used. In this study we report the formation of subwavelength image using a very thin silver lens in the wavelength range where its permittivity is negative. Taking into account the absorption effect, and applying Fourier transformation of the wave arriving at the image plan, our numerical calculation shows that a good quality image in terms of contrast and resolution could be formed at a distance between the object and the image that is a little larger than twice the lens thickness. This differs from the result obtained by a superlens of metamaterials with both negative permittivity and permeability, which produce a perfect image at a distance exactly twice the lens thickness.

References

[1] J. B. Pendry, *Phys. Rev. Lett.* **85** (2000) 3966.
[2] S. A. Ramakrishna, *Reports on Progress in Physics* **68** (2005) 449.
[3] N. Fang, H. Lee, C Sun, and X. Zhang, *Science* **308** (2005) 534.

Acoustical and acousto-optic properties of chalcogenide As_2S_3 glass waveguide on $LiNbO_3$

Eugeny Kolosovsky[1], Rinat Taziev[1] and Andrei Tsarev[1]

[1] *Institute of Semiconductor Physics, Siberian Branch of Russian Academy of Sciences*
Prospect Lavrenteva, 13, Novosibirsk, 630090, Russia

tsarev@.isp.nsc.ru

We had studied the detail structure of acoustic modes (Rayleigh wave, Sezawa wave and high-order Lamb waves) and acousto-optic interaction in chalcogenide As_2S_3 glass waveguide on $LiNbO_3$. It was found the large increase of diffraction efficiency at As_2S_3 thickness 0.8 μm, SAW frequency 750 MHz and optical wavelength 1.55 μm.

Summary

We study propagation of surface acoustic modes in layered chalcogenide As_2S_3 glass waveguide on $LiNbO_3$ substrate. The basic acoustical mode is a surface acoustic wave (SAW) (Rayleigh wave), which exists in the structure at any film thickness. Other modes can exist only at thicknesses larger the critical one. This layered structure can support simultaneously different acoustic modes (see Fig.1a), which differ in the velocity and spatial distribution of displacement, when thickness of layer is comparable with acoustical wavelength, and the velocity of shear waves is less than one in the substrate. In essence, it is the Lamb modes in a chalcogenide layer disturbed by presence of acoustic contact with piezoelectric substrate (lithium niobate). First of such modes, corresponding to the first antisymmetric Lamb wave is refered as a Sezawa wave [1]. For the acousto-optic (AO) interaction it is better to use Rayleigh wave that have to excited at free surface (without the film) on $LiNbO_3$, then gradually transforms to the same mode on the layered structure by means of gradually changed chalcogenide layer thickness from zero up to optimum value 0.8 μm. At this optimum thickness the structure provides a great increase of the diffraction efficiency (see Fig.1b) at SAW frequency 750 MHz and optical wavelength 1.55 μm. This As_2S_3 glass waveguide on $LiNbO_3$ is very perspective for construction of multi-reflector filtering devices with AO tuning [2]. For example, it provides wide tunability ~40 nm (within total C- or L-band), small linewidth (~0.1 nm), remarkably large number of tuning optical wavelength (up to 200), small operation power (~ 3 mW) and fast switching time (~2 μs), simultaneously.

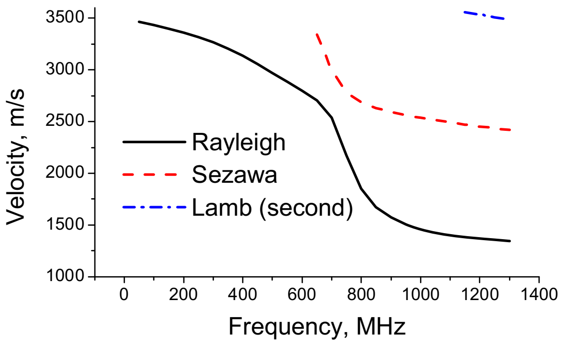

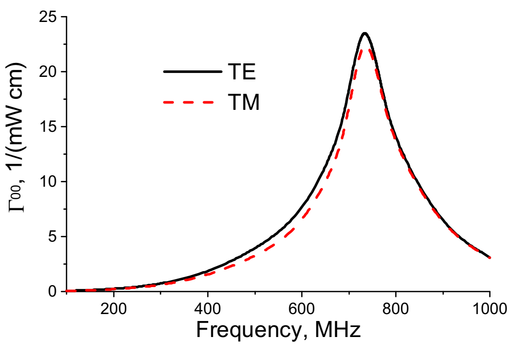

a) b)

Fig. 1. Acoustical and acousto-optical properties of 0.8 μm layer of As_2S_3 on $LiNbO_3$. (a) Dispersion of SAW and Sezawa wave velocities; (b) Simulation of the coupling coefficient Γ_{00} for TE_0 and TM_0 modes. Here Γ_{00} is the measure of AO efficiency: $\eta = sin^2[\Gamma_{00}P_aL]^{1/2}$, where P_a is acoustic power, L is the SAW aperture.

References

[1] H.F. Tiersten, J.Appl.Phys., **40**, 770-789 (1969).

[2] A.V.Tsarev, E.A.Kolosovsky, Optoelectronics, Instrumentation and Data Processing, **42**, 93-104 (2006).

Optimization studies of single-transverse-mode 980 nm ridge-waveguide lasers

Antti Laakso[1], Mihail Dumitrescu[1], Pasi Pietilä[1], Mikko Suominen[1] and Markus Pessa[1]
[1] *Optoelectronics Research Centre, Tampere University of Technology, Tampere, Finland*
antti.i.laakso@tut.fi

The paper presents a simple method for determining the ridge profile that ensures a stable single-mode operation in ridge-waveguide lasers. 2D Mode Solver simulation results have been compared to the results obtained with the commercial simulation package LASTIP and with experimental measurements.

Summary

While many 980 nm applications are targeting high-power multimode lasers, there is an increasing need of single-transverse-mode (STM) edge-emitting lasers for fiber amplifiers. The simplest structure that ensures STM operation is the ridge waveguide (RWG) structure. However, there are very few studies that even attempt a systematic analysis of the whole RWG solution space.

Our 2D Mode Solver (MS) is based on solving the 2D scalar Helmholtz equation with a variable discretization step in both transverse dimensions. Results obtained with the 2D MS were compared, for a restricted number of geometry variants, with more accurate simulations performed using the more powerful LASTIP software package from Crosslight Software Inc [1]. The simulation results were used to choose a few dimensional variants that have been fabricated and characterized in order to determine the RWG geometries that ensure stable STM operation.

In order to predict the modal behavior, it is important to compare the modal gains of different transverse modes. Since the carrier density distribution is not available in the MS approach, we use the approximation that the local gain is constant under the ridge, and zero elsewhere for all transverse modes. Under this assumption the ratio $(G_1\text{-}G_m)/G_1$ (where G_i is the modal gain of the i-th mode) is simply equal to the ratio $\Gamma_{1m}=(\Gamma_1\text{-}\Gamma_m)/\Gamma_1$, where Γ_m is the quantum well confinement factor calculated over the active region that is strictly under the ridge. Since Γ_2 is bigger than Γ_4, Γ_6 etc. and Γ_3 is bigger than Γ_5, Γ_7 etc., it is enough to study the ratios Γ_{12} and Γ_{13}.

The MS simulations predict that STM operation can be obtained for RWGs ranging from relatively narrow and deep ridges to relatively wide and shallow ones. Although the results suggest that for narrow ridges the STM operation can be achieved over a relatively wide range of un-etched cladding thicknesses (t) for a fixed ridge width, the lowest possible value of t should be always targeted in order to minimize the lateral current spreading and the threshold current.

The LI-curves obtained from LASTIP simulations indicate a similar modal behavior with the one determined by the MS simulations. The maximum values obtained for Γ_{12} and Γ_{13} with the MS and with LASTIP, indicating the un-etched cladding thickness t at which the STM operation is ensured, were very close to each other. Moreover, experiments made for 3 µm and 4 µm wide ridges confirmed that the relatively simple and efficient MS approach can be used to evaluate effectively the RWG geometry at which a stable STM operation is achieved.

Wider ridges are generally preferable due to their better electrical properties. However, as the ridge width increases, the overlap of the areas in which the ratios Γ_{12} and Γ_{13} are both high decreases. Therefore, STM operation is harder or impossible to achieve for wide ridges. The position of the high Γ_{12} and Γ_{13} areas depends on the vertical near field profile, and the overlap of high Γ_{12} and Γ_{13} areas can be tuned by altering the vertical layer structure. Simulations showed that by adding a current confining layer to the p-side cladding, STM operation together with good electrical properties can be achieved for wide-ridge RWG structures.

References

[1] LASTIP software information, www.crosslight.com

Theoretical investigation on the modification of the emission efficiency of a 2D-PC cavitiy assisted by metal layers

V. Marrocco, M.A. Vincenti, M. De Sario, V. Petruzzelli, A. D'Orazio
Dipartimento di Elettrotecnica ed Elettronica - Politecnico di Bari
Via E. Orabona 4, 70125 Bari
dorazio@poliba.it

F. Prudenzano
Dipartimento di Ingegneria dell'Ambiente e per lo Sviluppo Sostenibile - Seconda Facoltà di Ingegneria, Taranto
Via del Turismo 8, 74100 Taranto

Summary
Metals can strongly improve PBG properties of a photonic crystal without significant loss in the gap region: to this aim some authors have proposed different designs and experiments about the possibility of enhancing the PBG properties of the classic dielectric-based 2D-PC using noble metals as coating layers [1]. Other reserch groups have proposed to sandwich a 1D thick slab with gold cladding to achieve a better performance in the operation of lasing at the band edge, thus reducing the coupling of the fundamental mode to the leaky modes via metal interfaces [2]. An interesting work [3] also shows the potential of the surface plasmons arising at the metallo-dielectric interfaces in controlling the spectral response on the surface of a photonic crystal in reflection, absorption and emission in the near infrared region.
In this work we theoretically investigate the effects of the presence of a metal layer placed in the substrate of a two-dimensional photonic crystal cavity, designed in the visible spectral range. The simulations are performed using FDTD codes, which are able to take into account the material properties and to properly model the noble metal dielectric functions. The analysis takes inspiration by the fundamental issue concerning the reduction of the scattering losses related to a 2D-PC cavity in the substrate region, in order to enhance the emission efficiency in the vertical direction, as already done for LED application. We compare the use of a simple metal layer, such as PEC, to that of a noble metal, which gives the opportunity of exploiting the surface plasmon resonances arising at the metal-dielectric interface.

References

[1] V. Poborochi, T. Tada and T. Kanayama, A. Moroz, "Silver-coated silicon pillar photonic crystal: enhancement of a photonic band gap", Applied Physics Letters, vol. 82, n. 4, pp. 508-510, January 2003.
[2] J.Van Campenhout, P. Bienstaman, R. Baets, "Band-edge lasing in gold-clad photonic-crystal membranes", IEEE Journal on Selected Areas in Communications, vol. 23, n. 7, pp. 1418-1423, July 2005.
[3] I. Puscasu, M. Pralle, M. McNeal, J. Daly, A. Greenwald and E. Jonson, R. Biswas and C.G. Ding, " Extraordinary emission from two dimensional plasmonic-photonic crystals", Journal of Applied Physics 98, 013531 (2005).

Simulation of Pulse Propagation over Piecewise Regular Multimode Fiber Link Excited by Singlemode Laser Source

Anton V. Bourdine[1] and Vladimir A. Burdin[1]
[1]*Department of Communication Lines, Povolzhskaya State Academy of Telecommunications and Informatics (PSATI), 67, Moscow Av., Samara, Russia;*
burdin@psati.ru

Time domain model of piecewise regular multimode fiber link with conventional silica graded-index multimode optical fibers, excited by singlemode laser source, under taking into account DMD, launch conditions, high order mode chromatic dispersion, mode mixing and power diffusion is represented.

Summary

We present time domain model of piecewise regular multimode fiber optic link with conventional silica graded-index optical fibers, excited by singlemode laser source. Proposed model allows to take into account following distortion factors: differential mode delay (DMD), launch conditions, chromatic dispersion of high order modes, mode mixing and power diffusion. Unlike to conventional methods for analysis of pulse propagation over multimode fibers [1], solution is based on representation of link in the form of cascade of coupled regular fiber segments with sufficient low length, thereby fiber parameters of each segment are assumed constant, and mode coupling is absent. Each splice of regular segments is considered as splice of non-identical fibers without any misalignments, and mode interaction is estimated by mode coupling coefficient matrix calculation. Proposed solution requires multiple computations of the fundamental and higher order mode parameters. To estimate propagation constant, group velocity, chromatic dispersion and other mode parameters, we apply extension of modified Gaussian approximation method [2]. This method is sufficient accurate, simple and fast [4]. Launch condition simulation also applies mode field Gaussian approximation to estimate mode coupling coefficients under particular offset or tilt. Some results of simulation of pulse (initial width 0.386 ns) propagation over 1 km of conventional graded-index multimode fiber 50/125 under 1% core diameter and refractive index profile random variations through the each 10 m, are represented on Fig. 1.

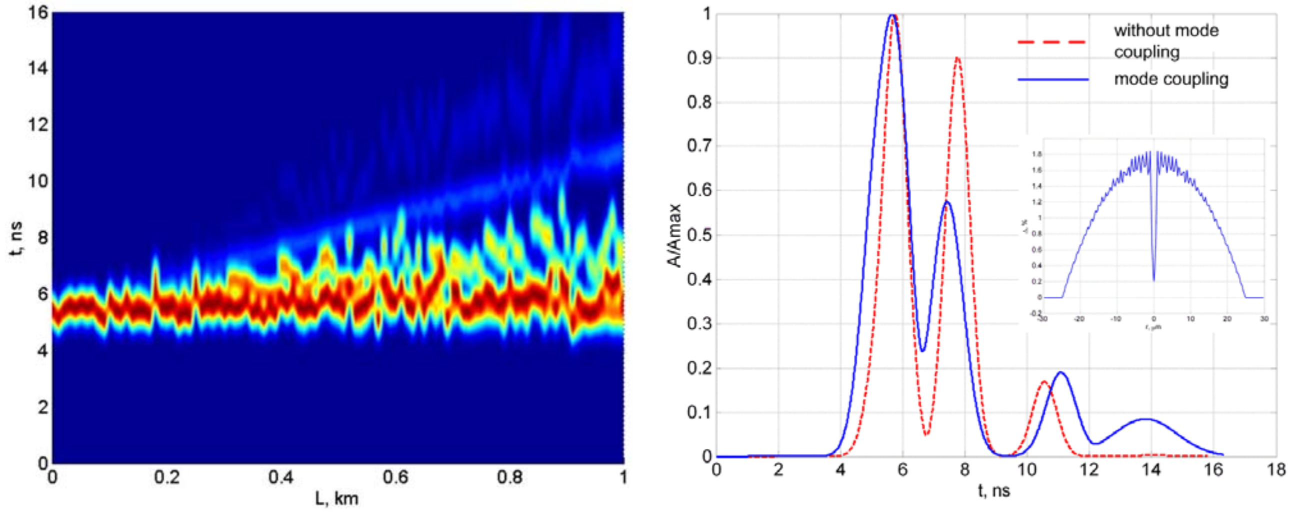

Fig 1. Results of pulse propagation simulation over 1 km multimode fiber link: (a) pulse propagation diagram; (b) output pulse form. Launch conditions: singlemode laser source (λ=1310 nm) coupled to link fiber under offset 12 μm.

References

[1] J.J. Ramskov-Hansen, E. Nicolaisen, *Applied optics*, **17**, 2831 – 2835 (1978).
[2] A.V. Bourdine, *Proceedings of SPIE*, **6605**, 660509-1 – 660509-13 (2006).

Using Optically Induced Forces in Numerical Structural Optimization

Thorsten Liebig and Daniel Erni
General and Theoretical Electrical Engineering (ATE), Faculty of Engineering, University of Duisburg-Essen, 47048 Duisburg, Germany
thorsten.liebig@uni-due.de

A numerical structural optimization procedure is presented that utilizes optically induced force fields as a "natural" strategy for shape deformations in photonic components. The proposed methodology has supposedly proven successful to reveal largest possible quality factors Q for e.g. two-dimensional (2D) simply-connected dielectric microcavity volumes.

Summary

The force field is calculated from the Maxwell's stress tensor $\bar{\boldsymbol{T}}$ at the boundary of a dielectric particle that is illuminated by a TM-polarized plane wave at the particle's resonance. The time-averaged optical force $\langle \boldsymbol{F} \rangle_t$ exerted on such object enclosed by the surface S is calculated as [1, 2]:

$$\langle \boldsymbol{F} \rangle_t = \int_S \langle \bar{\boldsymbol{T}} \cdot \boldsymbol{n} \rangle_t \, \mathrm{d}s = \int_S \left\{ \frac{1}{2} \Re[(\boldsymbol{D} \cdot \boldsymbol{n})\boldsymbol{E}^*] - \frac{1}{4}(\boldsymbol{D} \cdot \boldsymbol{E}^*)\boldsymbol{n} + \frac{1}{2} \Re[(\boldsymbol{B} \cdot \boldsymbol{n})\boldsymbol{H}^*] - \frac{1}{4}(\boldsymbol{B} \cdot \boldsymbol{H}^*)\boldsymbol{n} \right\} \mathrm{d}s \quad (1)$$

Shape relaxations of objects according to optically induced force fields are governed by energy minimization. Inverting the forces (i.e. the area-density of the force $\langle \bar{\boldsymbol{T}} \cdot \boldsymbol{n} \rangle_t$ on the surface S) will therefore provide a "natural" strategy for energy maximization. In the context of a resonant microcavity this is tantamount to tracking down the largest possible quality factor Q. Figure 1 shows the evolution of such an optimization scenario, where the boundary of a circular dielectric micropillar that supports a resonant whispering-gallery mode is deformed using a maximal stepsize of 0.1nm per iteration step. With this optimization strategy we were able to enhance the quality factor Q by 40%. Further investigations include waveguides as well as grating structures.

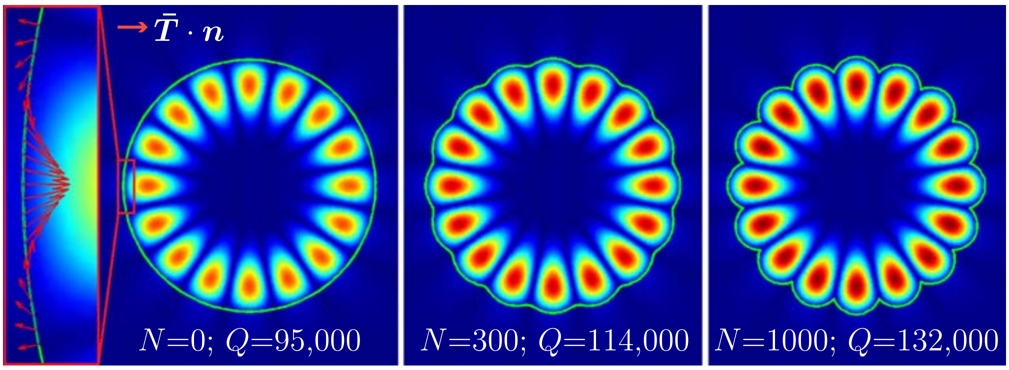

Fig. 1. Computed distribution of the magnetic field $|H_z|$ within an evolving 2D dielectric micropillar ($r = 1\mu$m, $\epsilon_r = 10$, embedded in air) at three different iteration stages N. The structure is excited by a plane wave from the left at a resonance wavelength of 1649 nm.

References

[1] J. A. Stratton, *Electromagnetic Theory*, McGraw-Hill Book Company, N.Y. and London (1941).
[2] L. Novotny, *Forces in Optical Near-Fields*, Appl. Phys. Lett. **81**, 123-141 (2001).

Simulation by FDTD of multi-reflector ROADM on SOI with variable reflector's width and position

Andrei Tsarev[1]

[1] *Institute of Semiconductor Physics, Siberian Branch of Russian Academy of Sciences*
Prospect Lavrenteva, 13, Novosibirsk, 630090, Russia

tsarev@.isp.nsc.ru

Analysis by FDTD of ROADM based on multi-reflector beam expanders is extended to complicated case of variable reflector's width and position. Additional reflector's shifts are needed to compensate parasitic phase change coursed by variable reflector width (to control reflection coefficients), which are used to provide the high side-lobe suppression.

Summary

The paper described recent results of theoretical investigation of novel reconfigurable optical add/drop multiplexer (ROADM) on Silicon-on-Insulator (SOI) structures employing multi-reflector (MR) filtering technology [1]. Heterogeneous optical waveguides with side *p-n* doping of wide and thin silicon core has a quasi-single-mode behavior and it is the best compatible with 2D-grating for fiber-to-waveguide coupling and ROADM's polarization diversity. Reflectors of beam expanders are built in as nano-grooves with back filling. Reflector's widths are monolithically changed with reflector number (see Fig.1a) in order to have optimal variation of reflector coefficient to provide frequency response with the high side-lobe suppression. Unfortunately, variable reflector's width produces parasitic phase changes those substantially disturb frequency response of ROADM. We study this effect and propose compensation algorithm of these phase changes by additional shifts in position of reflectors (see Fig.1a). Simulation by the 2D FDTD of frequency response (see Fig.1b) of ROADM that contains 3 beam expanders with 32 variable reflectors proves validity of new device conception. This multi-reflector ROADM with variable reflector's width and position could find application for flexible redirection wavelength channels in intelligence all optical networks.

Acknowledgment. The author thanks Company RSoft Design Group, Inc for providing Rsoft Photonic CAD Suite 8.0 including FullWave software (see http://www.rsoftdesign.com) for FDTD simulations.

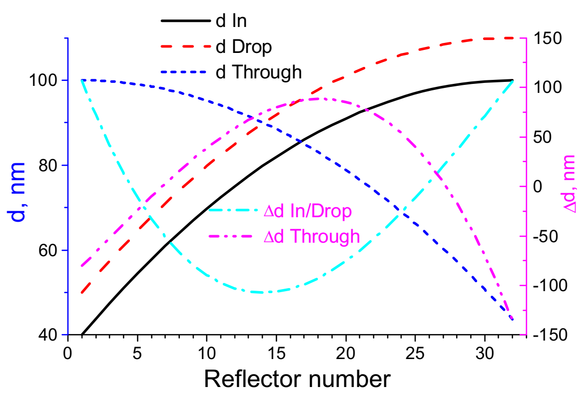

a)

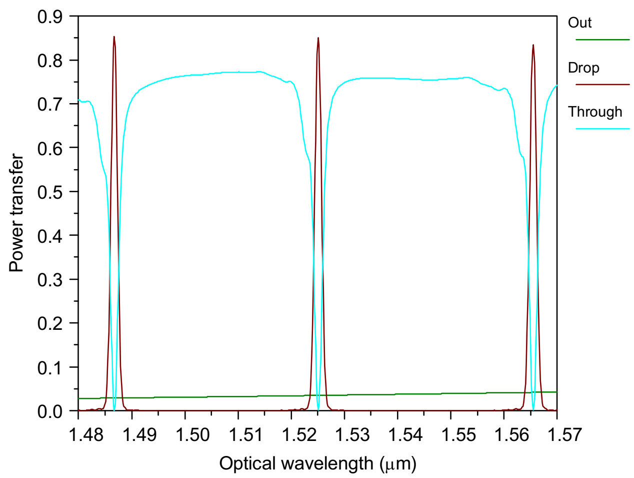

b)

Fig. 11. Simulation by 2D FDTD of MR-ROADM with 3 beam expanders and 32 reflectors with variable reflector width. a) Variation of width *d* and shift *Δd* of reflector position as a function of reflector number; b) Frequency response for TM polarization. Waveguide core width W = 5 μm, period of reflectors d_x = 10 μm, beam expander period d_z = 40 μm, n(reflector) = 1.7, FWHM = 1.5 nm, FSR = 40.4 nm.

References

[1] A. V. Tsarev, F. De Leonardis, and V. M. N. Passaro, Opt. Express, **16**, 3101-3113 (2008).

Impact of Waveguide Sidewall Roughness on the Output Uniformity and Phase of MMI Splitters.

Kehinde O. Latunde-Dada[1] and Frank P. Payne[1]
[1] *Department of Engineering Science, Oxford University, Parks Road, Oxford, OX13PJ, United Kingdom.*
kehinde.latunde-dada@keble.ox.ac.uk

In this paper, we develop a model for the effects of waveguide sidewall roughness on the output uniformity and phase of a 1x2 3-dB MMI splitter.

Summary

In a symmetric 1x2 MMI splitter, unwanted asymmetric modes can be generated in the MMI section as a result of scattering of the symmetric guided modes by sidewall roughness. The presence of asymmetric modes at the output of the MMI will result in degradation of both the uniformity and phase of the MMI response. If, as a result of sidewall scattering, the modal amplitude of the j^{th} asymmetric mode at the MMI output is ε_j and the overlap of this with the fundamental mode of the output waveguides is q_j then it can be shown that the output uniformity S of the MMI is given by:

$$S = \frac{40\sqrt{\sum_{j\ \mathrm{odd}} \left(\varepsilon_j q_j\right)^2}}{\log_e 10} \qquad (1)$$

where the sum is over the asymmetric modes of the MMI section. We assume that the amplitudes ε_j of the asymmetric modes generated by scattering are given by $\varepsilon_j = \sqrt{P_j(L)}$, where $P_j(L)$ is the power in the j^{th} asymmetric mode at the output of the MMI section of length L and is computed using coupled power equations [1] to be given by:

$$P_j(L) = \sum_{k\ \mathrm{even}}^{n} \left[\frac{(j+1)^2 (k+1)^2 \pi^2 \lambda}{8 w_1^4 n_r} \right] . \frac{2\sigma^2 L_c}{1+L_c^2(\beta_j - \beta_k)^2} . P_k(0) \qquad (2)$$

where w_1 is the width of the MMI section, n_r is the waveguide effective index, λ is the propagating wavelength, σ is the r.m.s roughness, L_c is the roughness correlation length, and β_j is the mode propagation constant. The power in the k^{th} symmetric mode at the input to the MMI section is $P_k(0)$. The length, L does not appear explicitly in (2) as it has been absorbed into the MMI imaging length.

In a similar manner, the phase error, $\delta\varphi$ between the outputs of the MMI can be shown to be given by:

$$\delta\varphi = 2\sqrt{\sum_{j\ \mathrm{odd}} \sum_{k\ \mathrm{even}} q_j^2 q_k^2 \left(\frac{(j+1)(k+1)\pi\lambda}{2 w_1^3 n_r} \right)^2 \frac{\sigma^2 L_c}{1+L_c^2\left(\beta_j - \beta_k\right)^2}} \qquad (3)$$

It is straightforward to extend our analysis to higher order waveguides and multiple input splitters.

References

[1] D. Marcuse, *Theory of dielectric optical waveguides,* Chapman and Hall, New York (1983).

Optical modeling of laterally-corrugated ridge-waveguide gratings

Mihail Dumitrescu[1], Antti Laakso[1], Jukka Viheriala[1], Mikko Suominen[1], Markus Pessa[1]
[1] *Optoelectronics Research Centre, Tampere University of Technology, Tampere, Finland*
Mihail.Dumitrescu@tut.fi

The paper presents an improved procedure for the calculation of the longitudinal effective index profile induced by a lateral corrugation in the ridge waveguide. The procedure has been used for designing laterally-corrugated ridge waveguide structures for distributed feedback lasers operating at 980 nm.

Summary

The conventional distributed feedback (DFB) and distributed Bragg reflector (DBR) edge-emitting laser designs are based on incorporating a grating deep into the semiconductor epilayer structure, either inside the laser waveguide itself or close enough, so that the optical field is strongly coupled with the grating. Such embedded gratings require two or more epitaxial-growth steps, bringing in a lot of difficulties and problems associated with overgrowth. All those difficulties and problems can be avoided by the use of weakly-coupled surface gratings, which have the supplementary advantage of a limited interaction with carrier flow and, therefore, can be analyzed and designed using optical modeling. However, the weak coupling of the surface grating with the optical field requires a much more accurate optical modeling since weakly-coupled structures are significantly more sensitive to relatively small calculation errors.

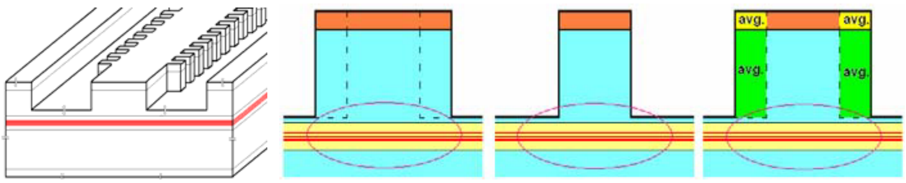

a. b. c. d.

Fig. 1 Laterally-corrugated ridge waveguide structure: (a) general view, (b) wide-ridge section, (c) narrow-ridge section, (d) transverse section with weighted-average refractive index regions (avg.) in the areas of the grating

The usual way of calculating the longitudinal effective refractive index distribution is to apply a mode solver (MS) separately to the grating slices. The grating slices for the laterally-corrugated ridge waveguide structure (RWG) exemplified in Fig. 1a are given in Fig. 1b and 1c. The disadvantage of this 'classical' approach derives from the fact that the mode solver assumes that the modeled slice structure is indefinitely long. Due to the difference in optical confinement between the corrugated RWG slices the MS-derived transverse optical field distributions are different in the slices. However, the real transverse optical field distribution cannot change substantially within the short-range periodicity of the grating. In order to take into account the slow variation of the transverse optical field distribution, our approach was to derive the transverse optical field distribution using a 2D 'weighted-average' transverse refractive index distribution. In this 'weighted-average' transverse refractive index distribution, the refractive index in the grating regions (marked 'avg.' in Fig. 1d) was considered as the average of the refraction index in the corresponding regions of the wide-ridge and in the narrow-ridge slices, weighted with the filling factor of the grating. The effective refractive index in the wide- and narrow-slice sections is then obtained by the convolution of the optical field distribution Ψ^a, obtained for the 'weighted average' 2D refractive index, with the refractive index distributions of each slice:

$$n^2_{\text{eff-slice\_i}} = \frac{\iint n_{slice\_i}^{\,2}(x,y)\cdot\Psi^a(x,y)}{\iint \Psi^a(x,y)}$$

The longitudinal refractive index distribution calculated by this procedure was used to derive the grating coupling coefficient and the group index and was checked against experimental results obtained for corrugated 980 nm RWG DFB lasers. Significant differences were found with respect to the effective refractive index values obtained by using the classical method of calculation, which yielded a smaller compatibility with experimental results. The experimental results have shown that, for weakly-coupled gratings, where the longitudinal effective refractive variation is small, the supplementary accuracy resulted from applying the 'weighted-average' procedure is important for properly designing the grating structure.

Optical Signal Processing Based on Planar Waveguides

Laurence W. Cahill and Thanh Trung Le
Department of Electronic Engineering, La Trobe University, Melbourne, Victoria, Australia 3086
l.cahill@latrobe.edu.au

This paper investigates possibilities for developing optical signal processing elements based solely on the combination of single mode waveguides and multimode interference couplers.

Summary

Signal processing functions such as the discrete Fourier transform, the fast Fourier transform, the Haar transform, the Hadamard transform as well as discrete wavelet transforms have been designed . using lenses, splitters, star couplers, fibres, directional couplers and multimode interference (MMI) couplers. In this paper we shall examine possible implementations of some signal processing functions using primarily MMI couplers and single mode waveguides.

The low-pass and high–pass filters associated with the Haar wavelet filter (or the Daubechies wavelet filter of order M=1) [1] can be written as

$$\begin{bmatrix} H \\ G \end{bmatrix} = \frac{1}{\sqrt{2}} \begin{bmatrix} 1 & 1 \\ 1 & -1 \end{bmatrix} \tag{1}$$

The above matrix is also the first order Hadamard transform [2]. The transfer matrix describing the relation between the input and output fields of a 2x2 restricted interference MMI coupler is

$$M = \frac{1}{\sqrt{2}} \begin{bmatrix} r & r^{-1} \\ r^{-1} & r \end{bmatrix} \tag{2}$$

where $r = \exp(j\pi/4)$. Hence the transfer function of the same coupler having additional lengths of a half-wavelength at the lower access waveguides is

$$T = \frac{r}{\sqrt{2}} \begin{bmatrix} 1 & 1 \\ 1 & -1 \end{bmatrix} \tag{3}$$

which is equivalent to equation (1) with an added phase change. This element can be used as a Haar wavelet filter and can also form the basis for the generation of a number of signal processing transforms. An example is the planar waveguide element shown in Fig.1, which when cascaded will produce the second order Hadamard transform of a four element column vector.

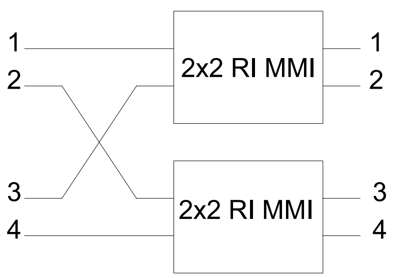

$$H_2 = \frac{1}{2} \begin{bmatrix} 1 & 1 & 1 & 1 \\ 1 & -1 & 1 & -1 \\ 1 & 1 & -1 & -1 \\ 1 & -1 & -1 & 1 \end{bmatrix}$$

Fig. 1. A signal processing element, which when cascaded, produces a second order Hadamard transform.

References

[1] G. Cincotti, *IEEE JQE* **38,** 1420-1427 (2002).
[2] A.R. Gupta et al, *Appl. Optics*, **42**, 2730-2738 (2003).

1D Grating Structures Designed by the Time Domain Topology Optimization

Lirong Yang[1], Andrei Lavrinenko[1], Ole Sigmund[2] and Jørn Hvam[1],

[1] *Technical University of Denmark,Department of Photonics Engineering , DK 2800, Denmark*

yang@com.dtu.dk

[2] *Technical University of Denmark, Department of Mechanical Engineering,DK 2800, Denmark*

We report on the time domain application of topology optimization to 1D photonic devices. The method is confirmed to converge to the global minimum when optimizing a Bragg grating structure.

Summary

The topology optimization (TO) has been proved to be a powerful frequency domain technique for designing efficient photonic structures with improved properties [1]. We attempt to show here its applicability to work within time domain methods, e.g. the Finite Difference Time Domain (FDTD) method. Only one group has reported similar effort in the dielectric antenna design [2].

It is well known that theoretically, BG are the best structures to minimize the transmission at certain frequencies. We try the TO aiming at minimizing the transmissions at these frequencies, and expect the resulting optimized structure to be a BG with the correct period and number of layers. Thus it confirms that the TO has reached global minimum.

The optimization starts out in a homogeneous medium, and 1D-FDTD is used to assess the structure's response to the excitation in every optimization iteration. The sensitivities for all the grid points in the design domain are calculated by the adjoint-variable method [3]. The optimization algorithm called the Method of Moving Asymptotes [4], uses these sensitivities to reevaluate how much it should change the grid points material properties. When the maximum change between iterations is small enough, the optimization is considered to have converged.

The resulting optimized layout structure (grey) is shown in Fig.1 where is it compared to the theoretical BGs (black). The resemblance between the two layouts as well as their spectra (Fig.2) is clear.

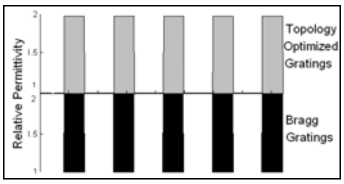

Fig.1. Layouts of the optimized gratings and the BGs.

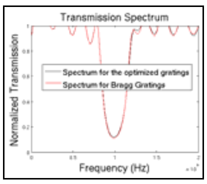

Fig.2. Transmission spectra of the optimized gratings and BGs.

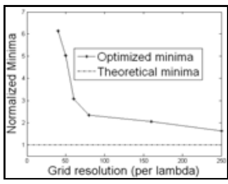

Fig.3. Convergence to the global minimum vs. resolution.

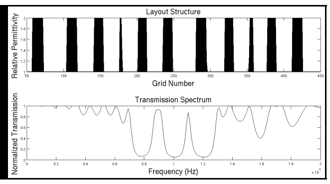

Fig.4. Layout and the spectrum of the optimized multi-channel filter.

For longer design domain, the convergence to the global minimum becomes more difficult. It can be improved by increasing the grid resolution (having more design elements per unit length). Fig.3. compares the optimized structures' transmission at the Bragg frequency to that of the BG, and shows that the optimized minimum gradually decreased to the BG minimum as more grid points are used.

A multi-channel filter is also tested to demonstrate the versatility of this optimization scheme. The resulting layout and the transmission spectrum are illustrated in Fig.4.

References

[1] P. I. Borel, A. Harpøth, L. H. Frandsen, M. Kristensen, J. S. Jensen, P. Shi, and O. Sigmund, *Opt. Express*, Vol. 12, Issue 9, pp. 1996-2001.

[2] T. Nomura, K. Sato, K. Taguchi, T. Kashiwa and S. Nishiwaki*, Int. J. Numer. Meth. Eng.,* vol. 71, 2007, pp. 1261-1296.

[3] N. Nikolova, H. Tam, and M. Bakr, *IEEE Trans. Micr. Th. Techn.*, vol. 52, 2004, pp. 1207-1216.

[4] K. Svanberg, *Int. J. Num. Meth. Eng*, vol. 24, 1987, pp. 359-373.

Optimization of an integrated-optical ring-resonator slow-light-based sensor

H. P. Uranus[1,2] , M. Hoekman[1], M. Dijkstra[1], H. J. W. M. Hoekstra[1], and R. Stoffer[3]

[1] *IOMS Group, MESA+ Institute for Nanotechnology, University of Twente, P.O. Box 217, 7500 AE Enschede, The Netherlands*

h.p.uranus@alumnus.utwente.nl, h.j.w.m.hoekstra@ewi.utwente.nl

[2] *Dept. of Electrical Engineering, University of Pelita Harapan, Lippo Karawaci, P. O. Box 453, Tangerang 15811, Indonesia*

[3] *Phoenix B.V., Hengelosestraat 705, 7521 PA, Enschede, The Netherlands*

A 3-D, vectorial, and multimodal model that incorporates realistic losses was developed to study the performance of Si_3N_4 based integrated-optical ring-resonator slow-light-based refractometric sensor. Efficient optimization of the coupler gap and tolerance analysis were also performed using the model.

Summary

Integrated-optical ring-resonators have since long been considered as good candidates for enhancing optical sensor performance [1]. Slow-light plays an important role for such enhancement [2]. The light slowness is a result of interplay between the waveguide losses and the coupling constant [2]. Furthermore, the optimal light slowness is a result of trade-off between sensitivity and insertion loss tolerable by the detection electronics. Obviously, optimization is an important part in designing a ring-resonator based sensor.

In this work, we develop a 3-D, vectorial, and multimodal model of ring resonator sensing circuit. The model combines the use of vectorial mode solvers, realistic loss model supported by measurement of prefabricated test structures, 3-D vectorial coupled-mode theory [3] and multimodal transfer matrix method and complex transmission coefficient approach . The model also takes into account the fact that waveguides outside and inside the sensing window are different, and uses realistic waveguide length coming out of mask layout design.

The model was applied to a Si_3N_4-based structure. The straight and ring waveguide cross-sectional structure and dimensions have been chosen as a compromise between single-modeness, available fabrication technology limitations, and losses for operation at visible wavelength. For such realistic structure, the model was applied to find the optimal coupler gap. By taking 20dB as insertion loss budget, operating the circuit at resonant wavelength nearest to 632.8nm, and taking realistic phase detection limit, a theoretical refractive index detection limit of 1.5E-9 RIU was obtained at the optimal gap size with acceptable fabrication technology accuracy tolerance.

Acknowledgement

The authors thank J. Čtyroký for the permission to use their film mode matching bend solver for this work. This work is supported by STW Technology Foundation through project TOE. 6596.

References

[1] C. Y. Chao and L. Y. Guo, *J. Lightwave Technol.* **24**, 1395-1402, (2006).
[2] H. P. Uranus and H. J. W. M. Hoekstra, *J. Lightwave Technol.* **25**, 2376-2384 (2007).
[3] R. Stoffer, K. R. Hiremath, M. Hammer, L. Prkna, and J. Čtyroký, *Opt. Commun.* **256**, 46-67 (2005).

Resonator chains of 2-D square dielectric optical microcavities

Manfred Hammer
MESA[+] Institute for Nanotechnology, University of Twente, Enschede, The Netherlands
m.hammer@math.utwente.nl

Chains of coupled square dielectric cavities are investigated. Resonant transfer of optical power can be achieved along quite arbitrary, moderately long rectangular paths, even with individual standing-wave resonators of limited quality. We introduce an ab-initio coupled mode model that helps to interprete the numerical results.

Summary

Coupled-resonator optical waveguides (CROWs) have been discussed already for some years [1] as a means to realize waveguiding along paths with small-size bends. Concepts based on series of microring resonators or sequences of defects in photonic crystal slabs [2] exist. As an alternative, in this contribution we consider chains of simple square dielectric cavities, that support a single specific standing wave resonance in the wavelength region of interest. In line with the fourfold symmetry of their resonant field pattern, the individual cavities are arranged sequentially on a discrete rectangular mesh, with guided-wave excitation at one end of the chain. The figure shows an example. Rigorous semianalytical simulations based on quadridirectional eigenmode propagation (QUEP) [3] enable convenient numerical experiments on these rectangular, piecewise constant configurations.

As some step towards an interpretation of the spectral features we look at an intuitive coupled mode theory (CMT) model for the resonator chains. The overall field in the chain is assumed to consist of bidirectional versions of the guided mode of the bus core, with variable local amplitudes, together with the identical, properly positioned resonant field patterns of the individual cavities, each multiplied by a single scalar coefficient. These latter fields can be approximated quite well by a superposition of suitable slab mode profiles, oriented along the two coordinate axes [4]. Then one proceeds along the hybrid CMT approach of Ref. [5]: By variational means one extracts a linear system of equations for the coefficients of the resonator fields, and for the amplitude functions of the bus modes, discretized in terms of finite elements, as unknowns. Note that no free parameters are introduced; the model, however, disregards any radiative losses (so far), and thus cannot be more than an approximation of the resonator chain in a kind of high-Q limit.

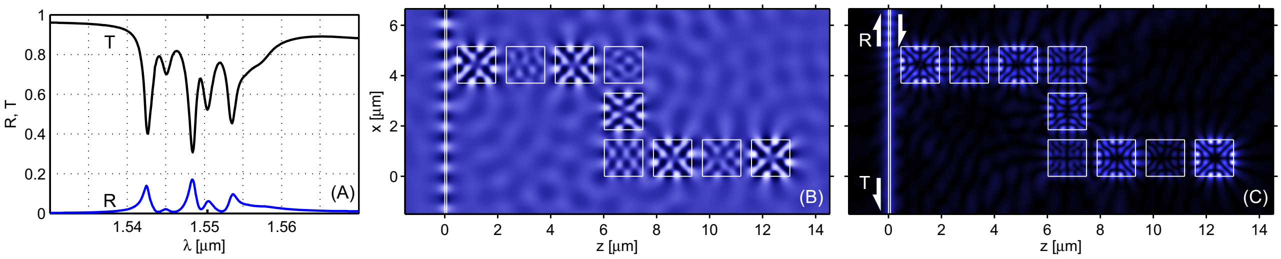

A chain of square microresonators, 2D-TE QUEP simulations [3] for a double bend configuration with refractive indices 1.45 *(background) and* 3.4 *(bus core, cavities), waveguide core width* $0.073\,\mu m$*, cavity width and height* $1.451\,\mu m$*, gaps* $0.4\,\mu m$*. Spectral guided-wave transmission and reflection (A); for vacuum wavelength* $\lambda = 1.5504\,\mu m$*: time snapshot of the physical principal electric field* E_y *(B), and field modulus* $|E_y|$ *(C).*

References

[1] A. Yariv, Y. Xu, R. K. Lee, and A. Scherer. *Optics Letters*, 24(11):711–713, 1999.
[2] J. Scheuer, G. T. Paloczi, J. K. S. Poon, and A. Yariv. *Optics & and Photonics News*, 16(2):36–40, 2005.
[3] M. Hammer. *Optics Communications*, 235(4–6):285–303, 2004.
[4] M. Hammer. *Optics Communications*, 214(1–6):155–170, 2002.
[5] M. Hammer. *Journal of Lightwave Technology*, 25(9):2287–2298, 2007.

Modeling of 2D Transient Responses in Stratified Cylindrical Structures

Nataliya Sakhnenko[1], Alexander Nerukh[1], Trevor Benson[2] and Phillip Sewell[2]
[1]*Kharkov National University of Radio Electronics, 14 Lenin Ave., Kharkov, 61166, Ukraine*
[2]*George Green Institute for Electromagnetics Research, University of Nottingham, University Park, Nottingham, NG7 2RD, UK*
e-mail: n_sakhnenko@yahoo.com

The transient electromagnetic field in a radially stratified dielectric cylinder with time-varying material properties is investigated by virtue of an analytical-numerical approach.

Summary

Multilayer cylindrical structures can be used as practical models in a wide variety of applications. Dynamic systems whose materials are varying in time have gained interest recently because they demonstrate new physical effects with a wide range of potential applications in optical communications and quantum information processing [1, 2].

To investigate the main features of electromagnetic transients evolving in complex cylindrical structure with time-varying materials a model problem is considered. The model problem is an investigation of the transformation of an electromagnetic field in a radially stratified cylindrical resonator placed in an unbounded lossless dielectric background medium. In a certain dielectric layer the permittivity changes its value at zero moment of time; this leads to a complex transition of the electromagnetic field which has existed in the resonator. The main goal of the investigation is to determine in what way the initial field transforms in response to the time variation of permittivity.

The solution of the problem presented consists of a strictly analytical formulation, deriving exact expressions which are then analysed using an analytical-numerical approach. By applying the Laplace transform directly to the wave equation, and including initial and boundary conditions at the circular interfaces, we arrive at a system of algebraic equations to find the unknown expressions. The resulting field in the time domain is obtained as the Laplace inverse transform via the residue series and a rapidly convergent integral along the branch cut in the complex plane. The analysis leads to a computationally straightforward and efficient method for obtaining transient fields.

Variation of the wave propagation velocity in one cylindrical layer of the structure leads to strong wave distortion. The field perturbation begins in the layer with the time-varying permittivity and propagates in opposite directions, occupying the other layers as well as the space outside the resonator. The transient waves evolve during reflections from the multiple dielectric interfaces. In the case when the initial field exists without an external source (e.g. the eigen-mode of the structure under consideration) then the time changing of the permittivity leads to a steady state regime where the frequency of the initial wave changes but the field pattern stays the same. Excitation of the higher modes with the same angular dependence as the initial one is possible in the case when the edge of the layer whose properties change is placed in the vicinity of the primary field amplitude maxima [3]. If the initial field has an external source then the temporal change of dielectric permittivity inside the resonator leads to a complicated transient process caused by the excitation of all modes of the resonator in its new state and an associated transformation of the near-field pattern.

References

[1] M. Yanik and Fan, S. *Physical Review* A. **71**, 013803 (2005).
[2] E. Reed, M. Soljacic, J. Joannopoulos, *Physical Review Letters*, **90**, n. 20, 203904 (2003).
[3] N. Sakhnenko, A. Nerukh, in *Proc. MSMW* 2007, Kharkov, Ukraine, 357-359 (2007).

Application of the Method of Single Expression for Analysis of Plane EM Wave Oblique Incidence on Multilayer Structures with Arbitrary Permittivity and Permeability

Hovik V. Baghdasaryan[1], Tamara M. Knyazyan[1], Tigran H. Baghdasaryan[2] and Grigori G. Eyramjyan[1]

[1] *Fiber Optics Communication Laboratory, State Engineering University of Armenia 105, Terian str., Yerevan 0009, Armenia*

hovik@seua.am

[2] *Optics Department, Physics Faculty, Yerevan State University, 1 Alex Manoogian str., 0025, Armenia*

Method of single expression (MSE) has been developed for the analysis of plane EM wave oblique incidence on multilayer structures comprising layers of arbitrary permittivity and permeability. Optical characteristics of the structures are obtained and discussed.

Summary

In the last years there is an increasing scientific and technological interest towards creation of new artificial materials with complex permittivity and permeability and their applications in specific devices possessing unusual electromagnetic properties [1-3]. In this connection, correct wavelength-scale analysis of optical characteristics of multilayer structures based on artificial materials is an important stage before their costly fabrication process. All existing computational methods require in advance the knowledge of a waveform in a layer, and as a consequence use refractive index for description of wave propagation in each layer of the structure. In the case of doubly negative permittivity and permeability this brings to uncertainty in the sign of refractive index. At the same time there is another method, namely the method of single expression (MSE) [4-6] applicable for boundary problem correct solution, where no refractive index is used in describing resultant amplitude of plane EM wave in constituting layers of a complex structure. The MSE operates directly with permittivity and permeability of a complex material independently from any combinations of their signs. The MSE has been recently extended for a correct electrodynamical analysis of plane EM wave normal incidence on a slab with complex permittivity and permeability [6].

In the current work a comprehensive electrodynamical simulation of optical properties of a multilayer structure comprising layers of arbitrary permittivity and permeability at wave oblique incidence is performed by the MSE. A complete set of mathematical expressions for incidence of TE and TM plane EM waves on multilayer structures having complex permittivity and permeability are derived for the first time. Reflectance and transmittance of the multilayer structures with arbitrary permittivity and permeability along with distributions of optical field amplitude and power flow density are analysed and discussed.

References

[1] J.B. Pendry, *Phys. Rev. Lett.* **85**, 3966 - 3969 (2000).
[2] M. Scalora, et al., *Optics Express*, **15**, 508-523 (2007).
[3] Pu Zhang, Yi Jin, and S. He, *Optics Express*, **16**, 3161-3166 (2008).
[4] H.V. Baghdasaryan: Method of Backward Calculation, in *Photonic Devices for Telecommunications: How to Model and Measure*, G. Guekos, Ed., Springer-Verlag, (1999).
[5] H.V. Baghdasaryan and T.M. Knyazyan, *Opt. and Quantum Electron.* **31,** 1059-1072 (1999).
[6] H. V. Baghdasaryan and T. M. Knyazyan, *in Conf. Proceed. ICTON 2006*, Nottingham, UK, Mo.B2.4, 13-18 (2006).

Modeling of Waveguide Structures with Crossed Discretization lines

Stefan F. Helfert and Reinhold Pregla
FernUniversität in Hagen, 58084 Hagen, Germany
Stefan.Helfert@FernUni-Hagen.de *R.Pregla@FernUni-Hagen.de*

It is shown how the accuracy can be improved when waveguide structures are analyzed. It has been found that the edges may cause problems. Therefore, this problem is treated as well.

Summary

When designing circuits, the accurate determination of the eigenmodes in waveguides is a crucial problem. One of the algorithms for ths purpose is the Method of Lines (MoL) [2]. We discretize in one direction (the horizontal in Fig. 1) and apply analytic expressions in the remaining ones. Now, to improve the performance (e.g. to analyze the rib waveguide shown in Fig. 1a), we treat the rib region in a special way: here we use additional discretization lines in vertical direction, allowing us to use analytic expressions also for the horizontal direction. The principle had been described in [3]. It should be stressed that we do not use a two-dimensional discretization.

The developed expressions were applied to determine the propagation constants of the benchmark-problem described in [1], where the normalized effective index B was computed. Fig. 1b shows the results for the quasi-TM polarization. Using crossed discretization lines (MoL-D2) improves the results (in terms of agreement with the literature) compared to results obtained with one direction of discretization (MoL-D1) alone. It should however be mentioned that the TE-case does not perform that good, requiring further studies.

A closer inspection shows that problems might be caused by the edges. Though this problem is known for a long time, a rigorous analytical solution is not known yet (to the best of the author's knowledge). Non of the (vectorial-)field components has to be zero at the edge, but some of them have poles there. Recently [4] the treatment of poles in finite difference schemes has been described. To treat the behavior of the fields correctly in the MoL we did some examinations that shall be shown as well.

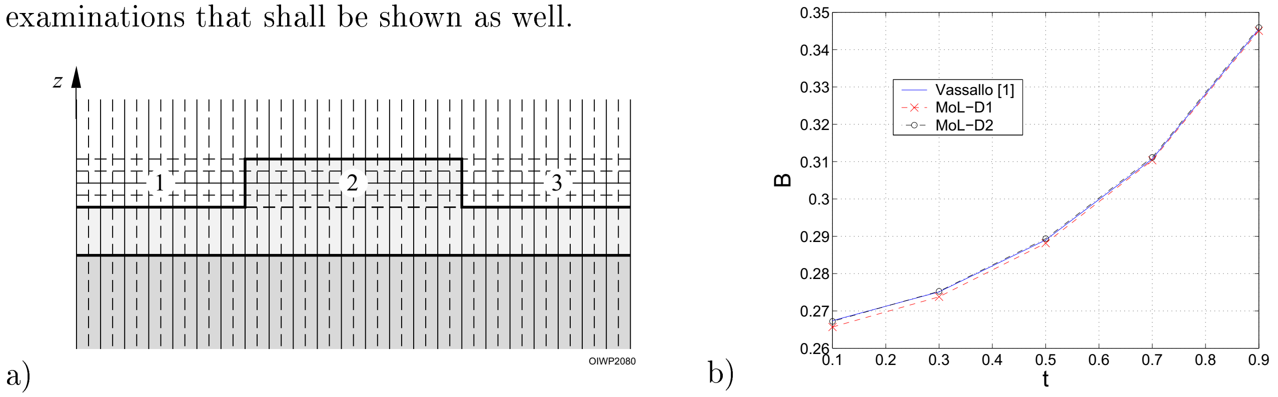

Fig.1. a) Rib-waveguide: discretization in horizontal direction and additional discretization in vertical direction in the rib; b) Normalized propagation constant B as function of the height of the guiding layer in a rib waveguide; Vassallo: results from [1], MoL-D1: horizontal discretization only, MoL-D2: vertical + horizontal discretization

References

[1] C. Vassallo, *Opt. Quantum Electron.*, vol. 29, pp. 95–114, 1997.
[2] R. Pregla and W. Pascher, in *Numerical Techniques for Microwave and Millimeter Wave Passive Structures*, T. Itoh, (Ed.), pp. 381–446. J. Wiley Publ., New York, USA, 1989.
[3] R. Pregla, in *OSA Integr. Photo. Resear. Tech. Dig.*, Victoria, Canada, 1998, vol. 4, pp. 139–141.
[4] G. R. Hadley, *J. Lightwave Technol.*, vol. 20, pp. 1219–1231, 2002.

Accurate Reconstruction of Gradient Index Profile of Planar Optical Waveguides by Two Sets of Measurements

Nikolai Nikolaev
Peoples' Friendship University of Russia,6 Miklukho-Maklaya St., Moscow 117198, Russia
ne_nikolaev@mail.ru

We demonstrate effective and accurate procedure of retrieval of gradient refractive index profile of planar waveguides using measurements of the propagation constant and the power fraction propagating into the external layer for two different external media.

Summary

With widened usage of gradient-index waveguides like plastic or polymer ones, reconstruction of gradient index profile of optical waveguides is of great demand for both synthesis and diagnostics purposes. All experimental techniques developed for the index profile retrieval require implementing some theoretical model for the reconstruction.

We reported previously on rigorous semi-analytical approach to reconstruct profiles of refractive index in gradient-index planar optical waveguides using Shift Formulae Method (SFM) [1, 2]. The profile was described by SFM formula with the shape determined by three parameters. To reconstruct it, values of propagation constants for three different external refractive indices from three measurements we used as an input data.

In this communication, we elaborated the technique of the gradient index retrieval by measurements for just two different external media (measuring propagation constant and a fraction of power which propagates into the external layer), which reduces measurements for obtaining the initial data to two sets, using two different external media. Mathematical model used to describe the profile [3-5] is flexible enough to represent smooth profiles as Gaussian one, complementary-error function profile and many others, including those with hollow centre. We show that this technique allows one to reconstruct the exact refractive index profile.

Compared with similar technique used with other methods [5], the Shift Formulae Method allows reconstructing the waveguide profile using less external effective indices, and with higher accuracy.

References

[1] N.E. Nikolaev and V.V. Shevchenko, *Proc. XIth International Workshop on Optical Waveguide Theory and Numerical Modelling*, April 4-5, Prague, Czech Republic (2003).

[2] N.E. Nikolaev and V.V. Shevchenko, *Optical and Quantum Electronics*, **39**, No 10-11, 891-902 (2007).

[3] N.E. Nikolaev and V.V. Shevchenko, *J. of Commun. Technology and Electronics*, 43, No 6, 651 (1998).

[4] V.V. Shevchenko, *Sov. J. of Commun. Technology and Electronics*, **31**, No 9, 28 (1986).

[5] K.S. Chiang, C.L. Wong, S.Y. Cheng, and H.P. Chan, *J. Lightwave Technol.*, **18**, 1412-1417 (2000).

Dynamical systems in nonlinear optics: Maxwell-Bloch models

John M. Arnold
University of Glasgow, Department of Electronics and Electrical Engineering, Oakfield Avenue, Glasgow G12 8QQ, United Kingdom
jma@elec.gla.ac.uk

A theory of nonlinear optics is developed, consisting of varieties of Maxwell-Bloch systems.

Summary

Maxwell-Bloch systems, consisting of electromagnetic wave equations driven by polarisation distributions that are determined quantum-mechanically, are prototype models of a wide range of dynamical systems in nonlinear optics, including harmonic generation, multiple wave mixing, soliton formation and laser amplification. In some simplified models, the Maxwell-Bloch system is completely integrable, meaning that there exists an infinite number of conserved quantities formed from polynomials of the fields and their derivatives. The known integrable systems are of two types: (i) reduced Maxwell-Bloch (RMB), in which the wave is approximated as unidirectional and the quantum system has a small number of degrees of freedom; (ii) envelope-wave systems with a 2-level atomic system as the polarisation element. In both cases the quantum system is nondissipative and the wave is lossless. When dissipation must be included in the models, the systems are no longer integrable, but in cases of weak dissipation approximate solutions can be described by means of perturbation theory in which the invariants are permitted to evolve slowly in time.

1-dimensional RMB systems with periodic spatial boundary conditions are very good models for self-oscillating self-pulsating lasers, exhibiting dynamical phenomena such as bifurcation, mode-locking and chaos. In these models dissipation in the quantum system is represented by adapting the population parts of the coherent density matrix to the form of rate equations, which permits the modelling of both saturable gain and saturable absorption in different sections of the atomic medium. Because these models are intrinsically dissipative, they are not exactly integrable. The theoretical question then arises as to how much can be said about the types of solutions of these dynamical systems, their stability and their trajectories. Qualitative methods are known for the study of aspects of this kind of problem in dynamical systems, but the particular RMB system has hardly been subjected to much systematic analysis in this way.

One interesting and potentially significant outcome of a qualitative analysis of the dissipative periodic RMB system is that there are two distinct regimes of mode-locking, the first being a conventional one in which saturable gain and saturable absorption, each with different relaxation times, cooperate to establish a stable intracavity pulse, and the second being pure soliton formation in the cavity with some weak assistance from the dynamical dissipation mechanisms. The soliton formation mechanism is preferred at shorter pulse time scales than those of the gain balance mechanism. It is not known what the stability conditions of these two mechanisms are when they co-exist, nor what dynamical trajectories link these states to each other, to bifurcations of CW or quiescent states, and other important dynamical properties.

Efficient Multiresolution Time Domain Analysis for Second Harmonic Generation Integrated Devices

R. Letizia[1] and S. S. A. Obayya[1]
[1] *University of Leeds, School of Electronics and Electrical Engineering, LS2 9JT Leeds, UK*
s.s.a.obayya@leeds.ac.uk

Summary

Despite its many capabilities, the numerical dispersion effect of conventional Finite Difference Time Domain (FDTD) scheme, demands a cell size of 15-20 times less than the minimum simulated wavelength (λ_{min} /15) and this results in a huge computational overheads in the analysis of Second Harmonic Generation (SHG) devices as they involve the propagation of half of the fundamental wavelength. Alternatively, the Multiresolution Time Domain (MRTD) approach for the analysis of SHG photonic devices is suggested here. The developed scheme relies on the use of interpolating scaling-functions in the context of method-of-moments in order to study the nonlinear effect in $\chi^{(2)}$ materials. The higher linear dispersion properties proved by this method allow the use of a much coarser grid resolution with a good accuracy relative to FDTD. As an application of the developed scheme, a new design for generating and selecting the SH frequency in a GaAs PhC-based device is proposed, Fig. 1. SH wave is generated in the "primary waveguide" through nonlinear effect. The process of SH selection is enhanced then, through a series of PhC-microcavities that are finely tuned to resonate at the SH frequency. Their arrangement maximizes the SH-transfer to the secondary waveguide. Coupling the waveguide to a tuned microcavity, is applied here for the first time, to the best of the authors' knowledge, to design a high efficiency SHG-based converter. Figure 2 shows the spectral distribution of both fundamental and SH waves at the output of the converter. It can be noted that only 0.5% of the fundamental field can be still detected and the efficiency has significantly increased to about 8.5% that is about three times higher than the best value reported in literature [1]. More results that show the efficiency of the proposed method will be presented.

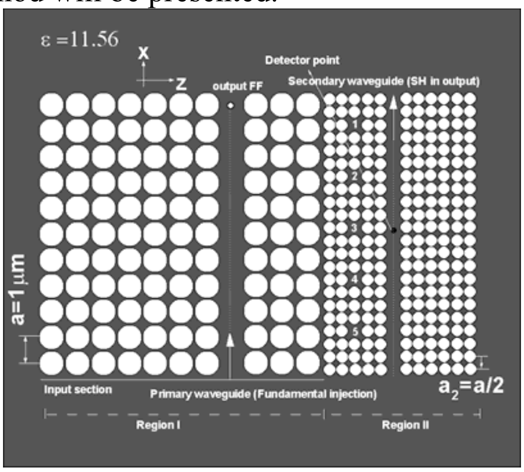

Fig. 1. Schematic diagram of frequency converter consisting of two PhC-waveguides (holes in GaAs with radius 0.475 μm) coupled through a row of microcavities.

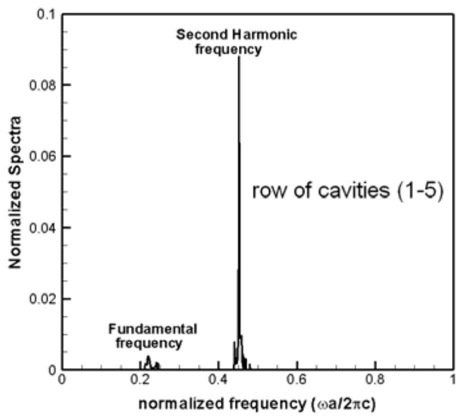

Fig. 2. Normalized spectra of the fundamental and SH waves at the output in the case of a row of five cavities (from cavity 1 to cavity 5).

References

[1] Satoh, N. Yoshida, S. Kitayama, and S. Konaka, *IEEE Trans. on Microwave Theory and Tech.*, vol. 54, n. 1, pp. 210-215, Jan. 2006.

A Novel Approach to Model Linear and Nonlinear Dispersion with ADE-FDTD

S. Schild[1], M. Ammann[1], N. Chavannes[2] and N. Kuster[1]
[1]*Foundation for Research on Information Technology in Society (IT'IS), ETHZ*
schilds@itis.ethz.ch

[2]*Schmid & Partner Engineering AG, 8004 Zurich, Switzerland*

A novel algorithm is derived based on ADE-FDTD that allows to model any combination of Drude- and Lorentz-Dispersion, Kerr-Effect and Raman-Scattering. Implemented in a full 3D simulation platform, it has been applied to various benchmarks and examples.

Summary

Applications in photonics and metamaterials involve media with frequency and intensity dependent polarisations. A novel finite-difference time-domain (FDTD) algorithm for arbitrary dispersive media (ADM) allows to model materials with linear multipole Drude- and Lorentz dispersion as well as Kerr-Effect and Raman-Scattering. The ADM algorithm is significantly faster than previously reported solutions [1] while providing full modularity. Moreover, it has proven stability conditions for every effect as well as the applied fixed-point iteration.

Methodology

The finite-difference formulation of the total polarisation $\mathbf{P}$ in the presence of Drude- and Lorentz-Poles, Kerr-Effect and Raman-Scattering is given by

$$\mathbf{P}^{n+1} - \mathbf{P}^n = \sum_{l,d=1}^{L,D} (\mathbf{P}_{l,d}^{n+1} - \mathbf{P}_{l,d}^n) + \epsilon_0 (R^{n+1}\mathbf{E}^{n+1} - R^n \mathbf{E}^n) + \alpha\epsilon_0\chi_0^3 (|\mathbf{E}^{n+1}|^2 \mathbf{E}^{n+1} - |\mathbf{E}^n|^2 \mathbf{E}^n).$$

To avoid the costly matrix inversion in each Newton-iteration when solving for the non-linearity in $\mathbf{E}^{n+1}$ and to preserve modularity, the new variable $I^n \doteq |\mathbf{E}^n|^2$ is introduced. It is shown that the update equation of I^n is badly conditioned for the Newton-method but can be solved efficiently through a fixed-point iteration with guaranteed convergence. Despite the fixed-point iteration converging slower than the Newton-iteration, the new formulation is faster as far less computations per iteration are required.

Results

The algorithm has been integrated into the EM simulation platform SEMCAD X. The modularity allows to use conventional solvers including hardware accelerated solutions to solve the linear part and to add the nonlinear contributions where necessary.

The algorithm was implemented and tested in full 3D using generic benchmark simulations of metamaterials simulating effects such as gap-solitons. Additionally, the algorithm has been verified by application and comparison to research examples in photonics. Specific considerations regarding the applicability of FDTD to nonlinear phenomena such as discretization, stability, and excitation are discussed.

References

[1] Greene, J.H. and Taflove, A., *Opt. Express*, Vol. 14, No. 18, 8305–8310, 2006.

Full vectorial modelling of femtosecond bullets for laser inscription of photonic structures

Holger Schmitz and Vladimir Mezentsev
Photonics Research Group, Aston University, Birmingham B4 7ET, United Kingdom
v.mezentsev@aston.ac.uk

Full vectorial analysis of nonlinear propagation of femtosecond (fs) laser pulse is presented. Full set of Maxwell's equations coupled to standard Drude model of the generated plasma is modelled. The results are compared with the orthodox models based on paraxial envelope approximation.

Summary

Microfabrication of photonics devices by means of intense fs laser pulses has emerged as a novel technology during the last decade [1]. A range of photonic structures and devices has been demonstrated recently based on permanent modification of refractive index after fs inscription (see e.g. [2] and references therein). This technology has the great potential but it also reveals intrinsic difficulties. A broad class of technological issues relates to the complexity of inherently nonlinear processes involved in fs pulse propagation and material modification. Additionally, there are numerous application–specific constraints to be considered, notably the common requirement for a refractive index modification pitch size much smaller than the inscribing wavelength. Nonlinear propagation of intense fs laser pulses is an extremely complicated phenomenon featuring complex multi-scale spatiotemporal dynamics of the laser pulses [3, 4]. From the numerical standpoint, the problem is extremely stiff as the propagating fs pulse undergoes very fast evolution. We have utilized a principal approach based on FDTD modelling of the full set of Maxwell's equations coupled to the conventional Drude model for generated plasma. Nonlinear effects are also included such self-phase modulation, multi-photon and plasma absorption. Such an approach resolves most problems related to extremely tight focusing, when paraxial approximation is not applicable and correctly describes creation of and scattering on inscribed structures of subwavelength size. Optimization has been performed in terms of the geometry of the distribution of the residual electron-hole plasma left behind the fs laser pulse. The recombination of this plasma is a primary mechanism for the energy transfer and eventual modification of the material. The plasma density relates to the material temperature [5]. After a complex thermoplastic relaxation [6] the frozen profile of refractive index has a spatial dimension of about a half of that of the original cloud of plasma [5]

References

[1] H. Misawa and S. Juodkazis, ed., *3D Laser Microfabrication. Principles and Applications*, Wiley–VCH, Weinheim (2006).

[2] V. Mezentsev, J. Petrovic, M. Dubov, I. Bennion, J. Dreher, H. Schmitz, and R. Grauer, *Femtosecond laser microfabrication of subwavelength structures in photonics,* Proc. SPIE 6459, paper 64590B (2007).

[3] A. Couairon,., A. Mysyrowicz, *Femtosecond filamentation in transparent media,* Physics Reports **441** 47-189 (2007)

[4] L. Berge, S Skupin, R Nuter, J Kasparian, and J-P Wolf, *Ultrashort filaments of light in weakly ionized, optically transparent media*, Rep. Prog. Phys. **70** 1633-1713 (2007)

[5] X. Zhang, X. Xu, and A. Rubenchik, *Simulation of microscale densification during femtosecond laser processing of dielectric materials*, Appl. Phys. **A79**, 945–948 (2004)

[6] J.S. Petrovic, V. Mezentsev, H. Schmitz, and I. Bennion, *Model of the femtosecond laser inscription by a single pulse*, Optical and Quantum Electronics, **39**, 939-946 (2007)

Design and control of metamaterials with negative refractive index

S.Anantha Ramakrishna
Department of Physics, Indian Institute of Technology Kanpur, Kanpur 208016, India
sar@iitk.ac.in

The design principles of metamaterials that show negative constitutive material parameters such as negative dielectric permittivity (ε), negative magnetic permeability (μ) and negative refractive index, and the control of the material properties by imbedding nonlinear media within the metamaterial structures will be discussed.

Summary

The past decade has seen the emergence of a new class of composite materials structured at subwavelength lengthscales that show a variety of novel electromagnetic and optical properties [1] such as negative refraction [2], electromagnetic invisibility [3] and imaging beyond the diffraction limit[4]. These materials which have been termed *metamaterials* depend on structural resonances and the accompanying dispersion for their properties. In this talk, I will discuss the design principles of these metamaterials and their propeties. By imbedding non-linear materials in critical locations within the metamaterial structure, one can utilize the large local field enhancements within these materials to control the properties of these materials. For example, I will discuss the bistability of split-ring resonator media when Kerr non-linear materials are imbedded within the gaps of the split-rings. The properties of metamaterials such as cut-wire media or split-ring resonator media can be well controlled by imbedding resonant atomic media within the structures. These ideas open the door to futuristic and robust metamaterials whose properties can be controlled by externally applied fields.

References

[1] For a review, see S.A. Ramakrishna, Rep. Prog. Phys. **68**, 449–521 (2005).
[2] V.G. Veselago, *Sov. Phys. – Usp.* **10**, 509 (1968)
[3] J.B. Pendry, D. Schurig and D.R. Smith, *Science* **312**, 1780–1782 (2006).
[4] J.B. Pendry, *Phys. Rev. Lett.* **85**, 3966–3969 (2000).

Transparent expressions for group velocity and sensitivity to index changes of Photonic Crystal Waveguide modes

Hugo J.W.M. Hoekstra[1] and Theo P. Valkering[2]

[1] *University of Twente, MESA+ Institute of nanotechnology, P.o. box 217, 7500 AE Enschede, The Netherlands*

h.j.w.m.hoekstra@utwente.nl

[2] *University of Twente, Faculty of Science and Technology, P.o. box 217, 7500 AE Enschede, The Netherlands*

On the basis of Maxwell's equations and Bloch's theorem basic relations for modes propagating in photonic crystal waveguides are derived. The physical meaning and possible experimental implications are discussed.

Summary

Slow light propagation of photonic crystal waveguide (PhC-WG) modes is currently widely investigated to study the strong matter-light interaction for among others nonlinear effects [1], time delays [2] and sensors [3, 4]. Hereby the group velocity is often considered to be a key parameter. For such studies and also for a better understanding of the underlying physics it is quite relevant to have simple, explicit expressions for the modal group velocity and the sensitivity to index changes in terms of the corresponding modal field or intensity pattern.

Such expressions will be derived in a straightforward way from Maxwell's equations and Bloch's theorem. In particular it will be established, in the frequency domain and including the effect of material dispersion, that the modal group velocity equals the ratio of the spatially averaged energy flow and energy density. The relations will be applied on a number of relatively simple structures. In addition to that, the potential of the derived relations for the interpretation of experimental results will be discussed.

Acknowledgements

This work was supported by NanoNed, a national nanotechnology program coordinated by the Dutch ministry of Economic Affairs and the STW Technology Foundation project TOE.6596.

References

[1] D.M. Beggs, T.P. White, L. O'Faolain and T.F. Krauss, *Optics Lett.*, **33**, 147-149 (2008)

[2]M.L. Povinelli, S.G. Johnson and J.D. Joannopoulos, *Optics Express* **13**, 7145-7159 (2005)

[3] X.Y. Mao et al., *Chinese Phys. Lett.*, **25**, 141-143 (2008)

[4] W.C.L. Hopman et al., *IEEE J. of Select. Topics in Quant. Electron.*, **11,** 11-16 (2005)

Finite Volume Time Domain Analysis of Nonlinear Photonic Crystal Devices

D. Pinto and S.S.A. Obayya
School of Electronic & Electrical Engineering, University of Leeds, Leeds LS2 9JT, UK,
Tel. +44 113 343 2079, Fax +44 113 343 2032, email: S.S.A.Obayya@leeds.ac.uk

In this work, photonic crystals (PhCs) composed of nonlinear material have been thoroughly investigated with an accurate finite volume time domain (FVTD) method. The power-dependent characteristic of the nonlinear PhCs have been used for the realization of a filter with tunable properties.

Summary

Nonlinear materials have attracted a great deal of interest for a variety of research applications because of the potential to design new devices to meet the needs of a range of optical systems [1]. Photonic bandgap (PBG) materials, also known as photonic crystals (PhCs), have attracted great research attention because of their capability to control the propagation of the electromagnetic waves. For this reason, the combination of nonlinear material with photonic crystals opens up a new frontier for the development of high-performance devices for all-optical ultra-fast applications.

In the literature various modeling techniques have been proposed for the simulation of optical devices. Recently, research efforts have been directed towards the use of finite volume time domain (FVTD) method in computational electromagnetic problems [2]. The beauty of FVTD is that it combines the versatile and flexible meshing capabilities of finite element time domain (FETD) method in addition to being explicit (no solution of large system of equation is required) where only field updates are performed at each time step as in finite difference time domain (FDTD) method. For this reason, in this work a FVTD method has been developed and extended to be capable to deal with nonlinear material with Kerr-like dielectric material with an istantaneous nonlinear response.

The structure analysed in this work consist of a 3-rings PhC cavity composed by a dielectric material with refractive index n^2_2 =11.4 in in which a triangular pattern with lattice constant a = 0.650225 μm of air holes (n_1 = 1.0) with radius r=0.2a have been drilled, as shown in Fig.1. The center of the cavity has been filled with a nonlinear material with a nonlinear coefficient n_{nl} = 1.43x10^{-17} m^2/V^2. The structure has been excited with sources with different level of power and the different spectra, obtained through FFT of the time-domain responses, are shown in Fig. 2. From this figure can be observed the power-dependent property from the different resonant wavelengths of the structure excited with different levels of power.

More results on the exploit of this tunability property of nonlinear PhC cavity in the realisation of power-dependent PhC filters will be presented.

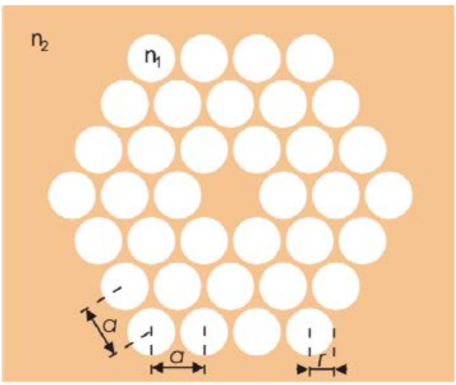

Fig. 1 Schematic diagram of the PhC cavity

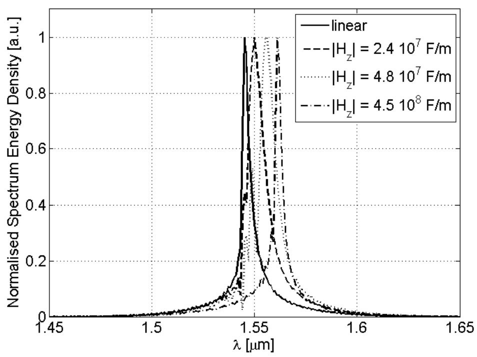

Fig. 2 Normalised spectra of the time domain responses of the cavity excited with different level of power

References

[1] H. Murata, M. Izutsu and T. Sueta, *J. Lightwave Technol.*, **16**, 833-840 (1998).
[2] S. Piperno, M. Remaki, and L. Fezoui, *SIAM J. Numer. Anal.*, **39**, 2089-2108 (2002).

Effects of Lattice Variations on Confinement in Photonic Crystal Microcavity using Green Tensor Method

Alexander A. Iskandar[1], Aimi Abass[1], Agoes Soehianie[1], Husin Alatas[2], May On Tjia[1] and Hugo J.W.M. Hoekstra[3]

[1] *Institut Teknologi Bandung, Physics of Magnetism and Photonics Group, Jl. Ganesa 10, Bandung 40132, Indonesia*

iskandar@fi.itb.ac.id

[2] *Bogor Agricultural University, Theoretical Physics Division, Jl. Raya Darmaga, Bogor 16680, Indonesia*

[3] *University of Twente, Integrated Optical Micro System Group, P.O. Box 217, 7500 AE Enschede, The Netherlands*

Electric field distribution in and around the 2D PC cavity was calculated for different lattice parameters using the Dyson formulation of the Green tensor. The results demonstrate the sensitive effects of structural variation of the photonic crystal on the effectiveness of field confinement in the cavity.

Summary

The Green's tensor method is known to offer remarkable advantages over the other computational schemes in avoiding the tricky treatment of boundary condition for finite system or finite computational domain and in its adaptability in handling small and subtle perturbations in the system. As such, it provides a powerful scheme for the development of numerical tools for modeling, simulation and exploration of structural variation giving rise to novel functionalities for photonic device applications.

We report in this paper the results of applications of a numerical program developed for the application of Green tensor method to the study of a 2D photonic crystal with defect. The Green tensor for more realistic background characterized by $\Delta\varepsilon(\vec{\mathbf{r}}'')$ was calculated from the homogeneous background Green tensor according to the Dyson formulation below,

$$\vec{\vec{\mathbf{G}}}(\vec{\mathbf{r}},\vec{\mathbf{r}}') = \vec{\vec{\mathbf{G}}}^B(\vec{\mathbf{r}},\vec{\mathbf{r}}') + \int_V d\vec{\mathbf{r}}''\vec{\vec{\mathbf{G}}}^B(\vec{\mathbf{r}},\vec{\mathbf{r}}'')\cdot k_0^2\Delta\varepsilon(\vec{\mathbf{r}}'')\vec{\vec{\mathbf{G}}}(\vec{\mathbf{r}}'',\vec{\mathbf{r}}') . \quad (1)$$

This allow the conversion of the implicit integral equation for finding the field solution into an explicit one as follows,

$$\vec{\mathbf{E}}(\vec{\mathbf{r}}) = \vec{\mathbf{E}}^0(\vec{\mathbf{r}}) + \int_V d\vec{\mathbf{r}}'\vec{\vec{\mathbf{G}}}(\vec{\mathbf{r}},\vec{\mathbf{r}}')\cdot k_0^2\Delta\varepsilon(\vec{\mathbf{r}}')\vec{\mathbf{E}}^0(\vec{\mathbf{r}}') . \quad (2)$$

The numerical calculation was implemented by a recursive scheme modified from a previously suggested one. This program was applied to the study of a 2D photonic crystal with a point defect structure was considered for its application as a microcavity for the TM wave. The electric field distribution in and around the cavity was calculated for different lattice parameters. The result demonstrated the sensitive effects of structural variation of the photonic crystal on the effectiveness of field confinement in the cavity.

References

[1] O.J.F. Martin, N.B. Piller, *Phys. Rev.* **E 58** (1998) 3909.
[2] O.J.F. Martin, A. Dereux and C. Girard, *J. Opt. Soc. Am.* **A 11** (1994) 1073.
[3] A.D. Yaghjian, *Proc. of the IEEE* **68** (1980) 248.
[4] J.M. Elson and K. Halterman, *Opt. Exp.* **12** (2004) 4855.

Application of Dirichlet-to-Neumann Maps in Numerical Modelling of Photonic Structures

Ya Yan Lu
Department of Mathematics, City University of Hong Kong, Kowloon, Hong Kong
mayylu@cityu.edu.hk

The Dirichlet-to-Neumann (DtN) map of a domain is an operator that maps the wave field on the boundary of the domain to its normal derivative. We describe applications of the DtN maps in numerical modelling for photonic crystals, optical waveguides and diffraction gratings.

Summary

While time domain numerical methods are widely used, frequency domain numerical methods can more easily take advantage of the geometric features. A photonic crystal (PhC) device, such as the Mach-Zehnder interferometer studied in [1], contains many unit cells, but there are only a very small number of distinct unit cells. The Dirichlet-to-Nuemann (DtN) map of a unit cell is an operator that maps the wave field on the boundary of the unit cell to its normal derivative. If we know the DtN maps of the unit cells, the numerical simulation of the PhC device can be carried out on the edges of the unit cells. This leads to a significant reduction in the total number of unknowns. In our earlier works, DtN maps have been used to develop efficient numerical methods for both boundary value problems (transmission and reflection spectra of finite PhCs [2, 3, 4]) and eigenvalue problems (band structures [5, 6, 7], line [8] and point [9] defect modes). In this paper, we report some recent applications of the DtN-map technique to 3D woodpile structures, leaky modes and weakly guided modes in PhC waveguides and to large PhC devices, such as the PhC Mach-Zehnder interferometer [1]. The DtN map technique is also useful for waveguide gratings where the structure is piecewise uniform in the propagation direction. The standard method relies on computing the eigenmodes in each uniform segment. The DtN-map method [10, 11] computes the DtN maps of each uniform segments instead. For diffraction gratings, the Fourier modal method has to use the crude staircase approximation when there are general sloping interfaces. Integral equation methods are somewhat complicated to implement due to their use of the quasi-periodic Green's function and lattice sums techniques. We report a DtN-map method where DtN maps of homogeneous sub-domains are calculated by much simpler boundary integral equations. Finally, we report some recent applications of the DtN-map method to modelling of second harmonic generation in both piecewise uniform waveguides [12] and photonic crystals.

References

[1] T. Fujisawa and M. Koshiba, *Journal of Lightwave Technology*, **24**, 617-623 (2006).
[2] Y. Huang and Y. Y. Lu, *Journal of Lightwave Technology*, **24**, 3448–3453 (2006).
[3] Y. Huang and Y. Y. Lu, *Journal of Computational Mathematics*, **25**, 337–349 (2007).
[4] S. Li and Y. Y. Lu, *Journal of the Optical Society of America A*, **24**, 2438–2442 (2007).
[5] J. Yuan and Y. Y. Lu, *Journal of the Optical Society of America A*, **23**, 3217–3222 (2006).
[6] J. Yuan and Y. Y. Lu, *Optics Communications*, **273**, 114–120 (2007).
[7] J. Yuan, Y. Y. Lu and X. Antoine, *Journal of Computational Physics,* **227**, 4617–3629 (2008).
[8] Y. Huang, Y. Y. Lu and S. Li, *Journal of the Optical Society of America B*, **24**, 2860–2867 (2007).
[9] S. Li and Y. Y. Lu, *Optics Express*, **15**, 14454–14466 (2007).
[10] L. Yuan and Y. Y. Lu, *IEEE Photonics Technology Letters*, **18**, 1967–1969 (2006).
[11] L. Yuan and Y. Y. Lu, *Journal of Lightwave Technology*, **25**, 3649–3656 (2007).
[12] L. Yuan and Y. Y. Lu, *Journal of the Optical Society of America B*, **24**, 2287–2293 (2007).

Analysis of waveguides bends and junctions

Reinhold Pregla, *Life Fellow, IEEE*
University of Hagen, Universitätsstrasse 27, 58084 Hagen, Germany
R.Pregla@FernUni-Hagen.de

In this contribution will be shown how optical waveguide bends and Y-junctions in different waveguide structures can be analyzed in an efficient way.

Summary

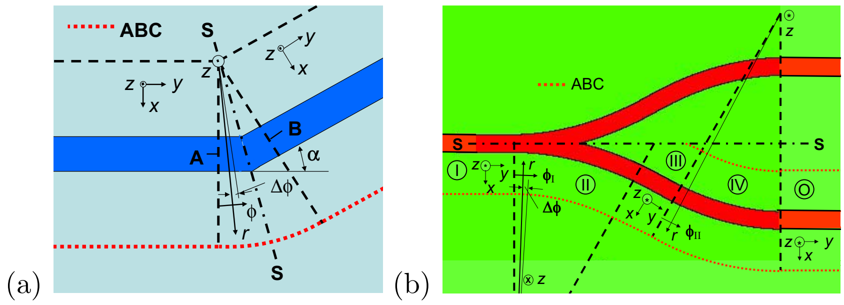

Fig.1. Bend (a) and Y-junction (b) in planar optical waveguides.

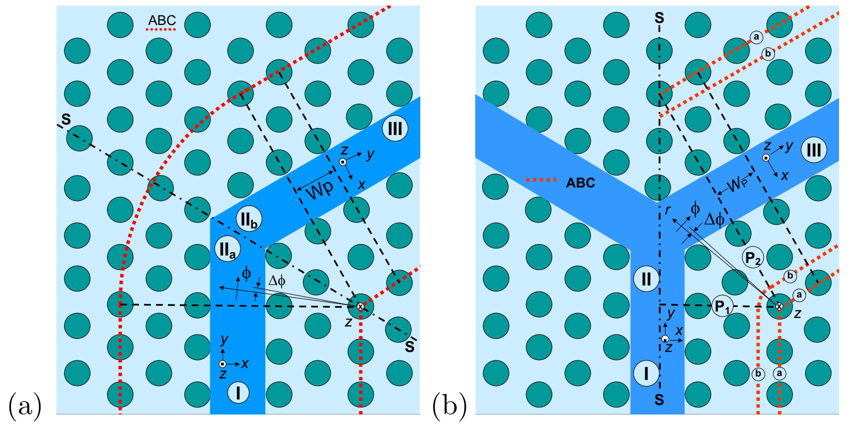

Fig.2. Bend (a) and Y-junction (b) in photonic crystals. The dark regions are introduced to indicate the main waveguide areas.

The Figures show somes examples of structures whose modeling shall be shown. To analyse them we use the Method of Lines (MoL)[1]. We divide the bends into suitable parts. The waveguide bends are symmetrical to plane S-S which devides the bends into an input and an output part. Each of these parts consists of homogeneous waveguide (Fig.1a) or a periodic waveguide (Fig.2a) and a bend section (in Fig.2b the parts IIa and IIb). We can obtain the properties from examining two cases, introducing an electrical or a magnetic wall in the symmetry plane. The sections I and III in Fig. 2b are periodic waveguide structures and can be analysed using Floquet modes with the algorithm described in [1]. The section IIa (IIb) in Fig.2a and the adequat section in Fig.1a are inhomogeneous. We use impedance/admittance transformation with finite differences in cylindrical coordinates for the ϕ−direction [2]. The Y-junctions (see Figs. 1b and 2b) are symmetric to the planes S-S. We introduce there again an electrical or a magnetic wall. In this way the analysis is performed with symmetrical and antisymmetrical modes. In Fig.1b we now have homogeneous parts in the input and output waveguide I and O and in the part IV. In Fig.2b we have homogeneous periodic parts in the sections I and III. In the inhomogeneous sections II we again apply impedance/admittance transformation with finite differences in cylindrical coordinates for the ϕ−direction. In section III in Fig.1b we perform this in Cartesian coordinates. The algorithm may also be used to analyse resonators that are important in nano technology[3].

References

[1] R. Pregla, "Analysis of Electromagnetic Fields and Waves: The Method of Lines", J. Wiley 2008.
[2] R. Pregla, *Optical and Quantum Electronics*, Vol. 38 (2006), pp. 3-17.
[3] R. Pregla, "Analysis of optical resonator structures", *ICTON 2008*, 22.-66.06.2008, Athens, Grease.

Use of the coupled modes theory for analysis of light scattering by the inclined reflector in optical waveguide

E.A.Kolosovsky[1], A.V.Tsarev[1]

[1] *Institute of Semiconductor Physics, Siberian Branch of Russian Academy of Sciences*
Prospect Lavrenteva, 13, Novosibirsk, 630090, Russia

tsarev@.isp.nsc.ru

We apply the theory of the coupled modes (CM) for the analysis of transmittance and scattering of guided TE mode by the inclined reflector located in an optical waveguide. Simulations by the CM method are very fast and are in excellent agreement with the computer experiments by the FDTD method.

Theory of coupled waves for optical beam scattering by the inclined reflector

We propose and investigate the new approach for the analysis of transmittance and scattering of guided *TE* mode by the inclined reflector located in an optical waveguide. Reflection of an inhomogeneous optical beam by the inclined reflector (see Fig. 1a) is executed for the first time semi-analytically under the theory of the coupled modes in view of interrelation and transformation of energy between all waves of discrete and continuous spectra of the optical 2D-waveguide (even and odd directed, radiating and evanescent). Results of calculation of light propagation through the inclined reflector in the form of thin (10-500 nanometers) homogeneous strip, obtained by our method and finite different time domain (*FDTD)* method are in excellent quantitative agreement (see Fig. 1b). Unlike *FDTD* our method has considerably higher (on one two order of magnitude) speed of calculation and needs smaller computer resources. Our results make a contribution in the theory of coupled mode and could be very interesting for analysis of multi-reflector filtering devices [2].

Acknowledgment. We thank Company RSoft Design Group, Inc for providing Rsoft Photonic CAD Suite 8.0 including BeamPROP software (see http://www.rsoftdesign.com) for BPM simulations.

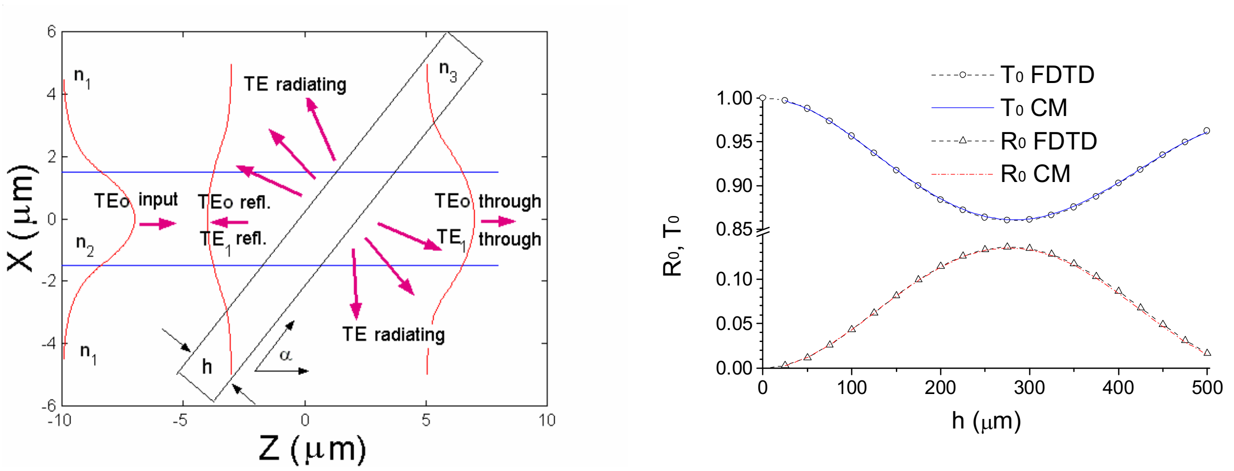

a) b)

Fig. 1. a) Geometry of optical beam studding the optical wave propagation in a waveguide with an inclined reflector by the theory of coupled modes. b) Reflection and transmitted coefficients R_0 and T_0 as a function of reflector width *h* for TE_0 mode propagated in the optical waveguide with the inclined reflector (n_3=2.4) placed under angle 45^0. SM – calculation under the theory of the theory of coupled modes, FDTD - calculation by method FDTD.

References

[1] D. Marcuse, Bell Syst.Technical J., **54**, 985-995 (1975).
[2] V. M. N. Passaro, F. Magno, A. Tsarev, Opt. Express, **13**, 3429-3437 (2005).

An Improved Perfectly Matched Layer in the Eigenmode Expansion Technique

Niels Gregersen[1] and Jesper Mørk[1]
[1] *DTU Fotonik, Department of Photonics Engineering*
Technical University of Denmark, Building 343, DK-2800 Kongens Lyngby, Denmark
ngr@com.dtu.dk

When employing the eigenmode expansion technique (EET), parasitic reflections at the boundary of the computational domain can be suppressed by introducing a perfectly matched layer (PML). However, the traditional PML suffers from an artificial field divergence limiting its usefulness. We propose a remedy.

Summary

In the EET [1] the structure is divided into layers along a propagation axis, and the field is expanded on the eigenmodes of each layer. In rotationally symmetric structures the eigenmodes can be described analytically leading to modest memory consumption and high performance. However, as with most simulation techniques the computational domain is bounded by metal walls, resulting in artificial parasitic reflections. These can be suppressed by implementing a PML [1], but at the cost of introducing a new artificial field perturbation.

As an example, we simulate the optical field in the vicinity of the nanowire analyzed in Ref. [2]. The geometry is illustrated in Fig. 1(a). A guided mode is traveling forward inside the wire and is diffracted at its top. The optical field for this geometry inside a metal cylinder of radius $R_0 = 2$ μm is illustrated in Fig. 1(b), and we observe an interference pattern indicating parasitic reflections. A regular PML can be implemented by changing the metal cylinder radius to $R^{PML} = R_0 + 0.1i$. The optical field illustrated in Fig. 1(c) shows that parasitic reflections are suppressed but also reveals an artificial field divergence creeping in from the sides at the layer interface. Adding more eigenmodes to the calculation only increases this artificial divergence.

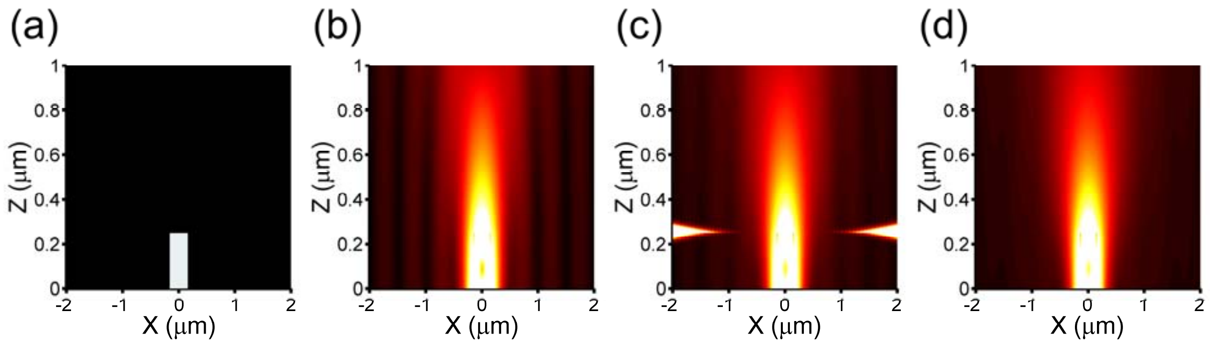

Fig. 1. Refractive index profile (a) and electric field amplitude without PML (b), with regular PML (c) and improved PML (d).

In this work, we show that when employing a regular PML with a fixed R^{PML}, the absorption at the boundary increases exponentially with the order n of the eigenmode, leading to numerical instability when the number of eigenmodes increases. We propose instead to fix the amount of absorption experienced by all eigenmodes by introducing a mode-dependent $R_n^{PML} = R_0 + f_n\, i$. The optical field using this improved PML implementation is illustrated in Fig. 1(d), and we observe that both the parasitic reflections and the field divergences are removed.

References

[1] P. Bienstman and R. Baets, Opt. Quantum Electron. **33**, 327-341 (2001).
[2] A. V. Maslov and C. Z. Ning, Opt. Lett. **29**, 572-574 (2004).

Interaction of light with subwavelength apertures: a comparison of approximate and rigorous approaches

Jan Fiala, Ivan Richter, and Milan Šiňor
Czech Technical University in Prague, Faculty of Nuclear Sciences and Physical Engineering, Department of Physical Electronics, Břehová 7, 11519 Prague 1, Czech Republic
ivan.richter@fjfi.cvut.cz

The interaction of an electromagnetic wave with various classes of subwavelength apertures is studied in detail, using several approximate and rigorous approaches. The attention is given to a comparison of these, revealing basic physical features of interaction. A practical aspect of structure realization is also mentioned.

Summary

A revelation of the transmission enhancement of the electromagnetic field through subwavelength structures (i.e. the observation that a periodic array of subwavelength apertures drilled in a metal film can reach the substantially higher transmission than expected), as was originally observed in [1], has initiated many questions and new studies in this area. This phenomenon was originally predicated to the excitation of surface plasmons and/or surface evanescent wave generation with Fabry-Perot resonances of evanescent waves in the aperture. But the question *what is the main contribution and the leading process* in the enhanced transmission phenomenon has not yet been fully answered since the physics is not completely understood. Also this work intends to contribute to this effort dealing with such light interaction with metal structures at the nanoscale. Particularly, we have analyzed in a detail the approximate physical models capable of, at least to some extent, understanding the physics of interaction and the effect of extraordinary transmission by propagating of light through various model subwavelength structures: single apertures, apertures with corrugations, on either input or both sides, and periodic aperture arrays. On the basis of the dispersion relation of *surface plasmon-polaritons* (SPP), the influence of SPP on the light propagation through the aperture was studied. Consecutively, the semi-analytical model was composed which is able to predict the enhanced transmission. Furthermore, the diffracted evanescent near-field was closely analyzed within the scope of the *diffracted evanescent wave model* (DEWM) and the influence of introduced surface corrugations was estimated. In a combination with the one-mode periodic model, the effect of the Fabry-Perot resonances of the fundamental aperture mode has also been studied. These studies led to the application of the so called *combined model* that appropriately combines the impacts of the DEWM and SPP model. The approximate analytical models were used in a combination with rigorous numerical methods (finite difference time domain method - FDTD and aperiodic rigorous coupled wave analysis ARCWA); their mutual comparison will be shown. As one of the examples of a primary interest here, the slit-groove diffraction problem has been intensively studied all over the world. The energy bounded to the fundamental mode of the aperture was rigorously analyzed in dependence on the mutual distance of the slit and groove [2] whereas Besbes *et al*. [3] confronted the data resulting from different rigorous numerical methods. As our contribution, we have compared the data from the approximate models to the rigorous results reaching a close correspondence with the combined model. Finally, practical aspects of structure realization will be also discussed.

References

[1] T. W. Ebbesen, H. J. Lezec, H. F. Ghaemi, T. Thio, P. A. Wolff, Nature **391**, 667 (1998).
[2] P. Lalanne, J. P. Hugonin, Nature Physics **2**, 551 (2006)
[3] M. Besbes et al., JEOS **2** 07022 (2007).

Variational coupled mode theory and perturbation analysis for 1D photonic crystal structures using quasi-normal modes

M. Maksimovic, M. Hammer, E. van Groesen
MESA+ Institute for Nanotechnology, AAMP group, University of Twente, The Netherlands
m.maksimovic@math.utwente.nl

Quasi-normal modes are used to directly characterize defect resonances in composite 1D Photonic Crystal structures. Variational coupled mode theory using QNMs enables quantification of the eigenfrequency splitting in composite structures. Also, variational perturbation analysis of complex eigenfrequencies is addressed.

Summary

We analyze resonances in coupled optical defect cavities realized in finite one-dimensional Photonic Crystals. Viewing these as open systems where waves are permitted to leave the structures, one obtains eigenvalue problems for complex frequencies (eigenvalues) and Quasi-Normal-Modes (eigenfunctions), see [1] and references therein. Single defect structures (photonic crystal atoms) can be viewed as elementary building blocks for multiple-defect structures (photonic crystal molecules) with more complex functionality. The variational CMT formalism using QNMs links the resonant behavior of individual PC atoms to the properties of the PC molecules via eigenfrequency splitting [2]. A variational principle for QNMs permits to predict the eigenfield and the complex eigenvalues in PC molecules starting with a field template incorporating the relevant QNMs of the PC atoms. Further, both the field representation and the resonant spectral transmission close to these resonances are obtained from a variational formulation of the transmittance problem using a template with the most relevant QNMs [1]. Restriction of the field template in variational CMT formalism to QNMs of the unperturbed structure leads to the perturbation theory approximations for the complex eigenfrequency. The method applies to both symmetric and nonsymmetric single and multiple cavity structures with weak or strong coupling between the defects [1, 2].

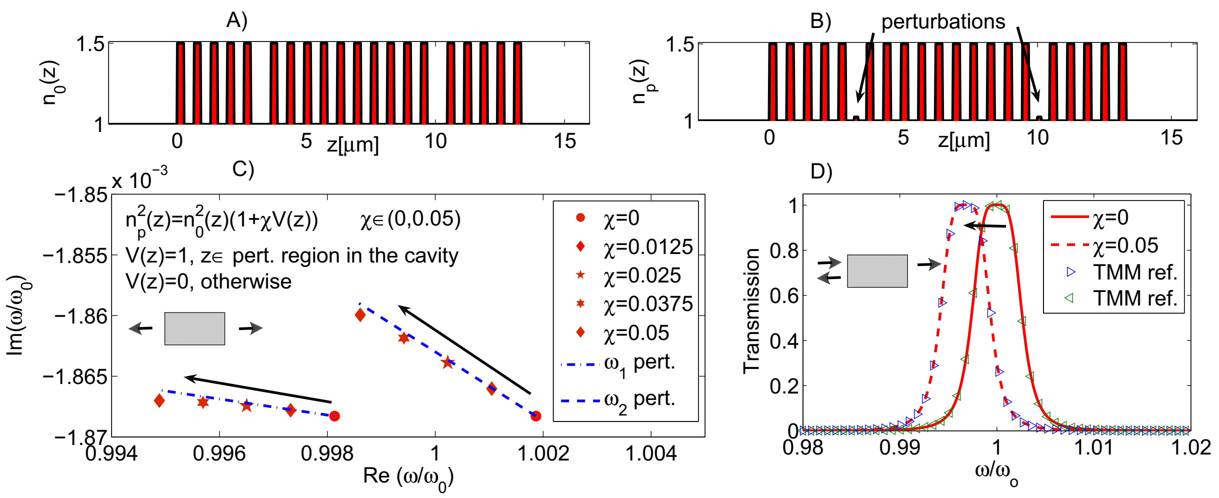

Fig. A) and B) refractive index distributions for the double cavity structure; C) complex eigenfrequencies (of defect resonances), direct computations and perturbation theory approximations; D) spectral transmittance, QNM approximation [2] based on exact QNM supermodes, and TMM reference; symmetric perturbations. The thicknesses of layers are quarter-wavelength (with half-wavelength defects) for reference frequency ω_0.

References

[1] M. Maksimovic, M. Hammer, E. van Groesen, *Optics Communications*, **281**, 1401–1411, (2008).
[2] M. Maksimovic, M. Hammer, E. van Groesen, *Proceedings of SPIE*, **6896**, 6896-05, (2008).

MESA+

Institute for Nanotechnology

http://www.mesaplus.utwente.nl/

PhoeniX

Software for micro- and nano technologies

http://www.phoenixbv.com/

nano ned

http://www.nanoned.nl/